

INFORMATION TO USERS

This manuscript has been reproduced from the microfilm master. UMI films the text directly from the original or copy submitted. Thus, some thesis and dissertation copies are in typewriter face, while others may be from any type of computer printer.

The quality of this reproduction is dependent upon the quality of the copy submitted. Broken or indistinct print, colored or poor quality illustrations and photographs, print bleedthrough, substandard margins, and improper alignment can adversely affect reproduction.

In the unlikely event that the author did not send UMI a complete manuscript and there are missing pages, these will be noted. Also, if unauthorized copyright material had to be removed, a note will indicate the deletion.

Oversize materials (e.g., maps, drawings, charts) are reproduced by sectioning the original, beginning at the upper left-hand corner and continuing from left to right in equal sections with small overlaps. Each original is also photographed in one exposure and is included in reduced form at the back of the book.

Photographs included in the original manuscript have been reproduced xerographically in this copy. Higher quality 6" x 9" black and white photographic prints are available for any photographs or illustrations appearing in this copy for an additional charge. Contact UMI directly to order.



University Microfilms International
A Bell & Howell Information Company
300 North Zeeb Road, Ann Arbor, MI 48106-1346 USA
313/761-4700 800/521-0600

Order Number 9217846

Concurrent fixture planning and analysis for machined parts

Lee, Soo Hong, Ph.D.

Stanford University, 1992

Copyright ©1991 by Lee, Soo Hong. All rights reserved.

U·M·I
300 N. Zeeb Rd.
Ann Arbor, MI 48106

OM

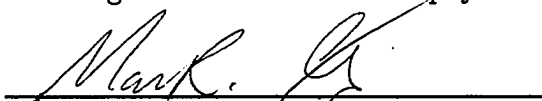
CONCURRENT FIXTURE PLANNING AND ANALYSIS FOR MACHINED PARTS

A DISSERTATION
SUBMITTED TO THE DEPARTMENT OF MECHANICAL ENGINEERING
AND THE COMMITTEE ON GRADUATE STUDIES
OF STANFORD UNIVERSITY
IN PARTIAL FULFILLMENT OF THE REQUIREMENTS
FOR THE DEGREE OF
DOCTOR OF PHILOSOPHY

By
Soo Hong Lee
September, 1991

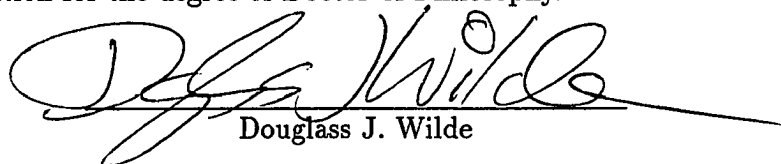
© Copyright 1991 by Soo Hong Lee
All Rights Reserved

I certify that I have read this dissertation and that in my opinion it is fully adequate, in scope and in quality, as a dissertation for the degree of Doctor of Philosophy.



Mark R. Cukosky
(Principal Adviser)

I certify that I have read this dissertation and that in my opinion it is fully adequate, in scope and in quality, as a dissertation for the degree of Doctor of Philosophy.



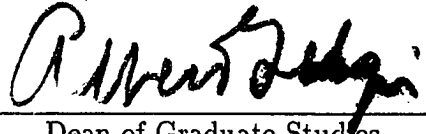
Douglass J. Wilde

I certify that I have read this dissertation and that in my opinion it is fully adequate, in scope and in quality, as a dissertation for the degree of Doctor of Philosophy.



Sheri D. Sheppard

Approved for the University Committee on Graduate Studies:



Robert D. Schaefer
Dean of Graduate Studies

Preface

Automated fixture analysis and planning are essential for unmanned manufacturing, particularly in small-batch machining and assembly. However, fixturing and fixture planning are among the least solved challenges facing unmanned, flexible manufacturing systems today. This thesis presents automated fixture analysis and planning as a component of a computational system for concurrent product and process design. The fixture analysis and planning system is called the fixture agent and is responsible for determining sets of fixturing arrangements to restrain and locate parts as they are machined. The fixture agent works with a geometry agent to obtain information about the geometry of a part and with a process planner to obtain information about the machining process. A set of rules and procedures provides the fixture agent with spatial and geometric reasoning capabilities (e.g., checking for accessibility and interference) and for choosing fixtures from a small library, according to the size and shape of the workpiece and the desired machining operations. The system also checks whether a fixture arrangement can fully locate and restrain a part by computing whether the set of contacts achieves kinematic “form closure” and “force closure.”

To properly handle more complex parts, the fixturing expert must also reason in more detail about forces. Therefore, the fixture agent has been designed to be able to reason at different levels of detail, employing fast geometric checks at the most superficial level and more time-consuming force and friction analyses at a deeper level, depending on the completeness of the machining plan. The focus of this thesis is on

the approaches used for analyzing fixture kinematics and clamping forces, including the analysis of friction. Since many fixture arrangements rely on friction, the ability to reason about friction is an important component of fixture planning. Limit surfaces in force/moment space are introduced as a convenient formalism to check whether parts will slip and to help in specifying clamping forces. For unknown pressure distributions, ways of producing a conservative boundary of limit surface are explored so that the fixture expert can assess the likelihood of slippage without knowing the details of the pressure distribution.

The final section of this thesis discusses the issues involved in turning a set of analysis programs and rules into an agent that can interact continually with other modules of a concurrent design system. A key aspect of the approach is to maintain a graph of dependencies among fixturing arrangements, machined features and geometric elements so that the effects of minor changes in the part geometry can rapidly be assessed, without computing a new fixture plan from scratch.

Acknowledgments

First of all I thank God for giving me the opportunity to study at Stanford University. I also thank my thesis advisor, Mark Cutkosky, for his constant, patient advice and encouragement throughout the last five years. I also thank Professors Douglass Wilde and Sheri Sheppard for their advice and suggestions for the final draft of this dissertation.

Without the help of my friends and colleagues in our research group, Prasad Akella, Rob Howe, Imin Kao, Ranjit Konkar, Warren Packard, Andrew Philpot and J. C. Tsai, much of the work covered in this thesis would not have been possible. I also thank Dr. Subbarao Kambhampati for many discussions with me regarding the implementation of the system.

I thank my wife, Suk-Yeon Lee, from the bottom of my heart for all she has done for five years. Besides being the mother of our two children, Stephanie and Joshua, she has supported me and given me constant encouragement and loving care. Finally I thank my parents for their constant encouragement and financial support.

This work was supported by the National Science Foundation under NFS Grant DMC-8618488 and DARPA under ONR N00014-88K-0620.

Contents

Preface	iv
Acknowledgments	vi
1 Introduction	1
1.1 Issues in Fixture Planning	4
1.1.1 Geometric analysis	4
1.1.2 Kinematic analysis	5
1.1.3 Force analysis	5
1.1.4 Deformation analysis	6
1.2 Terminology and notations	6
1.2.1 Terminology	6
1.2.2 Nomenclature	9
2 Literature Review	11

2.1	Surveys	11
2.2	Geometric analysis	12
2.3	Kinematic analysis	13
2.4	Force analysis	15
2.5	Deformation analysis	17
2.6	Fixture planning	18
3	Geometric analysis of fixtures	22
3.1	Checking for collisions: tool path pruning and definition of clampable regions	22
4	Kinematic analysis of fixtures	26
4.1	Complete location	27
4.2	Kinematic constraint	31
5	Force analysis with friction	34
5.1	Friction limit surfaces	34
5.1.1	The limit surface for a single contact point	35
5.1.2	Limit surfaces for multiple points of contact	38
5.1.3	Symmetry of the limit surface	40
5.2	Applying limit surfaces to fixturing	44
5.2.1	Two-dimensional procedure and example	44

5.2.2	Three-dimensional procedure and example	49
5.3	Discussion of limit surface accuracy	54
5.4	Comparison of the limit surface with other approaches	63
5.4.1	The COR locus method	63
5.4.2	Maximization force method	64
5.4.3	Minimization method	65
5.4.4	Polynomial solution method	68
5.5	Experimental results	69
5.5.1	Experimental measurement of clamping pressures	69
5.5.2	Comparison of measured and predicted limit surfaces for various contact shapes	73
5.6	Summary	78
6	Implementation of the fixture planner	80
6.1	Geometric interactions in fixture and process planning	81
6.2	Backtracking	86
6.3	Incremental planning	90
6.4	Working with incomplete information	92
6.5	Discussion	94
7	Conclusions and Future Work	100

Appendices	105
A A cylinder in a V-block and a vise-jaw	105
A.1 Equation of Equilibrium for a cylinder in a V-block and a vise-jaw	105
A.2 Example: Equation of limit surface of a cylinder in a V-block and a vise-jaw	108
B Initial fixture placement	110
B.1 Vise fixture type	110
B.2 Strap clamp fixture type	111
C Friction force versus slipping velocity	113
D Conservative limit surface proof	116
E Implementation of Interference Checking	119
F Experiment setups and mechanical drawings	122
F.1 Experiment procedure	122
F.1.1 Measurement of μ for indentation case	122
F.1.2 Measurement of external force and moment	123

List of Tables

List of Figures

3.1 A slot feature has four tool paths (TP1, TP2, TP3 and TP4), but TP3 is not feasible from fixturing stand point, because a tool holder collides with a part, so TP3 is pruned from the list of possible tool paths of the slot feature.	23
3.2 The fixture agent determines “clampable regions” in which fixtures will not produce collisions with cutting tools and then positions fixtures within the regions.	25
4.1 A system of forces can be combined into a force along a unique line and a couple in a plane perpendicular to this line. This equivalent force and couple combination is called a wrench.	27
4.2 Contact types and contact wrenches used in the fixture analysis (adapted from a table of contact types presented in Salisbury [1985])	28
4.3 The 3-2-1 rule of conventional fixturing satisfies the principle of complete location.	28
4.4 In (a), the block held in a vise is constrained by friction but is not located in the (x, z) plane and therefore does not have “complete location.” In (b), the block is indexed against a parallel bar and is unlocated only along the x axis.	30

4.5 Possible errors in clamping a block in a vise with two parallel faces (a-b) and solution involving one fixed and one pivoting face (c).	31
4.6 Contact wrenches for a rectangular part clamped in a vise with and without friction	32
4.7 Contact wrenches for a cylindrical part clamped in a vise with and without friction. In reality this configuration is not recommended; a V-Block would be used for such parts.	32
5.1 Examples of arrangements in the fixture library that require friction.	35
5.2 The limit surface of a single point contact becomes an ellipse.	36
5.3 Friction limit surface of three supporting points, obtained by scanning the COR over the (x, y) plane. The limit surface encloses “safe” forces and moments that will not produce slipping.	39
5.4 When the COR is not on a line of symmetry passing through the center of pressure, the friction force, f_t is not antiparallel to the direction of motion, $\frac{v}{ v }$	41
5.5 If the COR locations are scanned along the y axis, the resulting curve on the limit surface is not a planar curve, because the y axis is not a line of symmetry for the tripod pressure distribution.	42
5.6 A rectangular block is held in a vise. The details of the pressure distribution are not known and depend on the location of the cutting tool and the cutting conditions.	45

5.7 An approximating ellipsoid can be found for a fast, approximate method for determining a limit surface for arbitrary pressure distribution. Maximum moment point, $p_{max} = (f_{x_0}, f_{y_0}, m_{omax})$ is obtained when COR is at the origin. Also p_1 and p_2 can be found, where the circle in the (f_x, f_y) plane intersects the f_x and f_y	46
5.8 A rectangular block is held in a vise with a pressure distribution that is approximated by a tripod of forces that satisfies the same equilibrium conditions.	48
5.9 Projection of the limit surface in the (f_x, f_y) plane. If the clamping force is increased to $5,118N$ ($1,150lbf$), the cutting force no longer produces slipping.	48
5.10 A cylinder is held between a V-block and a plate with 3 line contacts. The ratio of translation to rotation about Z can be expressed by a screw angle θ	50
5.11 Projections of the limit surface for the first line contact, for which the l and n axes happen to be aligned with the x and y axes, expressed in the workpiece coordinate frame.	51
5.12 The final limit surface for a cylinder held in a V-block becomes an ellipse. 53	
5.13 Different friction limit surfaces produced by different contact assumptions that satisfy the same equilibrium equations.	55
5.14 A conservative lower bound on the limit surface for all possible pressure distributions known to lie primarily outside a central region	56
5.15 The ellipsoid has an approximation error depending on the angle of inclination, $\theta = \tan^{-1} \frac{f_{vertex}}{m_{omax}}$ (shown for the case of two strap clamps.)	56

5.16 For a given strap clamp figure configuration, several kinds of approximation are possible, but the point contact approximation, (c), gives the most conservative boundary of the limit surface.	58
5.17 A cross-section of a normalized limit surface for a disk contact. The dotted curve represents the actual limit surface and the solid curve represents the ellipsoidal approximation. The maximum error in m_o occurs at $\frac{r_{COR}}{r_{disk}} = 0.9$ and the maximum error in f_y occurs at $\frac{r_{COR}}{r_{disk}} = 0.6$ (The results would be the same for other cross-sections since this limit surface is axisymmetric.)	60
5.18 Comparison of limit surface and ellipsoidal approximation for a rectangular contact area. The actual limit surface is represented by the dotted line and the approximation by the solid line. The limit surface cross-sections are taken in the (f_y, m_o) plane, corresponding to scanning COR locations along the x axis. In this case, since the COR locus is the major principal axis, the errors in f_y and m_o are largest.	61
5.19 Comparison of limit surface and ellipsoidal approximation for a rectangular contact area. The actual limit surface is represented by the dotted line and the approximation by the solid line. The limit surface cross-sections are taken in the (f_x, m_o) plane, corresponding to scanning COR locations along the y axis. In this case, since the COR locus is the minor principal axis, the errors in f_x and m_o are smallest.	62
5.20 The pressure distribution was obtained by using an array of steel balls that indented a soft plate.	70
5.21 Load and indentation diameter relation for 1.778 mm thick lead plate and 4.763 mm diameter spherical indenter: comparison of results from three trials with theoretical result.	71

5.22 3-D perspective plot of a pressure distribution over a rectangular contact area, obtained by measuring ball indentation diameters. (Total clamping force = $\sum_{i=1}^{15} p_i = 890N.$)	71
5.23 Three shapes of workpiece to make an artificial pressure distribution.	73
5.24 Experimental results for uniform rectangular contact case	74
5.25 Experimental results for circular contact	75
5.26 Experimental results for four small islands of contact	76
5.27 Experimental result for two long islands of contact	77
6.1 A solid model of the component being machined.	82
6.2	83
6.3 The fixture agent was unable to find an adequate clampable region for this part with four slots, so it split the setup into two parts, shifting the clamps between them. Windows I and II show the initial and revised mergings of operations which are communicated back to the process planner.	86
6.4 Two possible total orders that are consistent with a partially-ordered setups graph and process plan. The two orders result in some different intermediate part geometries.	89
6.5 Dependencies among features, operations, and fixture setups and primitive geometric elements of features.	89
6.6 Since the setup for Hole-1 depends on face-1, a component face of Slot-1, the fixture agent needs to provide a new fixturing arrangement when Slot-1 is modified.	91

6.7	A flow chart of the checks involved in incremental fixture planning.	91
6.8	Solid model representation of a machined component with several interacting features. Part is shown before modification, in which Slot-3 is deleted and Hole-5 is relocated to the same face as Slot-2.	92
6.9	Process plan and sequence of setups before and after modifying the part in Figure 10. Setups 2 and 3 have been merged, and setups 1 and 4 have been reused without change.	94
E.1	Four hole features are interacting.	120
F.1	A measuring device of indented diameter.	124
F.2	Indented lead plates.	125
F.3	Experimental setup on MTS machine.	126
F.4	Mechanical drawing of pressure distribution measuring device.	127
F.5	Mechanical drawing of a workpiece with an island.	128
F.6	Mechanical drawing of a workpiece with four rectangular islands.	129
F.7	Mechanical drawing of a workpiece with two long rectangular islands.	130

Chapter 1

Introduction

Automated fixture analysis and planning are essential for unmanned manufacturing, particularly in small-batch machining and assembly. However, fixturing and fixture planning are among the least solved challenges facing unmanned, flexible manufacturing systems today. Thus it is common to see manufacturing systems in which CNC machine tools automatically cut parts and coordinate-measuring machines inspect them, but in which people are still required to locate parts on pallets and clamp them in place. The specification of fixtures for producing a part is likewise dependent on people, requiring the skills of a machinist or manufacturing engineer. As an alternative, this thesis explores automated fixture analysis and planning as a component of a computational system for concurrent product and process design. One of the goals of concurrent product and process design is to enable designers to quickly produce prototypes of new designs. To make this possible, process planning is done step-by-step, as the design evolves. The designer receives immediate feedback about possible manufacturing problems and can intervene in the planning if necessary. The software system for the project is called NextCut [Cutkosky and Tenenbaum 1990] and is inspired by human team design, in which designers and other specialists co-operate to solve problems and develop manufacturing plans. The fixture analysis, which forms the subject of this thesis, is performed by a module called the fixture

agent. The fixture agent interacts with other modules, including a geometric solid modeler and a machining sequence planner, so that fixturing and machining plans are developed concurrently as the design progresses.

An important part of the philosophy of concurrent design is that fast, approximate analyses are used to give immediate feedback to the designer during early design stages, while more detailed analyses are used during final design and process planning, when more information about expected cutting forces, tolerances, etc., is available. As a consequence, it is necessary for modules like the fixture agent to be able to reason at multiple levels of detail, so that simple questions such as "Can this part be held in a vise?" are answered with a minimum of computation, leaving numerical analyses for more difficult questions such as "Will the part slip if I cut it with a large end-mill ?"

Prior to the current work, the fixture agent had little "deep" knowledge of fixturing and instead relied primarily on rules and simple geometric and kinematic checks for choosing fixtures, based on the dimensions of the workpiece and the expected cutting operations. As such, it was limited to a small repertoire of machining operations. The work described in this thesis is an effort to model the process of work-holding more accurately and to provide the fixture agent with a more powerful set of tools for fixture planning and analysis, including rules, numerical procedures and symbolic reasoning.

The work in this thesis draws upon previous geometric and kinematic analyses of robotic grasp and motion planning, and fixture analysis. However, the main focus of this thesis is the analysis of fixturing with friction, a relatively unexplored subject. Although many common clamping arrangements rely on friction, the analysis of friction in fixturing has received very little attention. The approach to friction analysis developed in this thesis involves the use of limit surfaces in force/moment space. Limit surfaces form a convenient tool for reasoning formally about friction. They are also convenient for planning, since any series of anticipated forces and moments can be tested against a limit surface. If the forces and moments fall inside the surface,

the arrangement is “safe.” At the time the approach in this thesis was developed, no comparable analysis was found in the literature. Recently, however, an analysis by Sakurai [1990] has appeared in which friction is considered for parts held by strap clamps. Although Sakurai uses a different approach, involving optimization, to solve for the friction limits, the results he obtains are equivalent to those that the analysis in Chapter 5 obtains for the case of a part held by strap clamps. A comparison of different approaches to analyzing the possible slippage of parts subject to Coulomb friction is given in Section 5.4.

The importance of modeling friction becomes clear when it is recognized that common fixturing arrangements, such as a part clamped in a vise or held down with strap clamps, rely on friction for holding the part. In such cases, an obvious question is “How hard should one clamp?” Clamping harder than necessary may damage the part or produce deformations that reduce the final part accuracy. On the other hand, clamping too gently may permit the part to slip during machining, and be ruined.

Machinists learn to estimate clamping forces based on a variety of factors including the workpiece material (e.g., aluminum versus plastic), geometry (e.g., whether the part has thin walls or other easily deformed sections), the required tolerances and the expected cutting forces. The process of setting clamping forces is not entirely “open-loop” since the machinist feels the resistance in the crank of a vise and may tug on a clamped part to check that it is secure. Even so, the estimation of clamping forces is difficult and errors may occur, perhaps due to unexpected variations in cutting forces or the coefficient of friction. For unmanned manufacturing, it is necessary to have a way of replacing the machinist’s skill in assessing clamping forces and arrangements. Like the machinist, the fixture planner must consider geometric, kinematic and force constraints.

In Chapter 2, some of the issues involved in fixture planning are first reviewed. An approach to fixture analysis is then presented in Chapter 3, 4 and 5, concentrating on geometric, kinematic issues and the modeling of friction to predict whether a part will slip for a given set of forces. Limit surfaces are constructed in force/moment space

as a convenient formalism for reasoning about friction and for determining when and how clamped parts may slip. When used in the absence of deformation information, approximate limit surfaces are constructed, which permit estimates of the friction limits to be made. With more detailed information (e.g., pressure distributions determined from a finite-element analysis of the clamped part), precise limit surfaces could be constructed. In Chapter 6, the implementation of a fixture planning program is discussed. The analysis procedures of Chapter 3, 4 and 5 are embedded in a software module called the fixture agent, which interacts with a process planner and geometry module as part of a concurrent design system called Next-Cut. Conclusions and future work is shown in Chapter 7.

1.1 Issues in Fixture Planning

Fixture planning involves analyses at several different levels. In approximate order of increasing computational effort (and decreasing frequency of use) these are: geometric, kinematic, force and deformation analyses.

1.1.1 Geometric analysis

Geometric analysis in fixture planning has much in common with geometric analysis for robot grasp planning [Brost 1988, Jameson and Leifer 1986] and motion planning [Lozano-Perez 1983] and other subjects that involve spatial reasoning. Foremost, it is necessary that the proposed fixturing arrangement does not interfere with the expected tool path, that the fixtures do not restrict access to features being machined, and that the fixturing elements themselves can access desired faces or other features for clamping. For the fixture agent, rules are first applied to determine whether the workpiece is suitable for holding in a vise or with strap clamps, etc. Next, interference and access checks are performed, using approximate bounding volume representations of the features, clamping elements and swept tool paths for speed. After the geometric

constraints are satisfied, heuristics are applied to reduce the number of candidate clamping arrangements. These heuristics essentially try to maximize the clamping stability, but do not make use of the more formal analyses discussed in Chapters 4 and 5.

1.1.2 Kinematic analysis

Kinematic analysis of fixturing includes determining whether a fixture arrangement will correctly locate a part and whether it constrains the part with respect to cutting forces. Considerable work has been done on kinematic analysis of fixtures, and the main developments are reviewed in Section 2.3. For correct location, the fixturing elements should completely specify the position and orientation of the part with respect to desired datum surfaces, but should not overdetermine the location. For complete constraint, it is required that contact forces applied by the fixturing elements (with or without friction) completely span the vector space of possible cutting forces. As kinematic analysis is an important first step in performing the friction analysis which forms the main contribution of this thesis, the approach to kinematic analysis pursued in the fixture agent is described more in detail in Chapter 4.

1.1.3 Force analysis

Force analysis is concerned with checking that the forces applied by the fixtures are sufficient to maintain static equilibrium in the presence of cutting forces. For fixturing arrangements that rely on friction, this entails a friction analysis as discussed in Chapter 5. In contrast to the geometric and kinematic analyses, which can be applied when only the shape of the part is known, this analysis is useful only in the context of a complete machining plan with expected cutting forces.

1.1.4 Deformation analysis

Deformation analysis is the final and most computationally intensive step of fixture planning. The concern is that a part may deform elastically and/or plastically under the influence of cutting and clamping forces so that the desired tolerances will not be achieved. Deformation is particularly a concern with flexible parts and with parts in which a great deal of material is removed. The application of finite element analysis is described by Sakurai [1990] and Lee and Haynes [1987]. A finite-element analysis also permits an accurate assessment of pressure distributions on the clamping surfaces and, consequently, a more precise version of the friction analysis is described in Chapter 5. However, for many simple prismatic parts a deformation analysis will not be performed as part of fixture planning and, although it is an area of interest for future work, it will not be covered in this thesis.

1.2 Terminology and notations

1.2.1 Terminology

The terminology used in this dissertation is listed and briefly described in this section.

limit surface: A limit surface [Goyal *et al.* 1991] is a result of the process of mapping between motions and forces in force/moment space. By establishing a mapping between directions of sliding motion and corresponding forces and moments, one can solve the inverse problem of determining how a part will move in response to applied forces. Note that if the magnitude of a force, f_e , applied to a contact is smaller than that of the corresponding frictional force, $|f_t|$, the part will not slip. Limit surfaces are defined more fully in Chapter 5.

screw theory: Any rigid body displacement can be accomplished by a rotation about a unique axis and a translation along the same axis. A screw has been

defined by Ball [1897], as being a straight line in space with a scalar, called the pitch, assigned to it. The pitch can be regarded as the ratio of the magnitudes of two vector quantities acting along a straight line called the screw axis [Ohwovorole 1980]. Any set of six quantities, five of which are independent, may thus serve as screw coordinates.

convex set: A set such that for every two elements x and y , the line segment connecting them also belongs to the set itself [Fenchel 1953]. For example, X is a convex set if and only if

$$x, y \in X \longrightarrow \lambda x + (1 - \lambda)y \in X \text{ for all } \lambda \text{ with } 0 \leq \lambda \leq 1 \quad (1.1)$$

center of rotation (COR): The center of rotation [Peshkin 1986] is the point in a plane such that the instantaneous velocity of a rigid body moving in the plane can be expressed as a pure rotation about that point.

center of twist: The center of twist is the center of rotation for which the generalized load is a pure moment, i.e., the center of twist occurs at the minimum of the moment function [Goyal *et al.* 1991]. Zhukovskii [1948] calls the center of twist the “pole of friction”.

center of friction: The center of friction is the centroid of the frictional forces on a sliding body during pure translation [Goyal *et al.* 1991].

moment function: The moment function for a sliding body is the moment computed with respect to the COR [Goyal *et al.* 1991].

twist: A twist is a combined motion of rotation and translation. The most general three-dimensional displacement of a rigid body in Euclidean space can be accomplished by a twist about a unique axis, called the twist axis [Ohwovorole 1980]. The twist is equivalent to rotating about the axis while simultaneously translating along the axis. The motion is the familiar one of a bolt in a nut and is therefore called a screw displacement. The angular displacement is called the amplitude of the twist and the ratio of the translation to the amplitude is called the pitch of the twist.

wrench: A wrench is a combination of force and moment. Any system of forces can be combined into a force along a unique line and a couple in a plane perpendicular to this line. This equivalent force and couple combination is called a wrench and it can be regarded as the most general force [Ohwovorole 1980]. The line of action of the force will be called the wrench axis. The magnitude of the force is called the intensity of the wrench and the ratio of the couple to the intensity is called the pitch of the wrench.

force closure: Assuming the external forces acts to maintain contact between the fixturing elements and the object, is the object unable to move without slipping? Formally, a fixturing arrangement satisfies force closure if the union of the contact wrenches has rank 6 [Ohwovorole and Roth 1981, Mason and Salisbury 1985].

form closure: Form closure, or “complete kinematic restraint” refers to a finite set of wrenches applied on the object, with the property that any other wrench acting on the object can be balanced by a positive combination of the original ones. It is a way of defining the notion of a “stable grip” of the object, when friction is not taken into account. It has been pointed out by Reuleaux [1876] and Somov [1900] in the last century, and more recently by Lakshminarayana [1978], that the form closure of a two-dimensional object requires at least four wrenches, and that form closure of a three-dimensional object requires at least seven wrenches. In fixture analysis, the wrenches are contact forces applied by the locating and clamping elements.

quasistatic: A category of motion in which the compliance and friction forces dominate the dynamic equilibrium equations, and inertial and viscous terms can be neglected. This is usually true in low-speed motion [Mason 1986, Goyal *et al.* 1991, Peshkin 1986].

1.2.2 Nomenclature

The terms used in this dissertation are as follows:

coordinate frames:

$B(xyz)$: Body coordinate frame

$P(lmn)$: Coordinate frame at the contact point on the object

$O(XYZ)$: Stationary world coordinate frame

position and orientation vectors:

r_c : 3×1 vector giving the location of center of rotation with respect to the centroid of an object

r_{cp} : 3×1 vector giving the location of the centroid of an object

r_p : 3×1 vector describing the point of contact with respect to the centroid of an object

θ : a screw pitch angle

force/moment vectors:

f_c : a clamping force and moment ,i.e., a 6×1 vector of forces and moments applied at an interface between a workpiece and a fixturing element

f_e : externally applied force and moment on a workpiece, a 6×1 vector of forces and moments.

f_t : magnitude of a tangential force

f_n : magnitude of a normal force at a contact

$f_{t,max}$: maximum possible tangential force at a contact
(achievable when there is no moment)

m_{f_o} : a frictional moment with respect to the centroid of the pressure distribution of an object face

$m_{o,max}$: maximum possible moment at a contact (achievable when there is no force)

t_i : a contact twist at a contact i

T_F : contact twists at a face F

w_i : a contact wrench at a contact i

W_n : contact wrenches for a total number of contacts, n

Other parameters used in limit surface and slipping analysis:

μ : Coulomb coefficient of friction

Chapter 2

Literature Review

2.1 Surveys

Lewis and Bagchi [1987] compare the requirements for conventional fixturing systems with those utilized in automated factories. They also review modular fixturing systems and list the most labor-intensive areas associated with fixturing, namely the design, construction and testing of the fixturing system. Typically there is a great deal of indirect labor associated with support functions such as loading and unloading of workpieces onto the fixturing system, equipment maintenance, repair and operating problem diagnosis. As logical steps toward a computer-aided fixturing system, the authors assert that the following activities must be automated: (1) initial design; (2) design verification; (3) integration of fixture design with robotics for loading and unloading. The authors list what they feel are the most important research questions that must be addressed, including: process sheet design, part location, part clamping, design and selection of generic modules, and determination of proper clamping forces.

Cohen [1991] surveys many articles related to fixture design, analysis and planning. He also presents a methodology to integrate the automated design of fixtures with the planning of machining operations and presents his own rule-based system for the

assignment of features to setups and for the design of fixtures according to the 3-2-1 principle. This work is described further in Bidanda and Cohen, reviewed in Section 2.6.

2.2 Geometric analysis

Geometric analysis in fixture planning has much in common with geometric analysis for robot grasp planning [Brost 1988, Jameson and Leifer 1986] and motion planning [Lozano-Perez 1983]. Foremost, it is necessary that the proposed fixturing arrangement not interfere with the expected tool path, that the fixtures do not restrict access to features being machined, and that the fixturing elements themselves can access desired faces or other features for clamping. The problem of determining fixturing arrangements from the geometric analysis point of view has been addressed by a number of authors including [Sungurtekin and Voelcker 1986; Leu, Park and Wang 1986; Trappey and Liu 1990] .

Sungurtekin and Voelcker [1986] show how to determine, whether an NC program will produce a specified part without undesirable geometric side effects (e.g., collisions, cutter breakage) by using a machining verifier. Although the authors do not directly address fixturing, they deal with geometric and spatial reasoning that can be used in geometric analysis in fixturing, such as collision checking between fixture elements and tool paths. In particular, they establish the definitions of the operational swept region (OSR) and total swept region (TSR). The OSR corresponds to the volume of material that a cutting swept through space can actually remove. The TSR corresponds to the total swept volume of the tool and its holder. Thus, it is required that the sum of the feature volumes be contained within the sum of the OSRs and that the intersection of the TSRs with the final part shape be a null set. Conservative bounding-box approximations to the OSR and TSR are used for fixture planning in the fixture agent, as described Appendix E.

Leu, Park and Wang [1986] present a method of representing the geometries of translational swept volumes of three-dimensional objects, which can be constructed by the union of three types of primitives objects: blocks, cylinders, and spheres. Like Sungurtekin and Voelcker [1986], the authors do not directly address fixturing, but they present a technique which is applicable to collision detection in geometric analysis of fixturing, NC machining and motion planning.

Trappery and Liu [1990] propose an approach called Projective Spatial Occupancy Enumeration to simplify the complexities of representation and geometric reasoning for machined parts. The simplification is accomplished by rotating a 3-D object with respect to a certain face in which a user is interested, and then taking the X and Y coordinates only of each vertex to produce a 2-D projection on a plane in 3-D space. The advantage of the approach is that any complex part can be resolved into 2-D problems. By projecting the workpiece onto the working plane of the fixture baseplate, the authors define the 2-D projection as a matrix of elements which represent the decomposed cells of the workpiece. The fixture types and locations are then generated automatically, according to a set of heuristic algorithms, by manipulating the properties of elements in the matrix. A drawback of their system is that it cannot handle situations such as when a face has an enclosed feature like a hole.

2.3 Kinematic analysis

Kinematic analysis of fixturing includes determining whether a fixture arrangement will correctly locate a part and whether it constrains the part with respect to cutting forces. The problem of determining fixturing arrangements from the kinematic analysis point of view has been addressed by a number of authors including [Asada and By 1985; Asada and Fields 1985; Fields, Youcef-Tomi and Asada 1986; Chou, Chandru and Barash 1989; Mani and Wilson 1988].

Asada and By [1985] describe the basic concept of an adaptable fixturing system and its hardware implementation. The important contribution of this work is its

derivation of the condition (i.e., accessibility) for a fixture layout to locate a given workpiece uniquely at a desired location while also permitting the part to be inserted or detached from the fixture arrangement with a single motion. The authors show that the well-known 3-2-1 locating principle is good for prismatic parts. The fixturing of a plastic cover of an electrical appliance with complex shapes is used as a more general example. A limitation of the work is that there is no consideration of the magnitudes of clamping forces, i.e., it is a purely kinematic analysis.

Fields, Youcef-Toumi and Asada [1986] present a design of an automatically reconfigured fixture for sheet metal machining. The fixture consists of a universal fixture bed and a set of fixture elements, which are automatically assembled by a robot manipulator in order to build different fixtures. The main contribution of this paper is that the fixture construction is modified in such a way that the resultant accuracy of an assembled fixture is desensitized as much as possible to positioning errors of the robot manipulator used for assembly. Also the accuracy of workpiece fixturing is evaluated through analysis and experiments on the developed system. The authors show that a resultant part placement accuracy was found to be well within required aerospace tolerances of ± 0.81 mm (0.032 in).

Chou, Chandru, and Barash [1989] present a mathematical theory of automatic design of fixtures for general prismatic parts by using screw theory and statics. Four functions of fixtures, including *resting equilibrium*, *deterministic locating*, *clamping equilibrium* and *total constraint*, are analyzed. The paper focuses on a kinematic analysis of fixturing problems drawing upon earlier work on applying screw-theory to establishing whether parts are completely located by Ohwovorole [Ohwovorole 1980; Ohwovorole and Roth 1981]. Chou *et al.* argue that the correct order of analyses for fixture layout design is: 1) Deterministic Locating; 2) Clamping Stability; 3) Total constraint; and 4) Equilibrium of clamping forces. For satisfactory fixturing, they show that the intersection of contact twists, corresponding to the degrees of freedom at each contact, should be a null set and that the union of contact wrenches, corresponding to contact forces, should form a wrench matrix with a full rank (Rank 6). A limitation of this work is that it ignores friction forces, and the corresponding extra

contact wrenches.

Mani and Wilson [1988] divide fixturing elements into passive locating elements and active clamping elements. They take into account in specifying machining practice selection of passive and active fixturing elements, part loading, and clamping sequence. The fixturing plan includes a specification for the order in which clamping elements should be tightened. The kinematic planning is performed in four steps: 1) building triangles formed by lines of restraints applied at the mid-points of the three best rated edges, 2) matching the chosen triangles to assure complete restraints against part translation and rotation, 3) establishing the types of tool point, i.e., passive or active and soft or hard, and 4) devising a loading sequence for the part.

2.4 Force analysis

Force analysis is concerned with checking that the forces applied by the fixtures are sufficient to maintain static equilibrium in the presence of cutting forces. In contrast to the geometric and kinematic analyses, which can be applied when only the shape of the part is known, this analysis is useful only in the context of a machining plan. The analysis can be performed with, or without, consideration of the additional contact forces due to friction. The frictionless analysis is more conservative and when a fixturing arrangement can be found that will restrain a part without friction it may be preferred. However, many common fixturing arrangements rely on friction. The literature review on force analysis related to fixturing is divided into two parts: force equilibrium analysis, and friction analysis.

Force equilibrium analysis

Force equilibrium analysis in fixturing has been addressed by a number of authors including Lee and Haynes [1987]; Lee and Cutkosky [1991]; Chou [1990]; and Menassa and DeVries [1990.]

Chou [1990] builds upon the earlier kinematic and force analysis in [Chou, Chandru and Barash 1989] and considers the effects of cutting forces when designing a fixture arrangement. A methodology is proposed for locating clamping elements such that the cutting forces are neutralized. The methodology takes as input a cutting force field, computes the envelope of the force field and lays out locating and clamping elements such that all forces within the envelope can be accommodated. The envelope represents an upper-bound estimate for the effects of cutting forces, and in this respect, plays a similar role to the limit-surfaces discussed in Section 5.

Force equilibrium and Friction analysis

With the exception of [Sakurai 1990], no other work has been found that applies a friction analysis to fixturing. However, the analysis of workpieces slipping out of fixtures due to cutting forces is similar to the analysis of objects sliding across a flat surface, an area that has received attention from a number of investigators in robot motion planning. In this section, the contributions of investigators are briefly summarized. In Chapter 5.4 a more detailed comparison is made between the limit-surface method for expressing friction constraints, as used in this thesis, and other methods found in the literature.

Mason [1986], drawing upon classical work by [Zhukovskii 1948, Savvin 1965, Ishlinskii *et al.* 1981, Shvedenko 1986], investigates the motion of an object sliding on a plane, pushed by a manipulator. The problem is to determine the linear and angular velocities as a function of the force and moment applied by the manipulator or “pusher.” The ratio of linear to angular velocity is expressed in terms of the instantaneous center of rotation (COR) of the part. Since the details of the pressure distribution between the object and the planar surface are generally not known, one cannot uniquely solve for the COR. However, one can show, for example, that if the center of mass is to the right (left) of the applied force, then the object must rotate clockwise (counter-clockwise) as it slides.

Expanding on the results of Mason, Peshkin [1986] finds the set of possible motions of a part for a given pushing direction, by using a simple variational principle. He

expresses the set of possible motions as the “COR locus” of the part and shows that for certain shapes, a COR locus can be obtained despite incomplete knowledge about the pressure distribution of the part.

In certain cases, as when grasping a part with two fingertips that are equipped with a pressure-sensing tactile array, the pressure distribution over the contact area may be known. For this case, Bicchi and Dario [1987] show that the COR of the object can be found by solving a pair of polynomial equations. These calculations require measurement of the coefficient of friction, the total normal force, and the normal pressure distribution (using an array sensor).

Another approach to solving for the relationship between applied forces and sliding motion is presented by Sakurai [1990]. Sakurai’s approach assumes that the direction of the cutting force is known, and therefore it is only necessary to solve for the magnitude of the cutting force which will cause the part to slip. He shows that the actual magnitude of the applied force is the maximum possible magnitude for a force in that direction which also satisfies equilibrium and friction constraints. Then, since the direction of the applied cutting force is not, in fact, uniquely known, he scans over all feasible force directions to find the worst case. The clamping forces are chosen to prevent the part from slipping in the worst case.

2.5 Deformation analysis

The deformation of machined workpieces has been addressed by a few investigators. As mentioned in Chapter 1.1.4, deformation is primarily of concern with flexible parts. Although a deformation analysis is beyond the scope of this thesis, the results of previous deformation analyses are of interest because they would permit a more accurate estimation of the contact pressure distribution and, consequently, more accurate friction limit surfaces for fixture planning. A point worth noting about analysis of workpiece deformations is that (in contrast to many finite-element applications for which it is desired to obtain accurate values of stresses throughout the part) in the

case of workpiece fixturing we care only about:

- gross deformations of the part (which could affect tolerances);
- the integral of the pressure distribution over the clamping surfaces (i.e., the clamping forces);
- and the first polar moment of the pressure distributions (which affect the height of the limit surfaces, as discussed in Chapter 5.3).

Lee and Haynes [1987] present a method to compute the deformation of a workpiece by using a finite-element analysis in which the part is subjected to the clamping force and a simplified cutting force (i.e., a point load). The authors consider a block-shaped part and simplified boundary condition, they analyze the deformation of the block due to the clamping force.

Sakurai [1990] presents a finite-element analysis to model the elastic deflection of thin parts under the action of cutting forces. Although the analysis is very approximate, he points out that it is adequate for testing whether deflection may be a problem.

2.6 Fixture planning

A number of previous investigations have focused on fixture planning. For the most part, the previous work has considered only single-setup planning, i.e., finding a set of fixtures to hold a part in a single orientation as it is machined. (In Chapter 6.3 some of the issues associated with multiple-setup planning will be discussed).

Ferreira, Kochhar, Liu and Chandru [1985] present a fixturing expert system as part of their project on developing an automated machining cell. Their fixture planner is written in Lisp, using *If/Then* rules and separate files of facts which describe the part geometry and cutting plan. Most of the rules and facts are fairly straightforward (for

example the system tries to apply the 3-2-1 principle of fixturing if possible; if the part has several holes then the system tries to use some of the holes for fixturing.) An interesting part of the planner appears to be a collection of FORTRAN routines for "accessibility" and "reachability" checking. These routines are not described in any detail but they include functions for computing the areas of polygons, finding the locations of intersection points of polygons, and performing a stability analysis based on the locations of the contact points.

Englert [1987] proposes that both heuristic "craftsman" knowledge and analytical or empirical information must be integrated into a coherent framework to bring to fruition the ultimate goal of automated process planning. He summarizes currently used fixtures and discusses the development of a fixturing expert system, supported by approximate analyses of clamping forces and part deformation.

Kanumury, Shah and Chang [1988] describe a rapid prototyping system called Quick Turnaround Cell (QTC). The system is designed to integrate design, process planning, cell control and inspection. With regard to fixture planning, it is not clear whether the system deals explicitly with kinematic and force constraints (e.g., form closure, force closure). The magnitude of the clamping force is determined using empirical equations and graphs suggested by the HMT Handbook [Gnagopadhyada 1980].

Mani and Wilson [1988] provide a method for generating fixturing plans based on standard machining practice and the geometry of the part. The fixturing plan is based on two-dimensional geometric profiles obtained from a solid modeler. As discussed above, in Section 2.3, they require that the fixturing arrangement satisfy kinematic criteria for complete location and they divide fixtures into active and passive elements.

Bidanda and Cohen [1990] propose a rule-based fixture selection system, called Computer Aided Fixture Selection (CAFS), for axisymmetric or rotational parts. In some ways, rotational and prismatic parts have similar fixture planning requirements. Both types of parts must be located accurately and held securely to resist cutting forces. However, most fixture arrangements for prismatic parts are custom-designed using the

standard 3-2-1 fixturing rule to assure accurate location. By contrast, standard workholding chucks, mandrels and collets are usually used for rotational parts. Therefore, Bidanda and Cohen's planner can select a particular workholding device rather than designing any customized fixtures.

Sakurai [1990] describes a comprehensive process planner for parts held by strap clamps. The system begins by considering all the volumes of features to be removed for a given orientation of the part. If some features can be removed from more than one orientation, then they are considered for all possible orientations. The best clamping and locating surfaces are then identified and clamping and indexing elements are placed on these faces. At present it appears that the system uses only cylindrical indexing posts and strap clamps. Like other investigators reviewed in Chapter 2.3, Sakurai uses screw-theory for checking that the arrangement achieves complete kinematic restraint and location. An important consideration in Sakurai's work is to ensure that the part can be located with sufficient accuracy to produce the desired location tolerances on features to be machined. Next, the system checks for stability with respect to cutting forces. The values of cutting forces are obtained from a machining handbook. Since the actual toolpath is not known, the extreme locations of the cutter path for each feature are used (e.g., the corners of a pocket). Finally, the system checks for possible slipping of the workpiece using the maximum-force method reviewed in Chapter 2.4 and compared with the limit-surface approach use in this thesis in Chapter 5.4.

Hayes and Wright [1987 and 1989] present an expert system, Machinist, that automatically makes process plans for fabricating metal parts on a CNC machine. The expert system generates a process plan by integrating the feature interaction graph with a squaring graph, which outlines all methods for getting the raw material into a square and accurate shape with the minimum waste of material. To explore and model feature interactions, the authors used built-in pattern-operator pairs to spot the interactions and avoid the interactions, because cutting one feature may make it difficult or impossible to cut subsequent features. As a result of the feature interactions, the system finds feasible setup orders in which features can be produced.

A possible limitation of the system is that no analytic method is used to detect the interaction. The system relies on pattern-operator pairs which are based on the expert knowledge compiled from several machinists.

Chapter 3

Geometric analysis of fixtures

The geometric analysis of fixtures involves several steps, including: checking for collisions among tool-paths and fixture elements; checking that the faces of the part can be accessed for machining; selecting a preferred fixture type (e.g., vise versus strap clamps); selecting candidate clamping faces on the part; and positioning clamps on the candidate clamping faces. These checks are performed prior to the kinematic and force analyses discussed in the next two Chapters. Although these checks are fairly straightforward, they actually consume most of the fixture planning time and form the basis for most of the interactions with the process planner and the geometric modeling module as discussed in Chapter 6.3.

3.1 Checking for collisions: tool path pruning and definition of clampable regions

Prior to running the fixture agent, it is necessary to compute toolpath and feature interactions for the part. Such interactions are ubiquitous in machining and are therefore computed with every design or plan change. The checks are carried out using

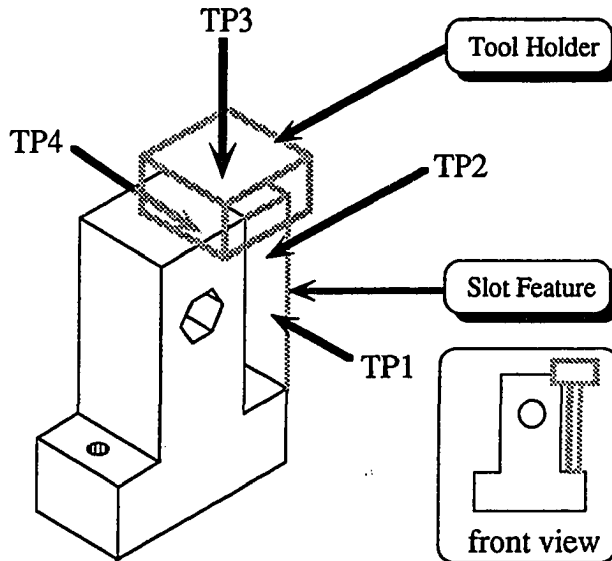


Figure 3.1: A slot feature has four tool paths (TP1, TP2, TP3 and TP4), but TP3 is not feasible from fixturing stand point, because a tool holder collides with a part, so TP3 is pruned from the list of possible tool paths of the slot feature.

bounding-box approximations of the material that a tool could remove from the part and of the total volume swept out by a tool, corresponding to Sungurtekin and Voelcker's [Sungurtekin and Voelcker 1986] OSR and TSR representations, respectively. The approximate swept tool volumes are also similar to "extended feature volumes" described by Karinthi and Nau [1989]. Details on the bounding-box algorithm[Lee and Cutkosky 1991b] are given in Appendix E.

Machining features have one or more possible tool approach directions, depending on the type of feature and the location of the feature on the component. A blind hole has one possible tool approach direction, while a through hole has two, and a slot on the corner of a cube has three. However, some of these approach directions may not be feasible due to intersections with the final part shape. Thus, the first step is to "prune" from the list of tool approach directions for each feature those that would intersect the finished part. The remaining list of directions for each feature, f_j , is called the set of "feasible tool approach directions" $TP(f_j)$. For example, the slot shown in Figure 3.1, has four tool approach directions (TP1, TP2, TP3 and TP4),

but $TP3$ is not feasible because the tool holder would collide with the part during machining. Therefore $TP3$ is removed from the list of feasible tool paths so that $TP(SLOT) = (TP1, TP2, TP4)$.

Similar tests are performed to see whether any of the tool directions in $TP(f_j)$ intersects one or more of the other features, f_k , removed from the part. If so, there is an ordering constraint such that f_k must be made prior to f_j .

As a result of the above two sets of tests, the fixture agent always begins with a list of feasible tool approach directions and with some constraints on the order in which features may be created. (Additional ordering constraints may be imposed by the machining process planner if it is run prior to invoking the fixture agent). The next step is to find candidate setups, by merging operations for features that could be made from the same tool approach direction. The merging is done so as to minimize the total number of different part orientations. Thus, if a face had four through holes and two blind holes, all 6 holes would be merged into a single setup such that the through holes and blind holes were made from the same direction.

The fixture agent then sends a request to the solid modeler to compute the geometry of the part at the start of each setup and tests this geometry against the swept volumes of the cutting tools and their tool-holders to determine safe regions on the part in which fixturing elements could be placed without producing collisions. These safe regions, or “clampable regions” are represented using the approximate cell decomposition method [Lozano-Perez 1983]. In Figure 3.2(a) the grid pattern shows the total clampable region for placing strap clamps. Figure 3.2(b) shows the refined clampable region, with the maximum length of strap clamps taken into account (the clamps cannot reach into the middle of the part). Although the cell decomposition method is not the most accurate representation of the clampable regions, it is used because it is easy to update as the dimensions and locations of features are modified; only a few cells must typically be added or deleted from the list.

Once the clampable regions have been determined, the fixturing elements are located with respect to the part using a heuristic objective function which essentially tries

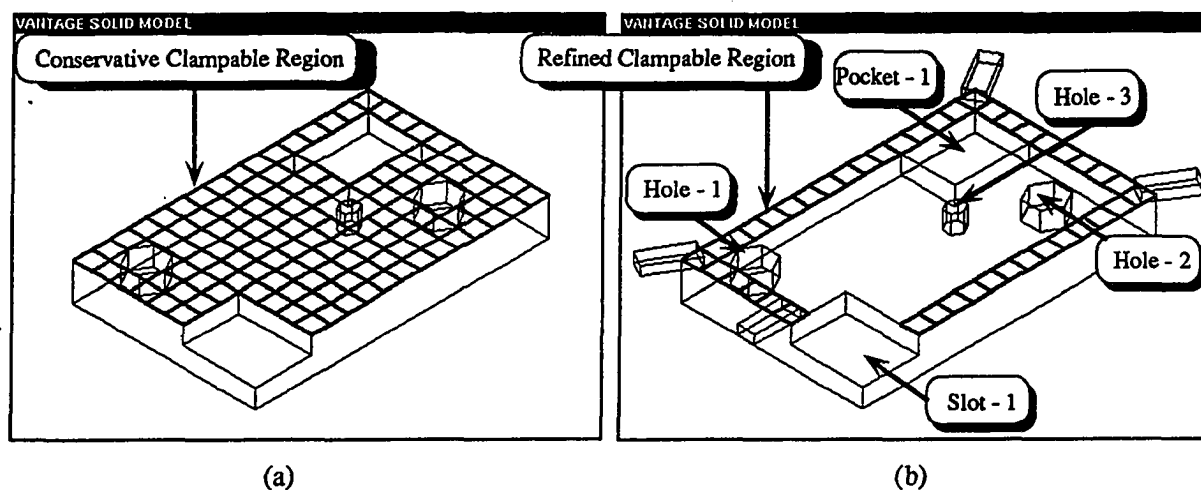


Figure 3.2: The fixture agent determines “clampable regions” in which fixtures will not produce collisions with cutting tools and then positions fixtures within the regions.

to maximize the stability of the arrangement. This initial placement is subjected to detailed kinematic and force checks as discussed in the following chapters. The details of the initial placement are slightly different for vise and strap-clamp fixtures and are summarized in Appendix B.

Chapter 4

Kinematic analysis of fixtures

The approach used by the fixture agent is similar to that of the kinematic analyses of other researches reviewed in Section 2.3, except that the extra contact forces due to friction are included. Furthermore it is recognized that many common clamping arrangements do not fully establish the position and orientation of a part. In this chapter, the kinematic analysis used in the fixture agent is described, focusing on those aspects that establish the framework for the force and friction analysis described in Chapter 5. From the kinematic analysis, a space of possible motions to scan over can be obtained. The reader is referred to [Salisbury 1985; Ohwovoriole and Roth 1981; and Chou, Chandru and Barash 1989] for a more detailed explanation of the underlying twist/wrench formalism. For the purposes of this chapter, it suffices to know that if a force, $\mathbf{f} = [f_x, f_y, f_z]^T$, is applied at a point, P , on a workpiece, the resulting 6-element wrench with respect to the origin is $\mathbf{w} = [\mathbf{f}^T, (\mathbf{r} \times \mathbf{f})^T]/|\mathbf{f}|$, as shown in Figure 4.1. The velocity or motion complement to a wrench is a twist. For a 6-element vector of rotational and translational motion at the origin, $[\omega^T, \mathbf{v}^T] = [\omega_x, \omega_y, \omega_z, v_x, v_y, v_z]^T$, the resulting twist at point p is $\mathbf{t}_p = [\omega^T, (\mathbf{v} + \omega \times \mathbf{r})^T]$ where $\omega = [\omega_x, \omega_y, \omega_z]^T$ and $\mathbf{v}^T = [v_x, v_y, v_z]^T$. Typical contact types and contact wrenches used in fixture analysis are summarized in Figure 4.2.

The kinematic analysis begins by dividing fixturing elements into two classes: *passive*

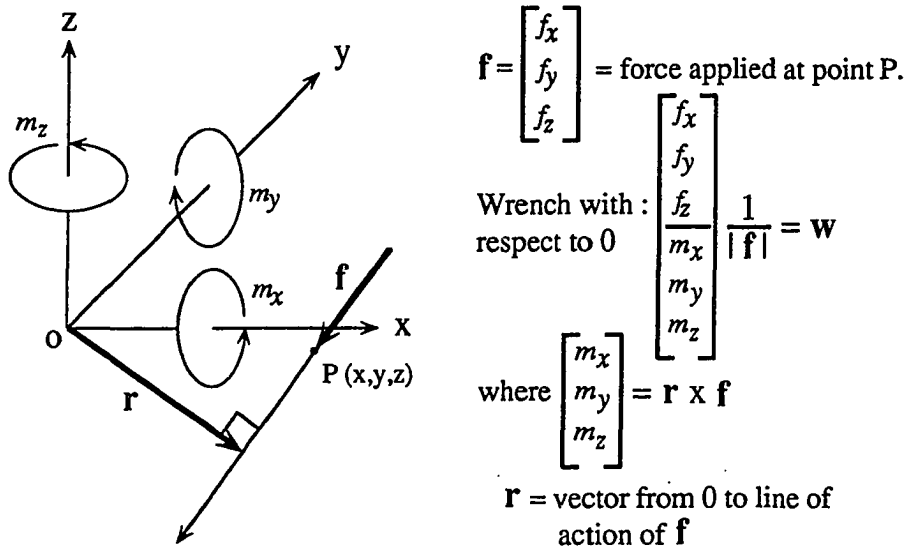


Figure 4.1: A system of forces can be combined into a force along a unique line and a couple in a plane perpendicular to this line. This equivalent force and couple combination is called a wrench.

and *active*. The passive elements provide stationary locating surfaces and include parallel bars, the fixed jaw of a vise, V-blocks and end stops. The active elements are movable and are used for applying forces. Active elements include hydraulic plungers, toggle clamps, strap clamps and the movable jaw of a vise. A fixturing arrangement of passive and active elements should satisfy the principles of *complete location* and *kinematic constraint* [Asada and By 1985] to be explained in the next two Sections.

4.1 Complete location

The requirement for complete location can be stated as follows [Ohwovorile 1987]:

Ignoring friction, the logical intersection of components of contact twists over all passive or locating elements should be null: Let null(A) be the null space of matrix A, then null(T_i), where T_i is a matrix of column vectors, t_i, becomes a wrench matrix, W_i and vice-versa. For complete location of part, it is required that

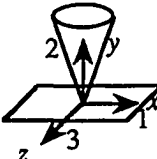
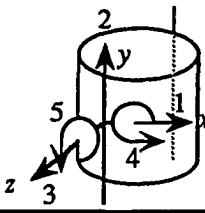
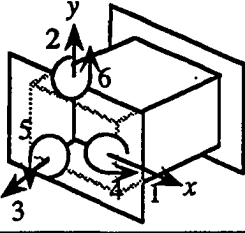
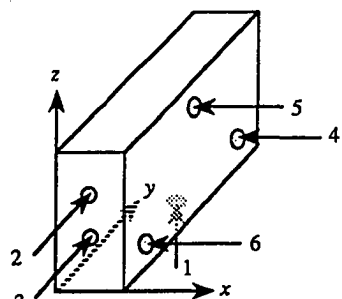
Contact Type	Without Friction		With Friction	
	Twist System	Wrench System	Twist System	Wrench System
Point Contact	 $t_1 = (1,0,0,0,0,0)$ $t_2 = (0,1,0,0,0,0)$ $t_3 = (0,0,1,0,0,0)$ $t_4 = (0,0,0,1,0,0)$ $t_5 = (0,0,0,0,1,0)$	$w_1 = (0,0,1,0,0,0)$ $w_2 = (0,0,0,1,0,0)$ $w_3 = (0,0,0,0,1,0)$	$t_1 = (1,0,0,0,0,0)$ $t_2 = (0,1,0,0,0,0)$ $t_3 = (0,0,1,0,0,0)$	$w_1 = (0,0,0,1,0,0)$ $w_2 = (0,0,0,0,1,0)$ $w_3 = (0,0,0,0,0,1)$
Line Contact	 $t_1 = (0,1,0,0,0,0)$ $t_2 = (0,0,1,0,0,0)$ $t_3 = (0,0,0,1,0,0)$ $t_4 = (0,0,0,0,1,0)$	$w_1 = (0,0,1,0,0,0)$ $w_2 = (0,0,0,1,0,0)$	$t_1 = (0,1,0,0,0,0)$	$w_1 = (1,0,0,0,0,0)$ $w_2 = (0,1,0,0,0,0)$ $w_3 = (0,0,1,0,0,0)$ $w_4 = (0,0,0,1,0,0)$ $w_5 = (0,0,0,0,1,0)$
Plane Contact	 $t_1 = (0,0,1,0,0,0)$ $t_2 = (0,0,0,1,0,0)$ $t_3 = (0,0,0,0,1,0)$	$w_1 = (0,0,1,0,0,0)$ $w_2 = (0,0,0,1,0,0)$ $w_3 = (0,0,0,0,1,0)$	Null Twist System	$w_1 = (1,0,0,0,0,0)$ $w_2 = (0,1,0,0,0,0)$ $w_3 = (0,0,1,0,0,0)$ $w_4 = (0,0,0,1,0,0)$ $w_5 = (0,0,0,0,1,0)$ $w_6 = (0,0,0,0,0,1)$

Figure 4.2: Contact types and contact wrenches used in the fixture analysis (adapted from a table of contact types presented in Salisbury [1985])



Coordinates of each contact point:

$$\begin{aligned}
 pt_1 &= (0.3, 1.0, 0.0) \\
 pt_2 &= (0.3, 0.0, 0.7) \\
 pt_3 &= (0.3, 0.0, 0.3) \\
 pt_4 &= (0.6, 1.5, 0.3) \\
 pt_5 &= (0.6, 1.0, 0.7) \\
 pt_6 &= (0.6, 0.5, 0.3)
 \end{aligned}$$

Figure 4.3: The 3-2-1 rule of conventional fixturing satisfies the principle of complete location.

$$\text{null}([\text{null}(\mathbf{T}_1), \text{null}(\mathbf{T}_2), \dots, \text{null}(\mathbf{T}_n)]) = [\emptyset] \quad (4.1)$$

where \mathbf{T}_i are the twist matrices of the contacts on a part.

As an example, the 3-2-1 rule of conventional fixturing shown in Figure 4.3 satisfies the principle of complete location since the block cannot move in any direction without breaking contact with the locating points. The contact twists for each face of the block are:

$$\mathbf{T}_1 = \mathbf{T}_{\text{point_contact}} = \begin{bmatrix} 1 & 0 & 0 & 0 & 0 & 0 \\ 0 & 1 & 0 & 0 & 0 & 0 \\ 0 & 0 & 1 & 0 & 0 & 0 \\ 0 & 0 & 0 & 1 & 0 & 0 \\ 0 & 0 & 0 & 0 & 1 & 0 \end{bmatrix} \quad (4.2)$$

$$\mathbf{T}_{23} = \mathbf{T}_{\text{line_contact}} = \begin{bmatrix} 0 & 1 & 0 & 0 & 0 & 0 \\ 0 & 0 & 1 & 0 & 0 & 0 \\ 0 & 0 & 0 & 1 & 0 & 0 \\ 0 & 0 & 0 & 0 & 0 & 1 \end{bmatrix} \quad (4.3)$$

$$\mathbf{T}_{456} = \mathbf{T}_{\text{plane_contact}} = \begin{bmatrix} 1 & 0 & 0 & 0 & 0 & 0 \\ 0 & 0 & 0 & 0 & 1 & 0 \\ 0 & 0 & 0 & 0 & 0 & 1 \end{bmatrix} \quad (4.4)$$

$$\text{null}([\text{null}(\mathbf{T}_1), \text{null}(\mathbf{T}_{23}), \text{null}(\mathbf{T}_{456})]) = [\emptyset] \quad (4.5)$$

By contrast, the block held in the vise of Figure 4.4(a) is not located in the (x, z) plane and has three degrees of freedom. Adding a parallel bar, as in Figure 4.4(b), reduces the number of degrees of freedom to one. In practice, such clamping arrangements are often acceptable. For example, a machinist may use the fixturing arrangement in Figure 4.4(b), locating the block in the x direction with a touch probe.

A corollary to the complete location principle is that the location of a part should not be over-determined. In other words, if any of the passive fixturing elements is removed, the logical intersection of the contact twists should no longer be null. To illustrate this principle, let us consider the contact twists for the fixed and movable jaws of the vise in Figure 4.4(a) or (b), and observe that they are redundant:

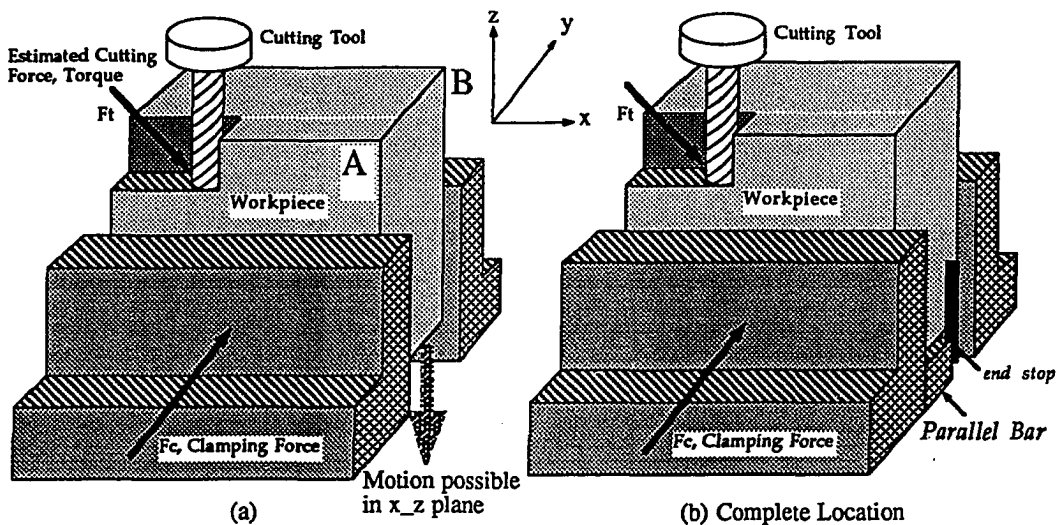
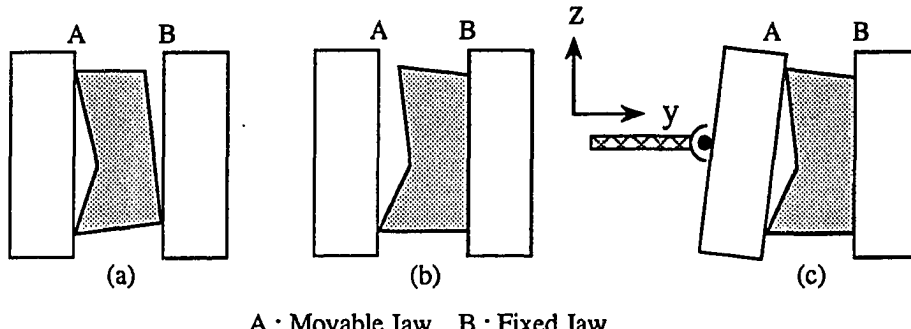


Figure 4.4: In (a), the block held in a vise is constrained by friction but is not located in the x, z plane and therefore does not have “complete location.” In (b), the block is indexed against a parallel bar and is unlocated only along the x axis.

$$\text{Twists from front face} = \mathbf{T}_A = \begin{bmatrix} 0 & 0 & 0 \\ 1 & 0 & 0 \\ 0 & 0 & 0 \\ 0 & 1 & 0 \\ 0 & 0 & 0 \\ 0 & 0 & 1 \end{bmatrix} \quad 6)$$

$$\text{Twists from rear face} = \mathbf{T}_B = \begin{bmatrix} 0 & 0 & 0 \\ 1 & 0 & 0 \\ 0 & 0 & 0 \\ 0 & 1 & 0 \\ 0 & 0 & 0 \\ 0 & 0 & 1 \end{bmatrix} \quad 7)$$

In other words, the parallelism of the block with respect to the x, z plane can be established using either the front “A” or back “B” faces of the block. Unfortunately, this ambiguity can result in a part that does not meet intended geometric tolerances. For example, suppose that the “A” face is not quite parallel to the “B” face, which



A : Movable Jaw. B : Fixed Jaw.

Figure 4.5: Possible errors in clamping a block in a vise with two parallel faces (a-b) and solution involving one fixed and one pivoting face (c).

a datum surface. The block should therefore be located with planar contact between the “B” face and the fixed jaw of the vise. However, if the vise has two rigid, parallel faces the block may adopt a number of orientations as shown schematically in the exaggerated views of cases (a) and (b) in Figure 4.5. A better approach is to use a vise with a ball-joint on the movable jaw as in case (c) (like the pivoted foot of a hobbyist’s C-clamp), that will adopt the orientation of face “A” and press face “B” firmly against the fixed jaw. The resulting arrangement also provides more reliable clamping, and a more accurate assessment of the friction limits, since the contact forces are better known. Similar principles have been used in robotic grippers for reliable locating and clamping by Wright and Cutkosky [1985] and have been proposed for modular fixtures by Mani and Wilson [1988].

4.2 Kinematic constraint

The requirement for kinematic constraint can be stated as follows:

Assuming that the clamping elements keep the part pressed against the locating elements, the resultant contact wrenches over all locating elements should have rank 6:

$$\text{Let } \mathbf{W} \equiv [\mathbf{w}_1, \mathbf{w}_2, \dots, \mathbf{w}_n], \text{ then } \text{Rank}(\mathbf{W}_n) = 6. \quad (4.8)$$

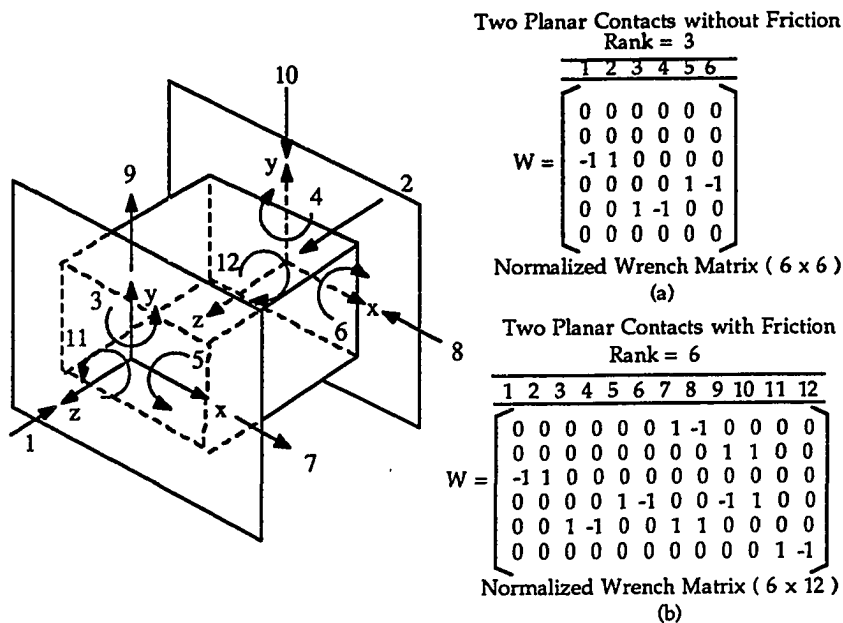


Figure 4.6: Contact wrenches for a rectangular part clamped in a vise with and without friction

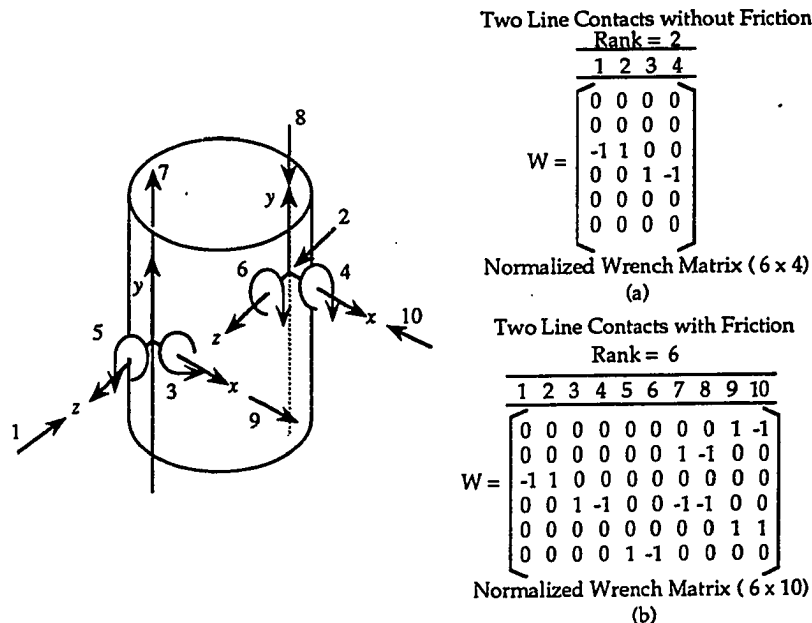


Figure 4.7: Contact wrenches for a cylindrical part clamped in a vise with and without friction. In reality this configuration is not recommended; a V-Block would be used for such parts.

For robotic grasping, this condition has been called “force-closure” [Nguyen 1988]. As Figures 4.6 and 4.7 show, a rectangular part and a cylindrical part clamped in a vise satisfy force-closure only if it is considered the additional contact wrenches due to friction between the vise jaws and the part. Of course, in this case we are relying on friction to keep the part from moving and would therefore have to proceed to the analysis of Chapter 5. A more conservative requirement would be to insist that a fixturing arrangement satisfy force closure even in the absence of friction. For example, a set of fixturing elements satisfying the 3-2-1 rule, as in Figure 4.3, will satisfy force-closure without friction as long as clamping elements are applied to keep the part pressed against the indexing elements. The concatenated matrix of wrenches for Figure 4.3 without friction is:

$$\mathbf{W}_n = \begin{bmatrix} 0 & 0 & 0 & -1 & -1 & -1 \\ 0 & 1 & 1 & 0 & 0 & 0 \\ 1 & 0 & 0 & 0 & 0 & 0 \\ 1 & -0.7 & -0.3 & 0 & 0 & 0 \\ -0.3 & 0 & 0 & -0.3 & -0.7 & -0.3 \\ 0 & 0.3 & 0.3 & 1.5 & 1 & 0.5 \end{bmatrix} \quad (4.9)$$

and $\text{Rank}(\mathbf{W}_n) = 6$. Where force-closure can be achieved without friction it is preferable. However, many commonly used fixturing arrangements, including the three pictured in Figure 5.1 from the fixture agent’s library, rely on friction. For such arrangements it is necessary to proceed to a force analysis with friction as described in the following chapter.

By satisfying the complete location and kinematic constraint, the fixture agent can provide a reliable locating and clamping. Also the kinematic analysis provides a space of possible motions to scan over that establish the framework for the force and friction analysis described in Chapter 5.

Chapter 5

Force analysis with friction

Once a fixturing arrangement has been found that is satisfactory from geometric and kinematic standpoints, it is necessary to determine suitable clamping forces. The force analysis begins by applying the equations of static equilibrium. However, since the fixturing arrangement is in general statically indeterminate, the equilibrium equations constrain the contact and friction forces, but do not uniquely determine them. The next step is to consider ways to determine when and how a clamped part may start to slip under the action of cutting forces and vibrations. This information is used to determine whether to increase clamping forces and/or modify the fixturing arrangement. This analysis builds upon recent work in robotics including grasp planning and the pushing of objects in a plane, as reviewed in Section 2.4.

5.1 Friction limit surfaces

Since the fixturing arrangement is statically indeterminate we cannot determine all the contact forces or pressure distributions without an elastic analysis. We therefore seek a force analysis that does not require knowledge of the pressure distributions over all contact surfaces, but which provides insight as to how and when a part might

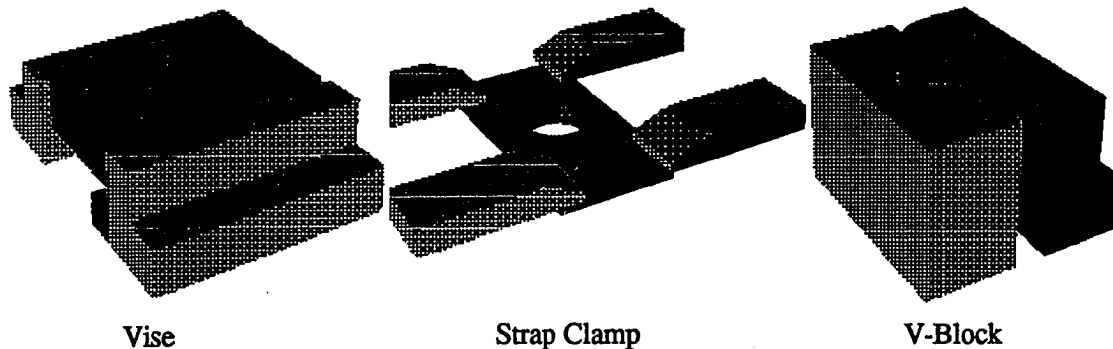


Figure 5.1: Examples of arrangements in the fixture library that require friction.

slip. This knowledge is useful for specifying clamping forces and/or adding extra fixturing elements to resist motion in the most vulnerable directions. In this analysis it is assumed that one can measure the forces applied by the active clamping elements and adjust them at will.

The friction analysis builds on recent work by Mason [1986], Peshkin [1986] and Goyal *et al.* [1991] on the sliding of objects pushed on a planar surface. The central idea is that once a part starts to slip, the instantaneous velocity and the resulting frictional force are uniquely related. By establishing a mapping between velocities and corresponding forces and moments, one can solve the inverse problem of determining how a part will slip in response to *applied* forces. The process of mapping between motions and forces results in a limit surface in force/moment space. Limit surfaces are convenient for planning, since any series of anticipated forces and moments can be tested against a limit surface. If the forces and moments fall inside the surface, the arrangement is “safe.”

5.1.1 The limit surface for a single contact point

As a starting point, consider a single point of contact against a face of a workpiece. For this special case, the limit surface will actually be a limit curve in force/moment

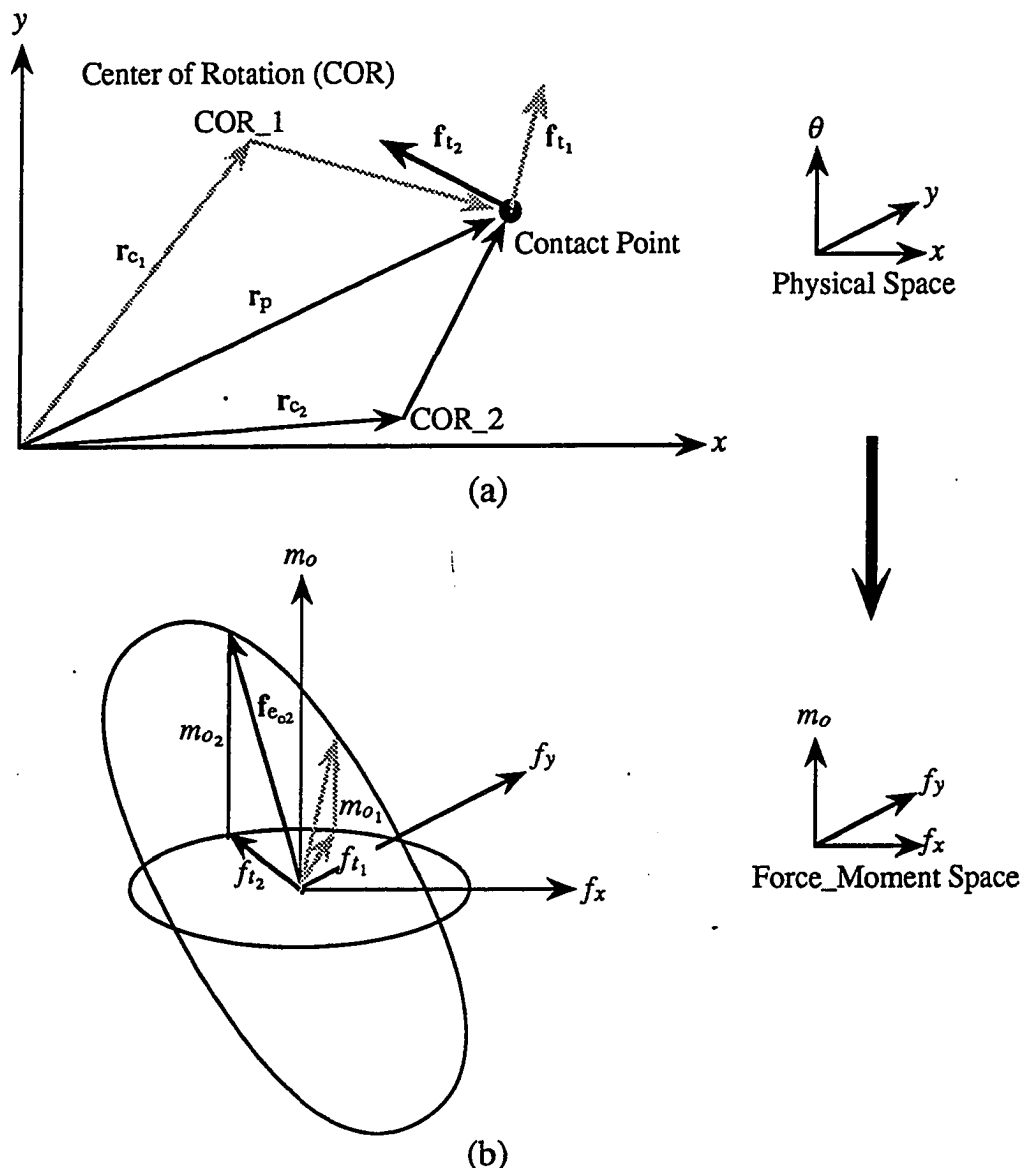


Figure 5.2: The limit surface of a single point contact becomes an ellipse.

space. Let a cartesian (x, y) coordinate system be embedded in the plane of the workpiece face. The contact point is located by a vector, \mathbf{r}_p , with respect to the origin, as shown in Figure 5.2(a). Until the part slips, the friction force is undefined; but as soon as it starts to move with a velocity $\mathbf{v} = [v_x, v_y]^T$, (corresponding to motion about an instantaneous center of rotation (COR) located at a point \mathbf{r}_c) the magnitude and direction of the friction force are known:

$$\mathbf{f}_t = [f_{tx}, f_{ty}]^T = \mu f_n \frac{-\mathbf{v}}{|\mathbf{v}|} \quad (5.1)$$

where $\mathbf{v} = \omega \times (\mathbf{r}_p - \mathbf{r}_c)$, $(\mathbf{r}_p - \mathbf{r}_c)$ is a vector from the COR to the contact, ω is the angular velocity with respect to the COR, μ is the Coulomb coefficient of friction and f_n is the magnitude of the normal force at a contact. The situation can be visualized by holding a pencil vertically against a tabletop. The force of the pencil pushing vertically upon the table is f_n and μ is the coefficient friction between the pencil and the table. Let \mathbf{f}_t be a force applied externally to the pencil, tangent to plane of the table (for example, the force that pushes the pencil along a sheet of paper). \mathbf{f}_t can be applied in any direction in the plane and as $|\mathbf{f}_t| \rightarrow \mu f_n$ the point of the pencil will slip in the corresponding direction, \mathbf{v} . Each direction of \mathbf{v} can be expressed as rotation about an instantaneous center of rotation (COR).¹

Associated with each force, \mathbf{f}_t , there is a moment taken with respect to the origin, m_o . Hence, the contact friction force, \mathbf{f}_t , is transformed to a resultant three-element force and moment vector at the origin: $\mathbf{f}_o = [f_{tx}, f_{ty}, m_o]^T$ (where $m_o = |\mathbf{r}_p \times \mathbf{f}_t|$ is the moment.) If one constructs the vector \mathbf{f}_o for every possible COR location, \mathbf{r}_c , and plots the results in three dimensional force/moment space, (f_{tx}, f_{ty}, m_o) , a limit curve shown in Figure 5.2 (b) is obtained. As Figure 5.2(b) shows, the projection of the limit surface forms a circle in the (f_x, f_y) plane corresponding to the constant magnitude of \mathbf{f}_t (as shown in equation 5.1). In the three dimensional (f_{tx}, f_{ty}, m_o)

¹In this point contact example the mapping from COR location to direction of motion, $\frac{\mathbf{v}}{|\mathbf{v}|}$, is not one to one since the COR can be anywhere along a line passing through the contact point and perpendicular to \mathbf{v} . For a finite area of contact, however, there will be a unique COR for each combination of $\frac{\mathbf{v}}{|\mathbf{v}|}$ and angular velocity, ω , of the contact area.

space, the curve becomes an ellipse² [Goyal *et al.* 1991]. The moment is largest when the center of rotation is on a line containing \mathbf{r}_p , and there is a singularity ($|\mathbf{f}_t|$ is undefined) when the COR is directly beneath the contact point (i.e., $\mathbf{r}_p = \mathbf{r}_c$).

Figure 5.2 also indicates how to use the limit curve to solve the inverse problem of predicting the slipping motion for an applied force. First, note that if the magnitude of a force applied to the contact, $|\mathbf{f}_e|$, is smaller than $|\mathbf{f}_t|$, the part will not slip. If one takes the resultant force and moment vector at the origin, $\mathbf{f}_{eo} = [f_{ex}, f_{ey}, m_o]^T$, and plots it in force and moment space, it can be seen that \mathbf{f}_{eo} lies in the plane of the ellipse. As $|\mathbf{f}_e| \rightarrow |\mathbf{f}_t|$, \mathbf{f}_{eo} will intersect the limit curve as the contact starts to slide in the direction of \mathbf{f}_e . Finally, if $|\mathbf{f}_e| > |\mathbf{f}_t|$, quasistatic equilibrium will not be satisfied and the contact will not only slip but will accelerate.

5.1.2 Limit surfaces for multiple points of contact

The 5.1.2 Limit surfaces for multiple points of contact_{tacts}. For two or more contact points, the limit surface encloses a volume of “safe” forces and moments that can be applied without slipping. Goyal *et al.* [1991] shows that the limit surface for a combination of contact points can be constructed as the Minkowski sum³ of the ellipses for each contact. He also shows that the unit normal where an applied force/moment vector, \mathbf{f}_{eo} , intersects the surface, gives the direction of slipping motion.

The limit surface can also be constructed for multiple contacts simply by scanning the COR over all points in the plane and plotting the resultant force and moment vectors. For example, the limit surface for a tripod of contact points, obtained by scanning the COR over the (x, y) plane, is shown in Figure 5.3. In this case, the

²Let a cartesian (X, Y) coordinate system be aligned with the plane of the limit curve in (f_x, f_y, m_o) space. The limit curve equation can then be expressed as $(\frac{X}{\mu f_n})^2 + (\frac{Y}{\mu f_n \sqrt{1+r_p^2}})^2 = 1$ where $r_p = |\mathbf{r}_p|$.

³The Minkowski sum, \oplus , is a natural generalization of vector addition. However, \oplus and scalar multiplication do not follow all the usual laws of vector space operations. Details properties and algebraic operations are shown in [Serra 1982].

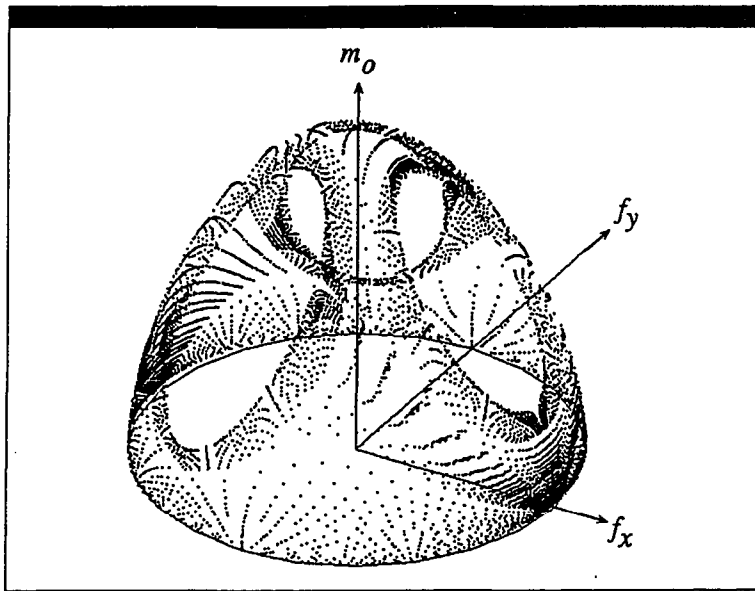


Figure 5.3: Friction limit surface of three supporting points, obtained by scanning the COR over the (x, y) plane. The limit surface encloses “safe” forces and moments that will not produce slipping.

limit surface encloses an approximately ellipsoidal volume with three facets. The facets correspond to singularities where the COR is directly under one of the three contact points. For larger numbers of contact points the facets shrink in size, and for continuous pressure distributions they vanish. For a continuous pressure distribution, the resultant friction force, \mathbf{f}_t , and moment, \mathbf{m}_o , are

$$\mathbf{f}_t = \int_A \mu \frac{\mathbf{v}_p}{|\mathbf{v}_p|} p(\mathbf{r}_p) dA \quad (5.2)$$

$$\mathbf{m}_o = \left| \int_A \mathbf{r}_p \times \mu \frac{\mathbf{v}_p}{|\mathbf{v}_p|} p(\mathbf{r}_p) dA \right| \quad (5.3)$$

where $p(\mathbf{r}_p)$ is the pressure at location \mathbf{r}_p within the contact area, A , $\mathbf{v}_p = \omega \times (\mathbf{r}_p - \mathbf{r}_c)$, and \mathbf{r}_c is the location of the COR.

In investigating the motion of an object pushed in a plane, Mason [1986] points out that a tripod of contact points is particularly useful since any pressure distribution that satisfies the equilibrium equations for stability with respect to the plane can be

approximated by a tripod with the same centroid:

$$[X] \cdot \mathbf{f} = f_n \begin{bmatrix} x_o \\ y_o \\ 1 \end{bmatrix} \quad (5.4)$$

where \mathbf{f} is a vector of the supporting forces, $[x_o, y_o]^T$ is the centroid location, $[X] = \begin{bmatrix} x_1 & x_2 & x_3 \\ y_1 & y_2 & y_3 \\ 1 & 1 & 1 \end{bmatrix}$ gives the locations of the contacts and f_n is the normal force (typically mg , a gravitational force.) If the locations of the contact points are fixed, then the magnitudes of the normal forces at each point are uniquely determined by equation (5.4). Therefore, a reasonable approximation would be to find a tripod that produces a limit surface nearly identical to the limit surface of the actual pressure distribution. But since the actual pressure distribution is unknown, there are many feasible approximating tripods corresponding to different locations of the contact points within the contact area. Mason [1986] and Peshkin [1986] therefore define loci of centers of rotation corresponding to the set of all possible tripods that satisfy equation (5.4) and lie within the contact area. The result is that while the exact motion of the sliding object cannot be predicted for an applied force and moment, bounds on the motion can be established.

5.1.3 Symmetry of the limit surface

For a single point of contact it is clear that the friction force is always antiparallel⁴ to the direction of sliding motion, as shown in Figure 5.2. By extension, it might seem for a sliding body with an area of contact, that the friction force in the contact plane, \mathbf{f}_t , must always be antiparallel to the sliding velocity, \mathbf{v} . However, if that were the case then the limit surface for any contact area and pressure distribution would always have circular cross-sections taken parallel to the (f_x, f_y) plane. This is because the direction of sliding motion is given by the unit normal, \mathbf{n} , to the limit surface

⁴Definition: \mathbf{v} and \mathbf{f} are *antiparallel* if and only if $\frac{\mathbf{v}}{|\mathbf{v}|} \cdot \frac{\mathbf{f}}{|\mathbf{f}|} = -1$.

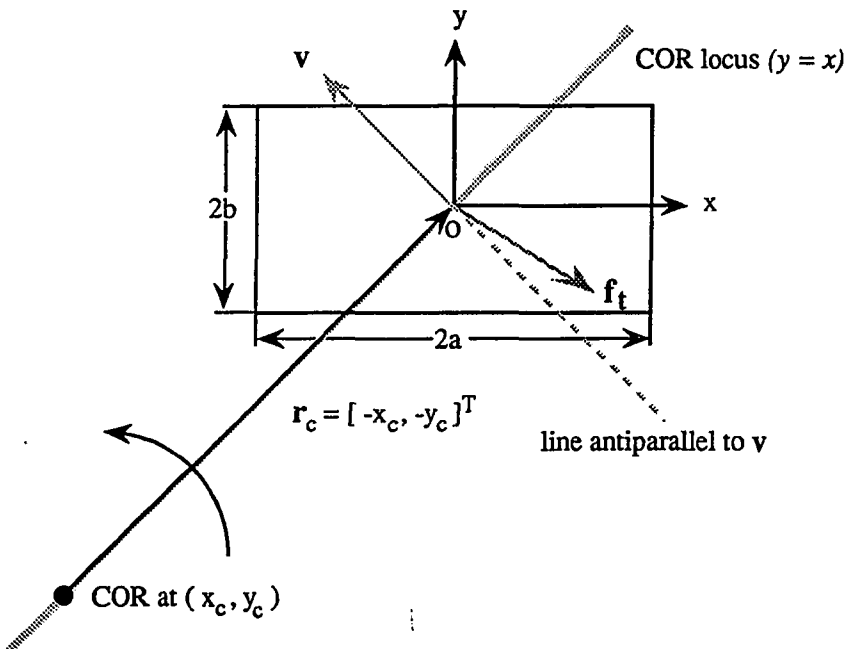


Figure 5.4: When the COR is not on a line of symmetry passing through the center of pressure, the friction force, f_t is not antiparallel to the direction of motion, $\frac{v}{|v|}$.

[Goyal *et al.* 1991]. Therefore, a necessary condition for the tangential sliding force to be antiparallel to the sliding velocity is that the projection of n on the (f_x, f_y) plane must always be parallel to f_t . Clearly, this will only be true if the limit surface is axisymmetric. Instead, as will be seen in this section, the only cases under which the tangential friction force is necessarily antiparallel to the tangential sliding velocity are: (i) when the sliding body is undergoing a pure translation (COR at infinity); and, (ii) when the COR is on a line of symmetry of the region passing through the centroid of the contact area. These cases are, however, of practical interest since they permit considerable time savings in computing the limit surface when they apply.

Let us begin by considering a rectangular region of uniform pressure, as shown in Figure 5.4. The rectangle has a width, $2a$ and a height, $2b$. As in the previous sections, we will place the origin at the center of pressure, which in this case is the center of the rectangle. The COR is at an arbitrary location on the (x, y) plane,

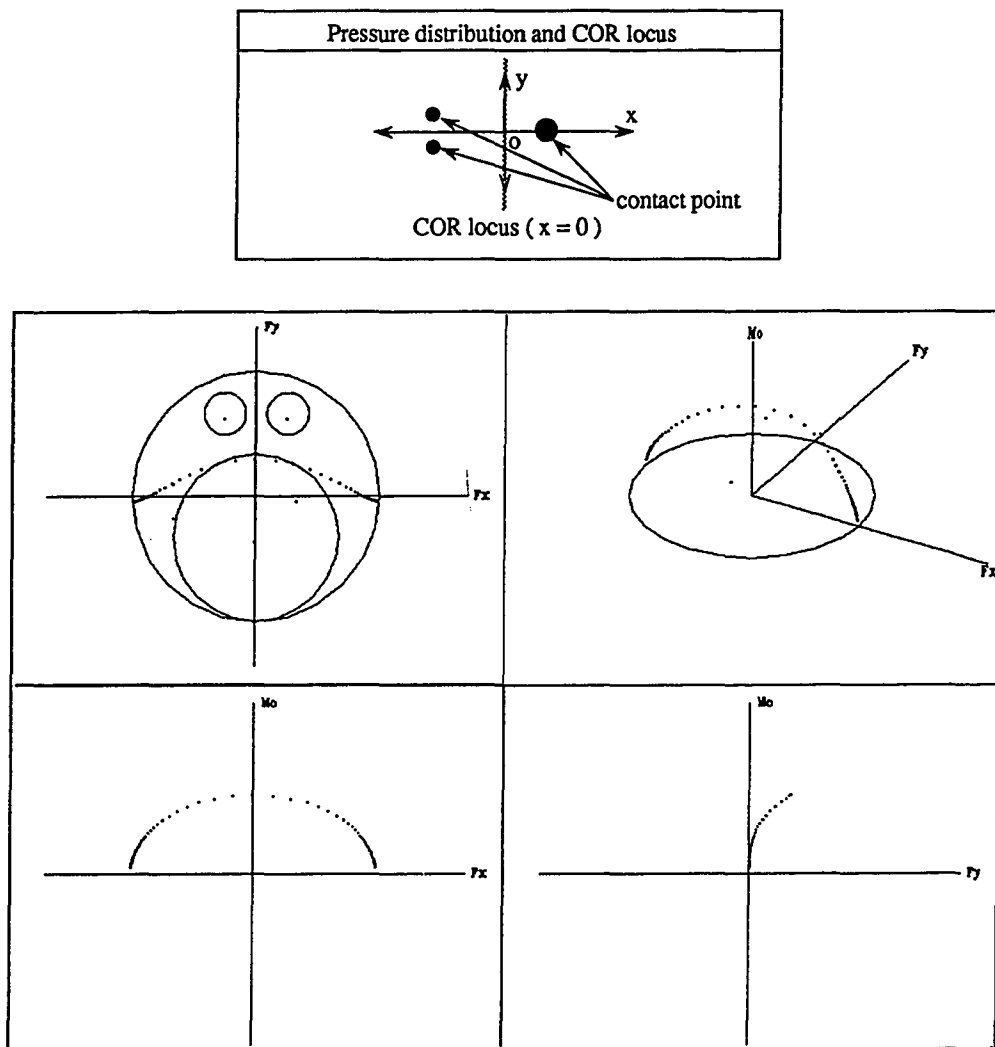


Figure 5.5: If the COR locations are scanned along the y axis, the resulting curve on the limit surface is not a planar curve, because the y axis is not a line of symmetry for the tripod pressure distribution.

located by a vector, $\mathbf{r}_c = [-x_c, -y_c]^T$ with respect to the origin.

- The friction force, \mathbf{f}_t , can be found by integrating equation (5.2). The result is given in Appendix C. For \mathbf{f}_t to be antiparallel to \mathbf{v} , we require that

$$\frac{y_c}{x_c} \cdot \frac{f_{t_y}}{f_{t_x}} = -1 \quad (5.5)$$

which, as the result in Appendix C shows, is generally not true. However, equation (5.5) *will* be satisfied if the COR is on a line of symmetry passing through the center of pressure. The possible cases are: $x_c = 0; y_c = 0$. Similarly, for the case of a square pressure area ($a = b$) it can be shown that the cases $x_c = y_c$ and $x_c = -y_c$ will additionally cause equation (5.5) to be satisfied, since the areas to left and right of these diagonal lines are mirror images in the case of a square.

An interesting result of equation (5.2), and its relationship to the COR location and the direction of \mathbf{v} , is that the limit surface will have the same degree of symmetry as the pressure distribution. Thus, a limit surface for a rectangular pressure area has two symmetric cross sections when viewed from above; the limit surface for a square has four; and the limit surface for an axisymmetric pressure distribution is axisymmetric because any line through the center of pressure will divide the circular region into two mirror images. Jameson [1985] essentially plots the cross-section of an axisymmetric limit surface when he plots his “contact stability region” for a spherical soft fingertip with a Hertzian contact pressure.

Another way to view the same result is to scan COR locations along a line that is not a line of symmetry for the pressure distribution, and to trace the corresponding locus of points on the limit surface. For example, consider Figure 5.5, which concerns the cross-sections of the limit surface for a pressure distribution consisting of three supporting points. If the COR locations are scanned along the line, $x = 0$, the resulting locus of points on the limit surface does not form a planar curve, but instead warps out of the (f_x, m_o) plane. Also, as expected, the limit surface has one axis of symmetry (about f_y) corresponding to the symmetry of the pressure distribution

about the x axis.

5.2 Applying limit surfaces to fixturing

5.2.1 Two-dimensional procedure and example

Now consider a simple example to explore how limit surfaces can be used for analyzing fixtures with friction. Figure 5.6 shows a rectangular block held in a vise which, in keeping with the kinematic principles of Chapter 4, has a ball joint on the movable jaw.

The part was located using a parallel bar, but the bar has been removed during machining to avoid possible interference with the tool. The cutting forces are expressed by a 6-element force/moment vector, $[f_e^T, m_e^T]$, which produces a resultant vector, $[f_{eo}^T, m_{eo}^T] = [J]^T [f_e^T, m_e^T]$ at the origin, where $[J]$ is a 6x6 cartesian transformation matrix [Craig 1989]. The clamping force, $f_c = [0, f_c, 0]^T$, produces an (unknown) pressure distribution over the two vise jaws. For equilibrium,

$$f_c = \int_A p(\mathbf{r}_p) dA \quad (5.6)$$

$$m_{fo} = \left| \int_A \mathbf{r}_p \times \mu \frac{\mathbf{v}_p}{|\mathbf{v}_p|} p(\mathbf{r}_p) dA \right| \quad (5.7)$$

where m_{fo} ⁵ is a frictional moment with respect to the origin and $\mathbf{r}_p = [x, y, z]^T$ is a vector from the origin on a contact face to an element of the contact area. It will be assumed that f_c is also known, perhaps because the vise is instrumented with strain gages. Also, since one of the vise jaws is pivoted, the center of pressure is at the center of the face (in line with the ball joint.)

⁵In most cases, the moment integral cannot be solved in closed form. Even for a constant uniform pressure for a ring/disk contact, it is expressed as complete elliptic integrals of the first and second kind [Goyal *et al.* 1991].

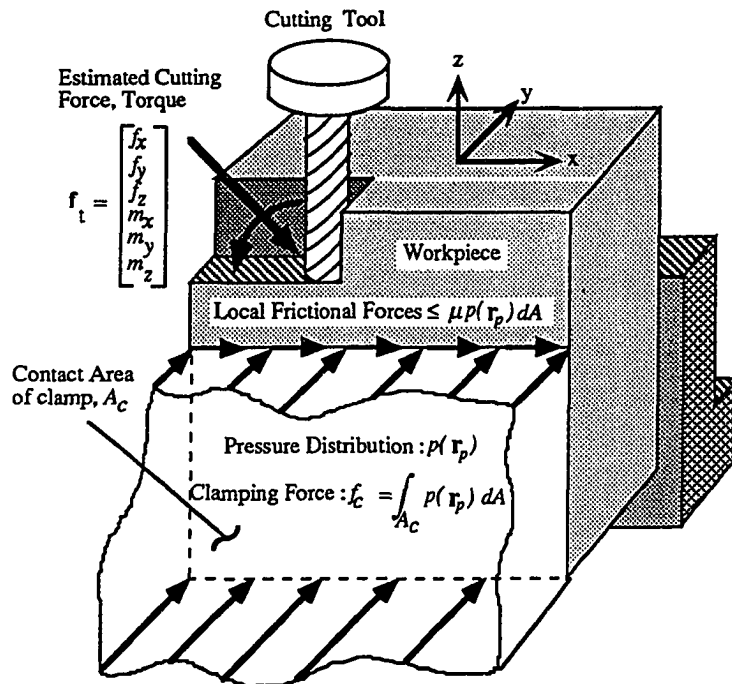


Figure 5.6: A rectangular block is held in a vise. The details of the pressure distribution are not known and depend on the location of the cutting tool and the cutting conditions.

It is necessary to clamp hard enough to prevent slipping, but not excessively hard. Now suppose that the pressure on the front face is primarily confined to three contact areas (perhaps due to a lack of flatness in the part) as indicated in Figure 5.8. In this case we could immediately construct a limit surface as in Figure 5.3.

However, it is too time consuming to construct such surfaces numerically for on-line fixture planning. For example, it took 5 CPU minutes on a 68020-based workstation to compute the limit surface in Figure 5.3 by scanning the COR location over the plane and approximately 2 CPU minutes to achieve a comparable resolution by the Minkowski sum method. The computational time for the COR scanning method increases as the product of the number of contact points and the number of COR locations. The computation time for the Minkowski sum method grows more rapidly. For n points of contact and a resolution of m points on the ellipse (see Figure 5.2) associated with each point, the computations grow as $(m + 1)^n$.

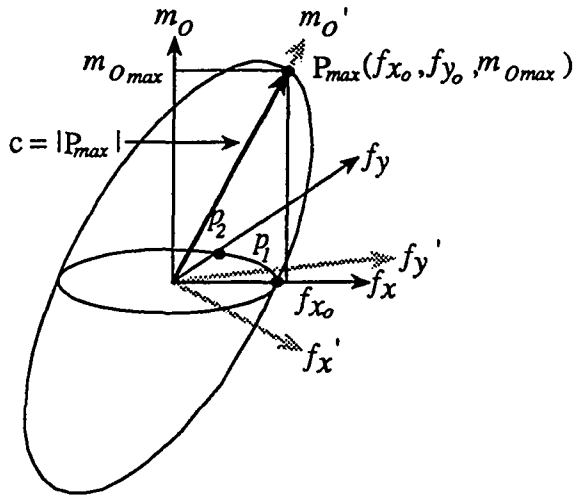


Figure 5.7: An approximating ellipsoid can be found for a fast, approximate method for determining a limit surface for arbitrary pressure distribution. Maximum moment point, $P_{max} = (f_{x_o}, f_{y_o}, m_{o_{max}})$ is obtained when COR is at the origin. Also p_1 and p_2 can be found, where the circle in the (f_x, f_y) plane intersects the f_x and f_y .

Fortunately, considerable time savings can often be achieved. For example, when using the scanning method, a non-uniform spacing in which COR locations are scanned slowly in the vicinity of supporting points and more rapidly elsewhere, gives good results. In addition, as seen from Section 5.1.3, for approximately symmetric pressure distributions, the COR need only be scanned along a few lines that pass through the origin, to obtain some representative projections on planar cross-sections. Similarly, for the Minkowski sum method, only the projections on a few sub-spaces are typically necessary. Nonetheless, it takes 15 CPU minutes on the same workstation to compute a limit surface comparable to that shown in Figure 5.3 for eight supporting points. Thus, there is a motivation to find a fast, approximate method for determining the limit surface for arbitrary pressure distributions.

Such an approach is to fit an approximating ellipsoid to the data. Since the ellipsoid has an analytic form, it can be rapidly determined whether the expected cutting forces and moments will be contained within it. In constructing the ellipsoid we first recall that the limit surface for any pressure distribution forms a circle on the (f_x, f_y)

plane. In addition, we know that the maximum moment will occur for the case where the COR is at the origin (which, in this case, is also the center of pressure). Using these constraints, an approximating ellipsoid is found as follows:

1. Find the point of maximum moment, $\mathbf{p}_{max} = (f_{x_o}, f_{y_o}, m_{o_{max}})$, (where the COR is at the origin) and plot it in (f_x, f_y, m_o) space. This defines the end points, and the tilt angles with respect to the f_x axis and f_y axis of the major axis of the ellipsoid. Let $c = |\mathbf{p}_{max}|$.
2. Find the (3×3) orthonormal transformation matrix, R , between the original (f_x, f_y, m_o) coordinate system and a new (f'_x, f'_y, m'_o) frame aligned with the major axis of the ellipsoid.
3. Find the points p_1, p_2 where the circle in the (f_x, f_y) plane intersects the f_x and f_y axes and express them in the (f'_x, f'_y, m'_o) frame as p'_1, p'_2 .
4. Solve for the ellipsoid (unknowns are a and b) that contains \mathbf{p}_{max} as its end point and includes the points p'_1, p'_2 :

$$\left(\frac{p'_{1x}}{a}\right)^2 + \left(\frac{p'_{1y}}{b}\right)^2 + \left(\frac{p'_{1z}}{c}\right)^2 = 1 \quad (5.8)$$

$$\left(\frac{p'_{2x}}{a}\right)^2 + \left(\frac{p'_{2y}}{b}\right)^2 + \left(\frac{p'_{2z}}{c}\right)^2 = 1 \quad (5.9)$$

where c is given by step 1.

For continuous pressure distributions, or pressure distributions with many contacts, the facets on the limit surface can be ignored. But for pressure distributions with just a few, concentrated pressure regions (e.g., clamping a thin piece of metal with two or three strap clamps), the volumes corresponding to the facets should be removed. This is accomplished by constructing planes corresponding to the facets:

$$\left(\left(\frac{x}{a}\right)^2 + \left(\frac{y}{b}\right)^2 + \left(\frac{z}{c}\right)^2 - 1 \right) \prod_{i=1}^{2n} (\mathbf{p}_i \cdot \mathbf{n}_i - d_i) < 0 \quad (5.10)$$

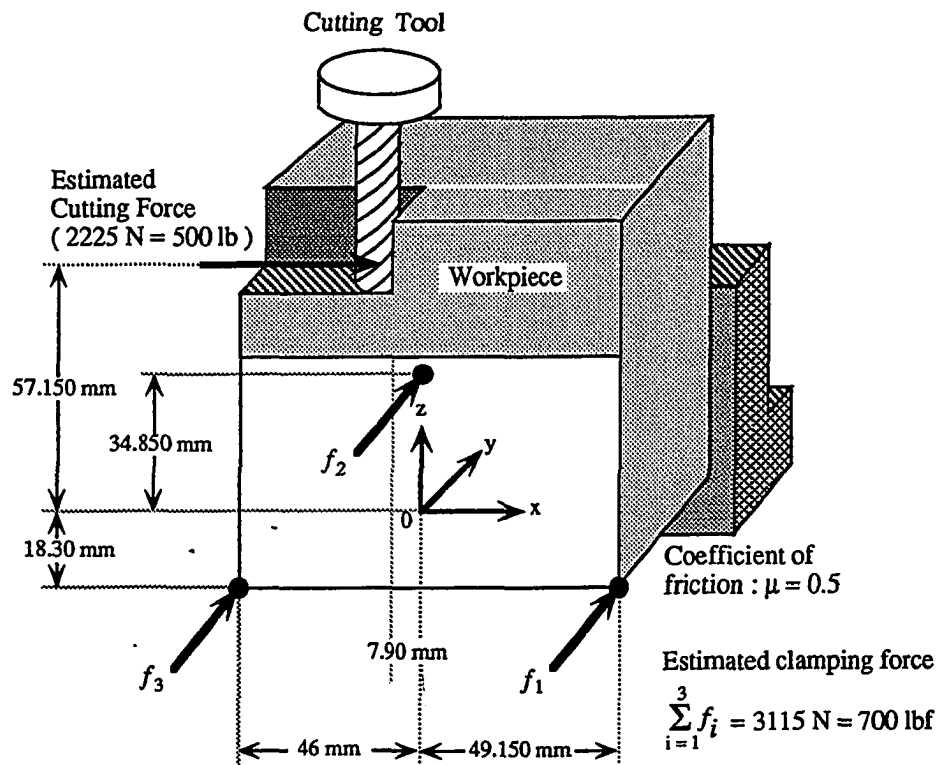


Figure 5.8: A rectangular block is held in a vise with a pressure distribution that is approximated by a tripod of forces that satisfies the same equilibrium conditions.

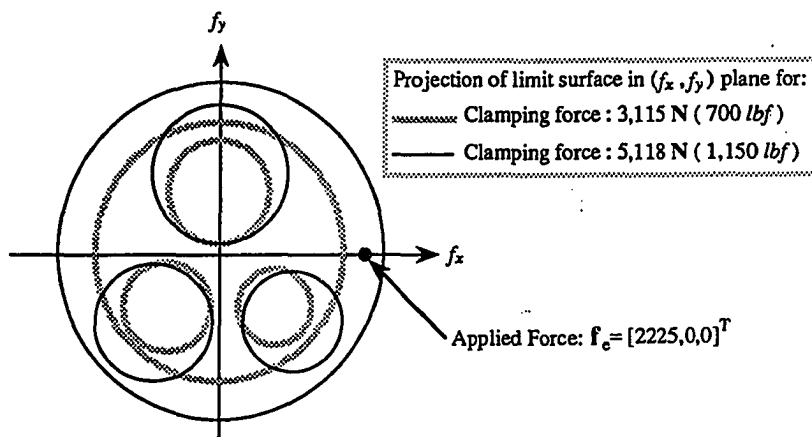


Figure 5.9: Projection of the limit surface in the (f_x, f_y) plane. If the clamping force is increased to $5,118\text{N}$ ($1,150\text{lbf}$), the cutting force no longer produces slipping.

where p_i , n_i and d_i represent a point on the facet, a normal vector on the facet and a distance from the origin to the facet respectively.

Returning to the example of Figure 5.6, let us assume that the cutting force is entirely in the (x, z) plane where $m_e = [0, 0, 0]^T$ and $f_e = [2225N, 0, 0]^T$. The coefficient of friction is assumed to be 0.5. The magnitudes of the contact forces, $\mathbf{f} = [f_1, f_2, f_3]^T$ (see Figure 5.8), are determined from equation (5.4):

$$\begin{bmatrix} 49.15mm & 0 & -46mm \\ -18.30mm & 34.85mm & -18.30mm \\ 1 & 1 & 1 \end{bmatrix} \cdot \mathbf{f} = \begin{bmatrix} 0 \\ 0 \\ 3,115N \end{bmatrix}. \quad (5.11)$$

As shown in Figure 5.9, the resultant force vector, $[f_{eo}^T, m_{eo}^T]$, is outside the limit surface and the part will slip. However, if we increase the clamping force to 5,118N (1,150lbf), the limit surface expands and the cutting force will no longer produce slipping.

5.2.2 Three-dimensional procedure and example

Although some fixturing problems are essentially planar (e.g., a block held in a vise or a plate held down with strap clamps), others require a three-dimensional treatment. To address such problems, it is necessary to extend the planar sliding analysis to include rigid bodies with up to five degrees of freedom⁶. As in the planar case, the limit surface represents a mapping between possible motions of the sliding body and corresponding forces and moments taken with respect to some reference frame. Also as in the planar case, the limit surface can be numerically generated by scanning over the space of all possible directions of motion and plotting the corresponding force/torque vectors. However, we now have six-element force/torque vectors that must be plotted in a six-dimensional force/torque space. While the resulting limit surfaces lack the intuitive appeal of the surfaces for planar problems, three-dimensional projections of the limit surfaces can be plotted on subspaces (e.g., m_x, m_y, f_z) for visualization.

⁶A part can have up to five degrees of freedom in sliding without breaking contact.

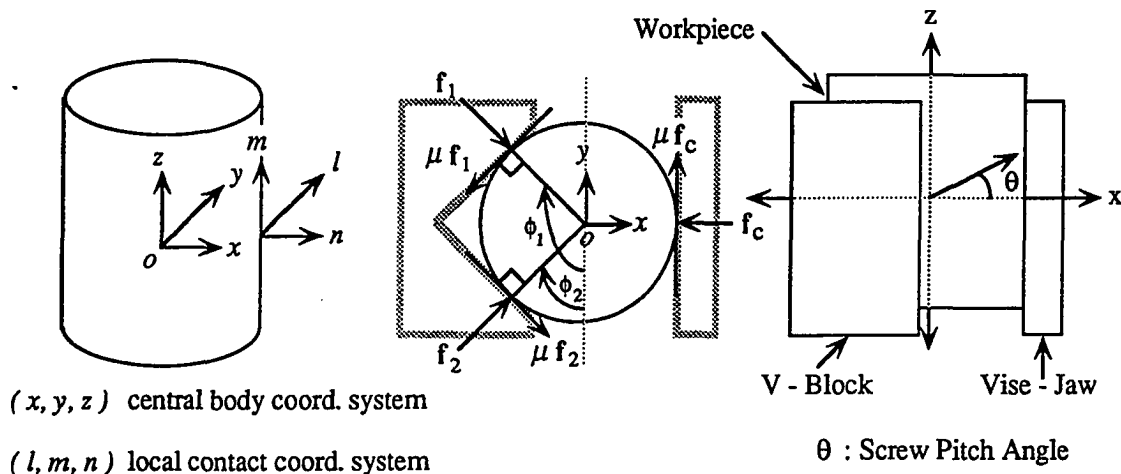


Figure 5.10: A cylinder is held between a V-block and a plate with 3 line contacts. The ratio of translation to rotation about Z can be expressed by a screw angle θ .

A potential drawback is that scanning over the space of all possible motions could be very time consuming. Fortunately, most fixture arrangements only have two or three degrees of freedom for sliding. This is basically a result of the need to locate and constrain the workpiece. A fixture arrangement with more than three degrees of freedom for possible sliding motions is unlikely to satisfy the force-closure requirements of Chapter 4 and would not locate the part adequately. Therefore, it is useful to apply the kinematic constraints of Chapter 4 *before* scanning over the space of possible sliding motions. The kinematic constraints produce a limit surface with non-zero projections on only a few subspaces.

Taking these issues into consideration, an approach to treating three-dimensional problems is as follows:

1. Determine the contact types and the sliding degrees of freedom (i.e., the instantaneous motions for which the contact types remain unchanged) by taking the logical intersection of components of contact twists, as in Section 4.1.

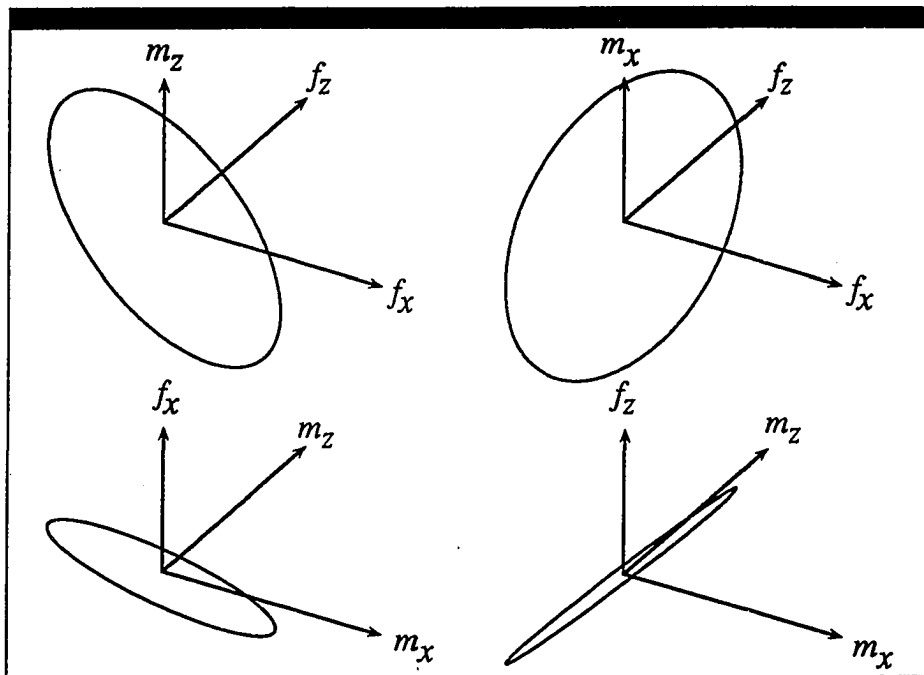


Figure 5.11: Projections of the limit surface for the first line contact, for which the l and n axes happen to be aligned with the x and y axes, expressed in the workpiece coordinate frame.

2. Find the limit surface, expressed in the contact coordinate frame, for each contact subject to the kinematic constraints from Step 1. These limit surfaces will typically be quite simple; perhaps just a circle or an ellipse in the tangent plane of the contact.
3. Transform the limit surface of each contact to a limit surface expressed in the central coordinate system of the workpiece. As the limit surfaces are transformed to the workpiece coordinates, they typically become more complex as extra torques are picked up due to the contact forces acting at some distance from the central axes. However, only projections of the limit surface on those subspaces in which motion is possible need be considered.
4. Take the Minkowski sum of the limit surfaces from Step 3 to obtain the surface for the entire arrangement. Again, it is only necessary to consider projections on the subspaces for which sliding motion is possible.

5. Test expected cutting forces and torques, expressed in the workpiece coordinate system, against the limit surface to determine whether the part will slip, and if so, in what direction it will move.

The approach can be illustrated by the case of a cylinder held between a flat plate and a V-block. Although this is a simple example, and the final result is perhaps obvious from symmetry, it is three-dimensional and will be solved as a general three-dimensional problem.

Example: Solving for the limit surface of a cylinder in a V-block as a 3D problem

Figure 5.10 shows a cylindrical workpiece clamped between a flat plate and a V-block. The arrangement results in three line contacts and, as we can see from Figure 4.7, it kinematically constrains the cylinder so that the only possible sliding motions are translations along the z axis and rotations about the z axis. In fact, all motions of the cylinder can be represented by a screw axis along the centerline of the cylinder and a finite pitch angle, θ , corresponding to a ratio of translation to rotation as shown in Figure 5.10. Therefore, we expect that the limit surface for this arrangement will have a non-zero projection only on the (f_z, m_z) plane. The first step is to apply the kinematic constraints to determine the vector space of possible motions, expressed in the local (l, m, n) coordinate system of each contact. The n axes are normal to the surface of the cylinder, the l axes are tangent to the surface of the cylinder and the m axes are aligned with the centerline of the cylinder, as in Figure 5.10. In this example, only translations along the l and m axes are possible for each line contact. The limit surface for each contact is therefore simply a circle in the (f_l, f_m) plane. (If the contact friction were anisotropic, perhaps due to fine grooves on the surface of the cylinder, the local limit surfaces could be expressed as ellipses.)

Transforming the local, circular limit surfaces to the (x, y, z) coordinate system of the cylinder results in more complicated surfaces, with torque components. The simplest of these is for the first contact, for which the l and n axes happen to be

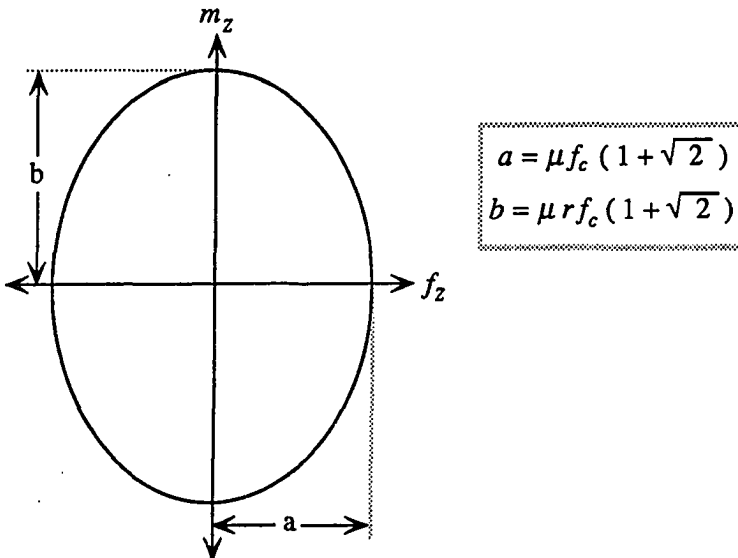


Figure 5.12: The final limit surface for a cylinder held in a V-block becomes an ellipse.

aligned with the x and y axes, respectively, so that a four-dimensional limit surface (f_x, f_z, m_x, m_z) results. The projections of the resulting limit surface on four three-dimensional sub-spaces $((f_x, f_z, m_z), (f_x, f_z, m_x), (f_x, m_x, m_z)$ and $(f_z, m_x, m_z))$ are shown in Figure 5.11. Not surprisingly, they are ellipses since the moments all vary as $r \times f$. The final step is to sum the limit surfaces, expressed with respect to the (x, y, z) coordinate system, for the three line contacts. Only the projections on the f_z and m_z plane need be considered since motions are possible only along and about the z axis. All other sliding forces and moments will cancel. As expected, the final result is an ellipse, as shown in Figure 5.12. The length of the major axis of the ellipse for a 90° V-block, as shown in Figure 5.10 ($\phi_1 = 135^\circ$ and $\phi_2 = 45^\circ$), for example, is $b = \mu f_c r (1 + \sqrt{2})$ and the minor axis is $a = \mu f_c (1 + \sqrt{2})$ where r is the radius of the cylinder and f_c is the clamping force. Derivations of a and b are given in Appendix A.2.

5.3 Discussion of limit surface accuracy

Once constructed, the limit surface for a two- or three-dimensional fixture arrangement can be compared against all anticipated forces to test for slipping. However, a number of practical issues remain to be solved before the method can be used in on-line fixture planning. The most important of these is that neither the pressure distributions nor the cutting forces are exactly known. Therefore, a conservative lower-bound on the limit surface is required that will apply to all feasible pressure distributions, and against which the expected cutting forces can be tested with some factor of safety. As it happens, many different pressure distributions have similar limit surfaces. For example, Figure 5.13 shows the limit surfaces for several tripods and for a uniform pressure distribution, all of which satisfy the same equilibrium conditions and have the same center of pressure as the tripod for the block held in a vise in the example of Section 5.2.1. Therefore, they could all theoretically have been applied to the same example. The intersection of all the limit surfaces in Figure 5.13 with the (f_x, f_y) plane is a circle of radius $f_t = \mu \sum f_{n_i}$, where $\mu \sum f_{n_i} = 3,115\text{N}$ (700lbf .) (For case (f), $f_t = \mu \int_A p(r)dA$, where $\int_A p(r)dA = 3,115\text{N}$.) However, the ability of the different contact arrangements to resist moments in the plane depends strongly on the spacing between the points. When the points are close together, as in case (b), the limit surface is very squat. Also note that an asymmetrical arrangement of the contact points results in a correspondingly skewed limit surface, whereas a symmetric arrangement gives a symmetric surface. In the extreme case where two of the contact points are nearly coincident as in case (c), the tripod limit surface approaches that of a dipod. Furthermore note that the case of a uniform pressure distribution is more conservative than case (a) since the maximum frictional moment is proportional to the first polar moment of the pressure distribution.

More importantly, it is evident that a variety of contact positions produce similar limit surfaces. In fact, if one is able to rule out cases such as (b) and (d) in Figure 5.13, one can construct a conservative limit surface that will handle all expected cases as shown in Appendix D. For example, Figure 5.14 shows a lower-bound on the limit

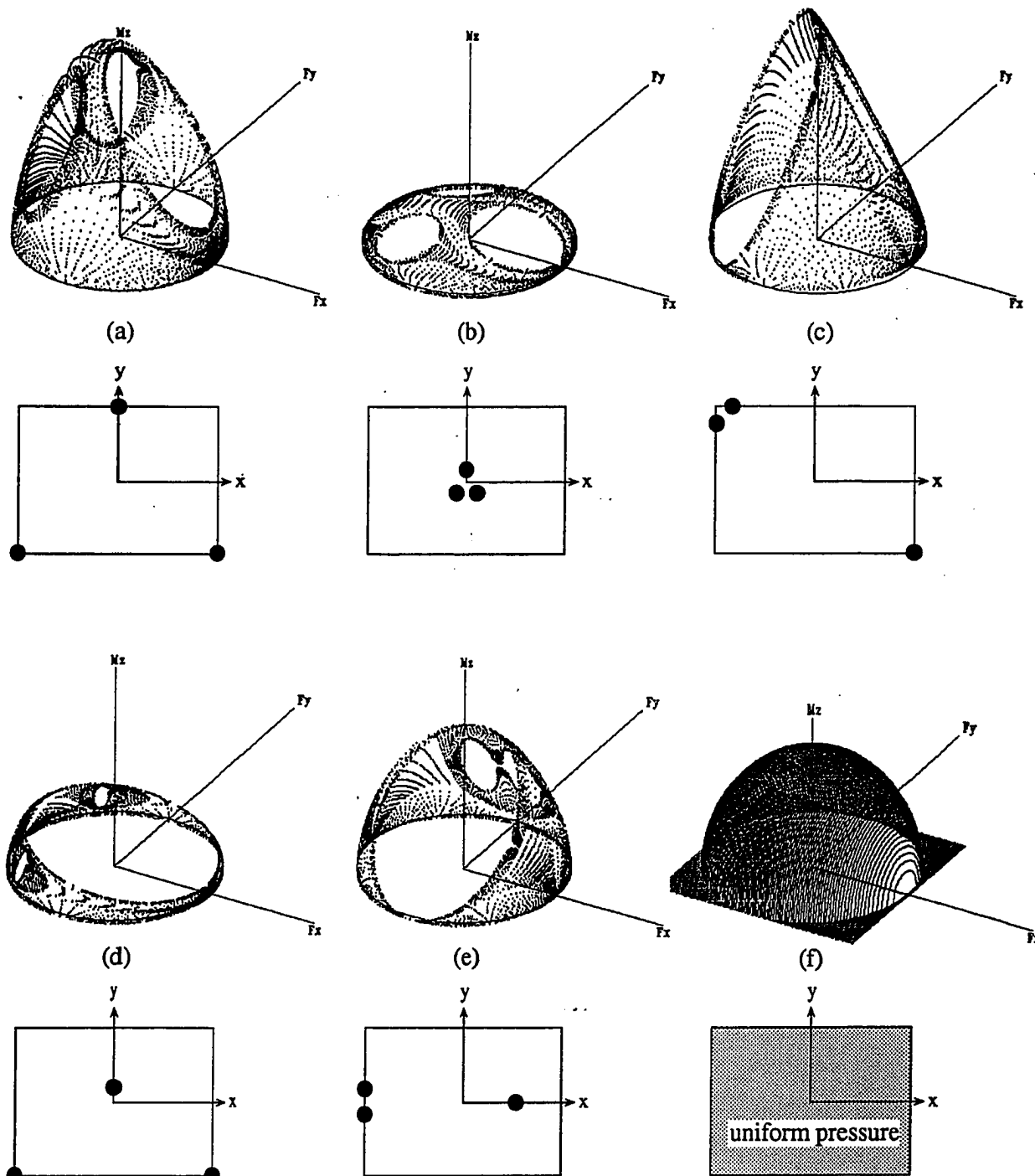


Figure 5.13: Different friction limit surfaces produced by different contact assumptions that satisfy the same equilibrium equations.

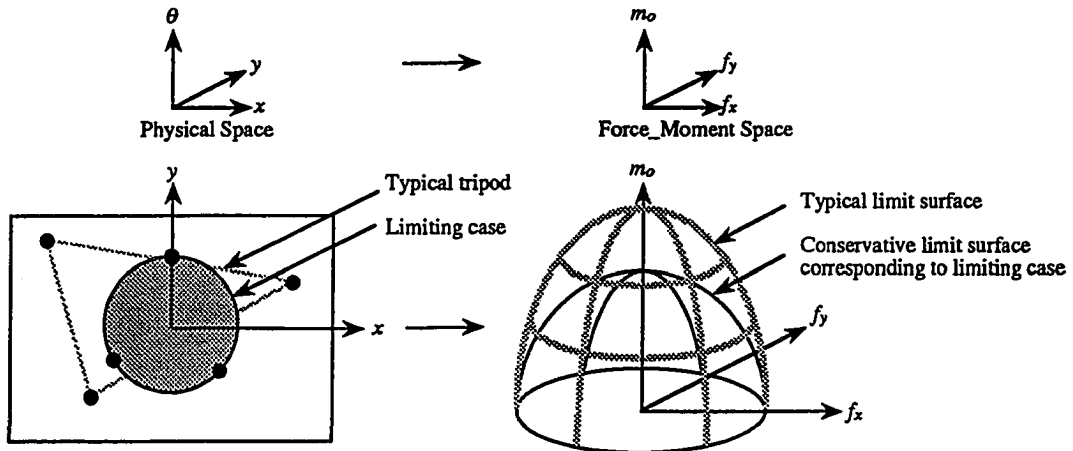


Figure 5.14: A conservative lower bound on the limit surface for all possible pressure distributions known to lie primarily outside a central region

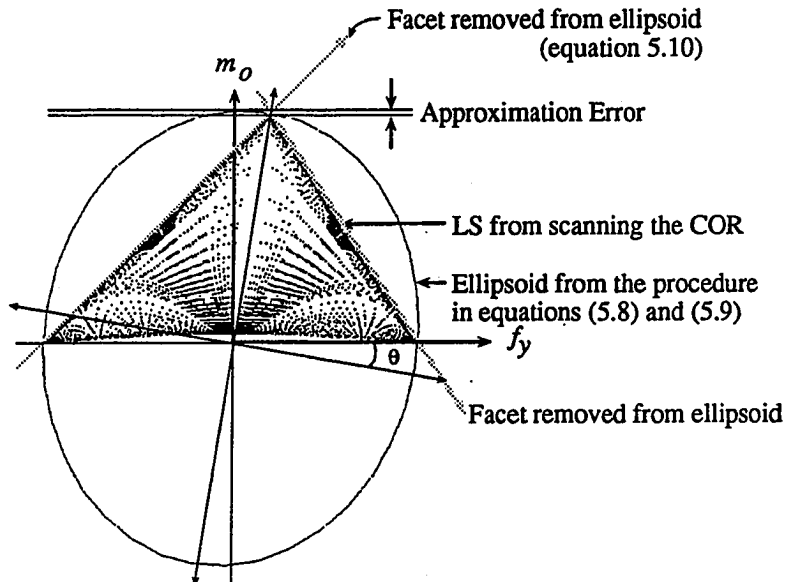


Figure 5.15: The ellipsoid has an approximation error depending on the angle of inclination, $\theta = \tan^{-1} \frac{f_{y_{\text{vertex}}}}{m_{o_{\text{max}}}}$ (shown for the case of two strap clamps.)

surface for all cases where all of the contact points are known to lie outside some central region. If a finite-element analysis were performed on the clamped part (e.g., following the approach in [Lee and Haynes 1987]), then the exact pressure distribution over the clamping surface could be obtained and the exact limit surface computed. However, for concurrent design it may be desirable to obtain a rough estimate of the friction limits when a finite-element analysis is impractical, either for reasons of speed or because the design is still in an early stage. In this case it is necessary to determine, perhaps using knowledge about the flatness of the clamped part, what the *approximate* pressure distribution is. Failing this, one might establish a space of "reasonable" pressure distributions and then compute the innermost limit surface, corresponding to the worst-case pressure distribution in that space. Unfortunately, it is not easy to find a conservative pressure distribution which represents a provable worst-case. For example, the worst-case pressure distribution in Figure 5.13 is case (b), corresponding to a plate that is warped so that the pressure distribution is concentrated near the center of the plate. But this case is clearly *too* conservative, since it implies that no moments can be resisted whatsoever.

For the case of strap clamps, the situation is somewhat better. It can be shown that approximating the contact areas between the strap clamps and the part as point contacts leads to a limit surface that is both conservative and reasonable (i.e., not so conservative as to rule out good clamping arrangements). In Appendix D it is shown that the limit surface for a series of point-contacts will be enclosed by the limit surface for strap clamps that satisfy the same equilibrium conditions. Figure 5.16 shows the case for a flat plate held by four strap clamps. As the assumed area associated with each strap clamp reduces from case (a) to case (b), and finally case (c), the limit surface shrinks slightly and develops a set of four facets.

A second practical issue involves the accuracy of the ellipsoidal approximation to the true limit surface. In particular, as seen in Figure 5.15, there is an error in the approximation when m_{omax} does not coincide with the end point of the ellipsoid. The relative magnitude of the error depends on the angle of inclination of the ellipsoid, which in turn depends on the degree of asymmetry in the contact arrangement. Thus,

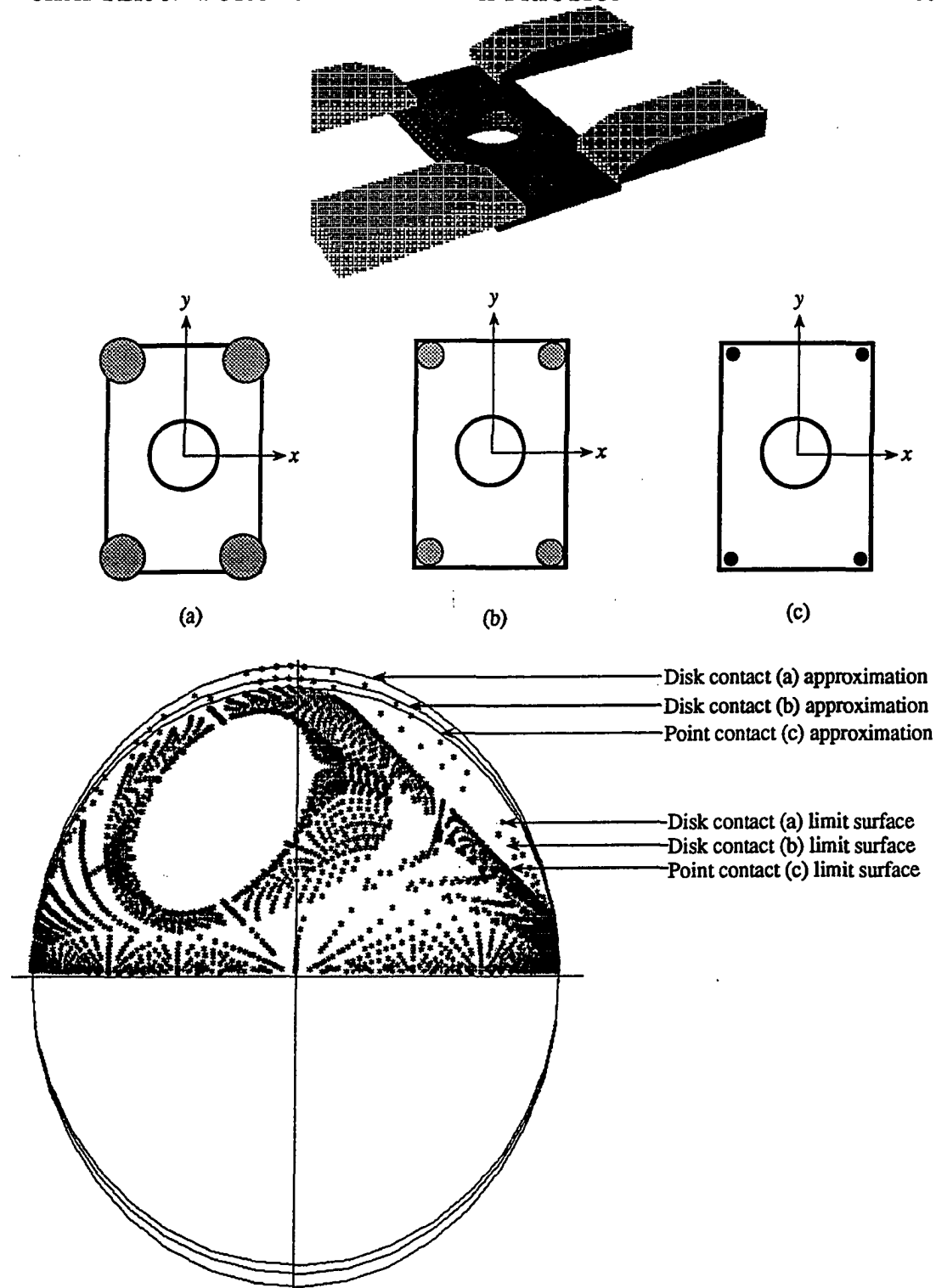


Figure 5.16: For a given strap clamp figure configuration, several kinds of approximation are possible, but the point contact approximation, (c), gives the most conservative boundary of the limit surface.

if one has prior knowledge that the contact pressure is highly asymmetric, one may wish to use a different procedure to find the ellipsoid that includes the circle of radius $\sum \mu f_n$ in the (f_x, f_y) plane, and is tangent to the horizontal plane defined by $m_o = m_{o\max}$ at the point $(f_x, f_y, m_{o\max})$.

For a particular pressure distribution, the approximation errors can easily be quantized. In the remainder of this section the maximum errors are explored for axisymmetric and rectangular pressure distributions (two distributions of practical importance in fixturing). For the case of an axisymmetric continuous pressure distribution the limit surface can be computed by evaluating equations (5.2 and 5.3) numerically and comparing the result with the corresponding ellipsoidal approximation from equations (5.10). The normalized errors in the tangential force, f_t , and moment, m are plotted in Figure 5.17 for the case of uniform pressure. (Normalized values of $\frac{f_t}{f_{t\max}}$ and $\frac{m_o}{m_{o\max}}$ are plotted so that the results are independent of the dimensions and load.) The maximum errors occur when the COR is near the periphery of the contact area. The COR location that produces the worst-case errors is a fixed fraction of the contact area radius for various clamping force. The maximum error occurred at $\frac{r_{error}}{r_{disk}} = 0.9$ when based on $(1 - \frac{m_o}{m_{o\text{true}}})$ and at $\frac{r_{error}}{r_{disk}} = 0.6$ when based on $(1 - \frac{f_y}{f_{y\text{true}}})$ for a disk contact.

When considering a rectangular contact area, the magnitudes of the errors associated with the ellipsoidal approximation depend on the direction along which the COR locus is scanned. In general, when one scans the COR locations along the maximum principle axis of the contact area, one gets the highest approximating errors. Thus, as shown in Figure 5.18 and 5.19, the approximation errors are largest when the COR locus is taken along the x axis.

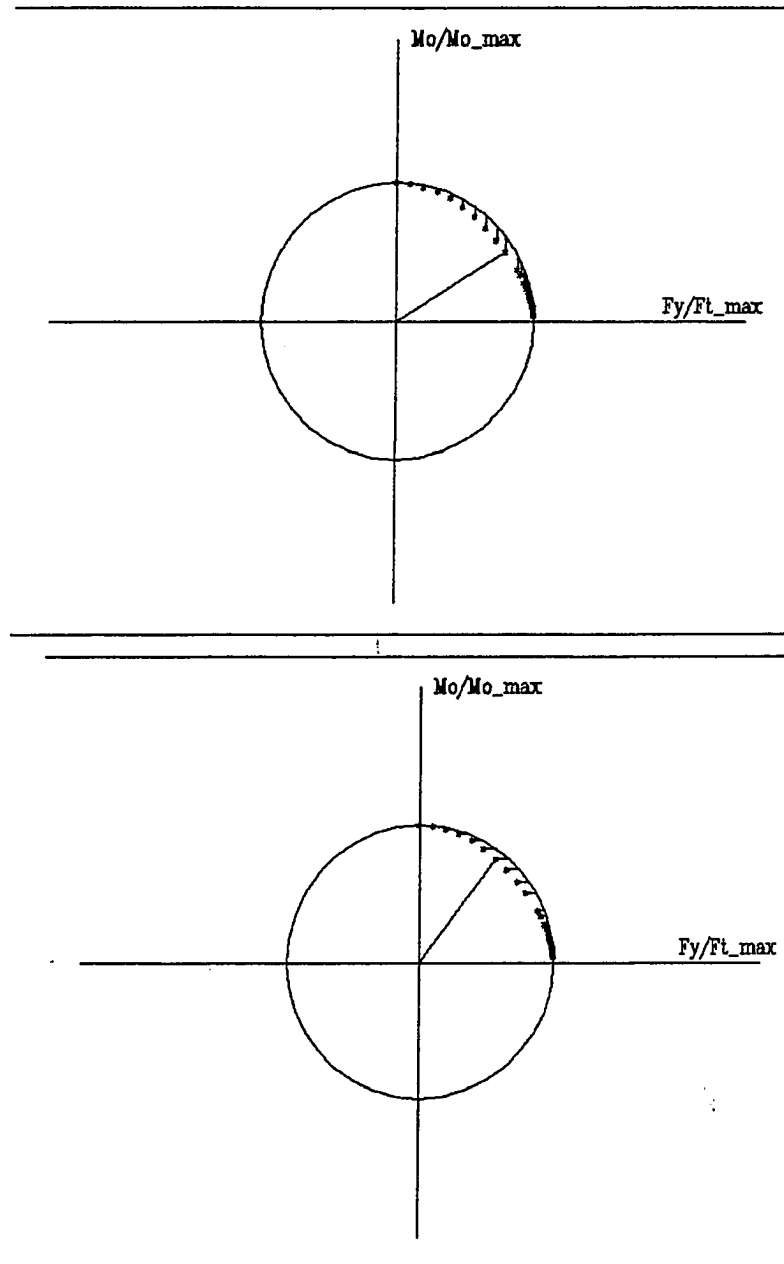


Figure 5.17: A cross-section of a normalized limit surface for a disk contact. The dotted curve represents the actual limit surface and the solid curve represents the ellipsoidal approximation. The maximum error in m_o occurs at $\frac{r_{COR}}{r_{disk}} = 0.9$ and the maximum error in f_y occurs at $\frac{r_{COR}}{r_{disk}} = 0.6$ (The results would be the same for other cross-sections since this limit surface is axisymmetric.)

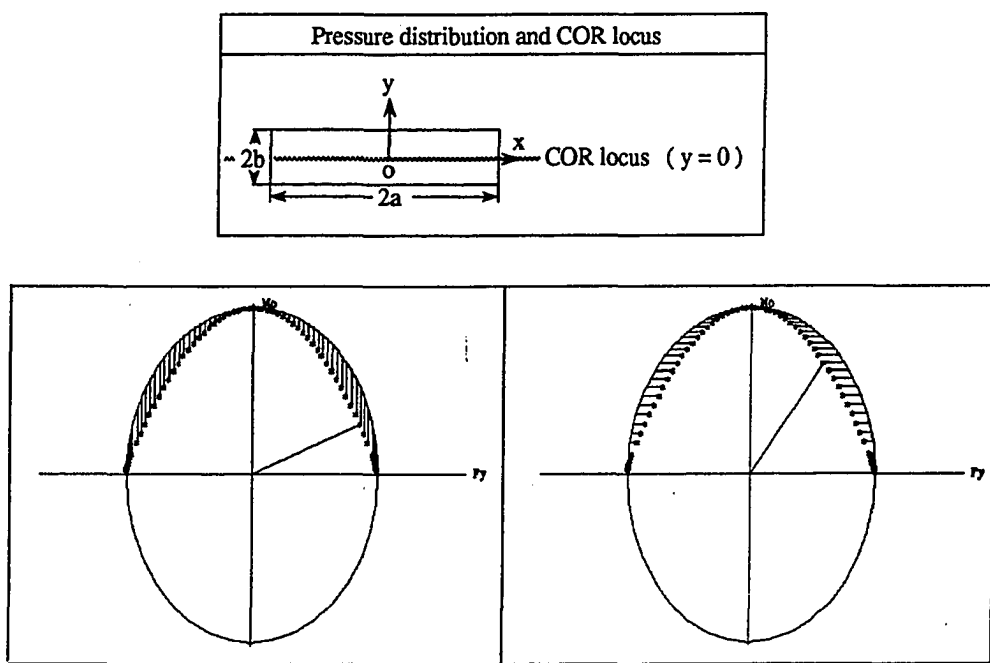


Figure 5.18: Comparison of limit surface and ellipsoidal approximation for a rectangular contact area. The actual limit surface is represented by the dotted line and the approximation by the solid line. The limit surface cross-sections are taken in the (f_y, m_o) plane, corresponding to scanning COR locations along the x axis. In this case, since the COR locus is the major principal axis, the errors in f_y and m_o are largest.

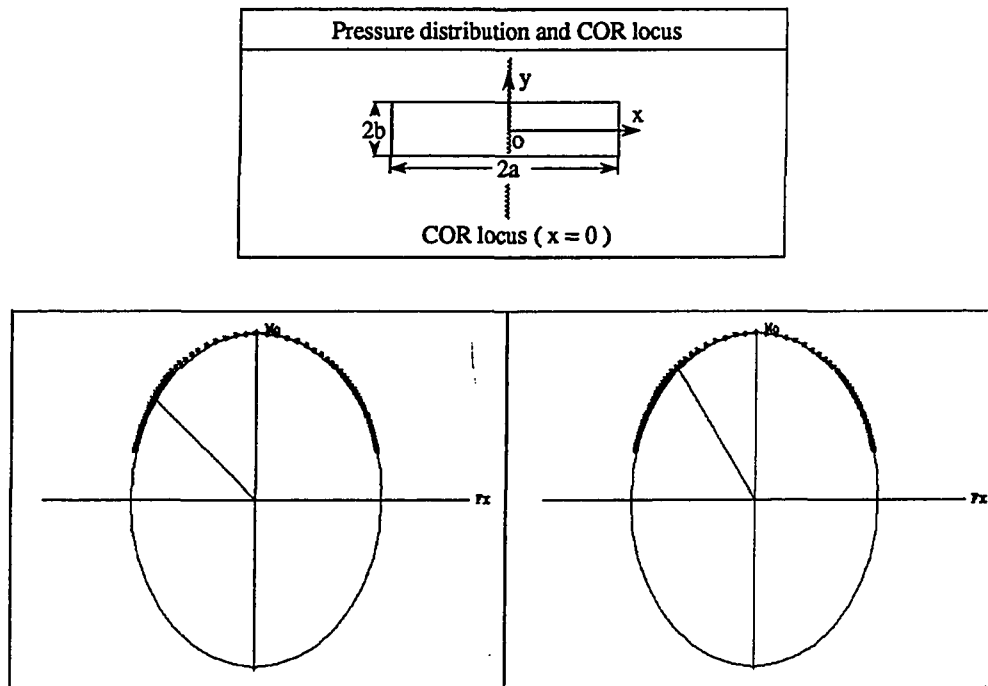


Figure 5.19: Comparison of limit surface and ellipsoidal approximation for a rectangular contact area. The actual limit surface is represented by the dotted line and the approximation by the solid line. The limit surface cross-sections are taken in the (f_x, m_o) plane, corresponding to scanning COR locations along the y axis. In this case, since the COR locus is the minor principal axis, the errors in f_x and m_o are smallest.

5.4 Comparison of the limit surface with other approaches

In this section the use of limit surfaces, obtained either by scanning over the space of possible motions or by Minkowski sums, is compared with other approaches to establishing the relationships among applied forces and moments and the corresponding direction of sliding motion. Since the other approaches in the literature have only been applied to planar examples, the discussion in this section will be confined to the case of a planar pressure distribution. As reviewed in Section 2.4, previous work on the sliding of objects on a planar surface has resulted in four other solution methods:

1. the COR locus method [Mason 1986]
2. the maximum force method [Sakurai 1990]
3. the minimum force method [Pham *et al.* 1990]
4. the polynomial solution method [Bicchi and Dario 1987]

In the following four sections these methods are briefly examined and compared with the limit surface approach investigated in this thesis. The results shed further light on the nature of the friction limits.

5.4.1 The COR locus method

Mason [1986] investigates the direction of motion of a sliding object propelled by a rigid "pusher." The first, and simplest, case addressed by Mason assumes that there is no relative sliding between the pusher and the object. In this case only one degree of freedom exists, corresponding to the instantaneous rotation of the object about its contact with the pusher. The origin is placed at the pusher/object contact and the pusher is assumed to move along a vertical axis (y axis). Applying the condition that

there must be no moment transmitted through the pusher/object contact results in a straightforward numerical solution to a polynomial, giving the location of the COR along a horizontal axis (x axis).

For the case in which sliding between the pusher and the object is possible, there are two degrees of freedom and the situation is analogous to the cases considered in this thesis, in which the COR can be anywhere in the (x, y) plane. In this case, the contact between the pusher and the object provides a known force magnitude (due to the friction between them). The resulting equilibrium equations contain the location of the COR implicitly. Therefore, Mason examines all possible directions for the velocity of the contact point, v_c that satisfy geometric and equilibrium constraints and are consistent with the velocity of the pusher, v . In other words, he basically first plots a COR locus and then finds the correct location of the COR along the locus by requiring that the correct value of the contact force be obtained. This approach is similar to the idea of scanning over the space of kinematically feasible motions, as used in this thesis, taking the special case in which the resultant force and moment on the object correspond to a point-contact force applied to the edge of the object by a pusher.

5.4.2 Maximization force method

The maximum force method is used by Sakurai [1990] to determine when a part clamped by strap clamps will start to slide. The basic idea is to determine the location of the COR by maximizing the inner product of a vector of the cutting forces and moments with a vector of the friction forces for all the strap clamps. The contacts between the strap clamps and the part are treated as point-contacts. The maximum is found subject to equilibrium equations, to the known magnitude of the friction force at each clamp and to the known direction of the externally applied cutting force. Because the direction of the cutting force is assumed to be known, a limit surface is not needed. In terms of the limit surfaces, this is equivalent to solving for the intersection of a line representing fixed ratios of f_{tx}/m_x and f_{ty}/m_x with the limit

surface. Sakurai points out that since the Kuhn-Tucker conditions are satisfied, and since the domain is convex, the maximum he obtains must be the global maximum that satisfies equilibrium conditions.

Although this method is limited to pressure distributions with points of contact (e.g., to strap clamps), it is considerably faster than constructing a limit surface. However, the main time savings is due to the assumption that the direction of the applied force is known (corresponding to known ratios of f_{tx}/m_s and f_{ty}/m_s). If the direction is not known then the process must be repeated for all possible force directions. This amounts to scanning over force-space instead of scanning over velocity-space. Moreover, during process planning, the limit surface is a useful construction which can be computed just once (for a given fixture arrangement) and against which any anticipated cutting forces can subsequently be checked.

5.4.3 Minimization method

In contrast to Sakurai [1990], Pham, Cheung and Yeo [1990] obtained the location of the COR for a rectangular pressure distribution by *minimizing* the magnitude of the externally applied force, f_e . They use the argument that of all possible locations of the COR, the actual one must be the one for which f_e is minimum, since it would obviously slip first for that location. The magnitude of the external force is obtained from a frictional moment, m_c , taken about the location of the COR.

The authors illustrate the approach for a rectangular contact area with uniform pressure. The situation is therefore as in Figure 5.4, except that in this case the external force is applied at the centerline of the rectangle, parallel to the x axis, at a height of y_n . The expression to be minimized is

$$m_c = f_e \cdot (R + y_n) \quad (5.12)$$

where R is the distance between the COR and the center of mass and y_n is the distance between the center of mass and the point of applied force, f_e . By differentiating f_e

with respect to R and setting the derivative to zero, a value of R is found which gives the location of the COR. The authors argue that the COR locus must be along the y axis since the velocity of the center of pressure must be parallel to the applied force, f_e . However, as we have seen in Section 5.1.3, this is only true when the COR locus happens to divide the contact region into symmetric images. As it happens, this is true for the particular case that the authors present. Indeed, if we apply this procedure to other cases in which the external force is not parallel to the x or y axes we do not obtain the correct result for the location of the COR. In general, the application of this minimization method will give a value for f_e which is greater than the correct value.

Minimum versus maximum force: discussion

At first, it might appear contradictory that two approaches, one of which solves for the maximum value of a product of the applied force and the second of which solves for the minimum value of an applied force, could both be used to solve for the motion (and consequently the friction force and moment) of a sliding body. However, there is an analogy in the literature on plasticity, involving two well-known methods for solving problems with plastic metal flow: the upper bound method and the lower bound method. The upper bound method begins by assuming a velocity field that satisfies geometric compatibility conditions. Plastic stress/strain-rate and yield criteria are then applied to solve for the required input pressure (e.g. the pressure on a punch). Equilibrium conditions are not applied, and the final solution for the input force is always greater than the true solution, approaching the true solution as the assumed flow field approaches the true flow field [Hill 1950].

On the other hand, the lower bound solution starts with an assumed stress field that satisfies equilibrium equations and applies plastic stress-strain-rate and yield criteria to solve for the required input force. Geometric compatibility is not enforced. This method always gives a value below the true solution, approaching the true solution in the case that the assumed stress field (and the corresponding velocity field) approaches the actual one [Hill 1950].

	Minimum force method by Pham, Cheung and Yeo [1990]	Maximum force method by Sakurai [1990]
Criterion	Minimum effort criterion	Maximum friction wrench criterion
Objective Function	$f_e = \frac{m_c}{R+y_n}$ <p>where f_e is a pulling force, m_c is a moment with respect to the COR, R is the distance between the COR and the center of mass and y_n is the distance between the center of mass and the point of application of the force, F.</p>	$\mathbf{I} = -\mathbf{w}^T \cdot \mathbf{Wf}$ <p>where \mathbf{I} is the magnitude of the inner product, \mathbf{w} is a vector giving the directions of the cutting forces and moments (i.e., a wrench) and \mathbf{Wf} is a vector of the friction forces (of known magnitudes, but with directions determined by the unknown COR location).</p> <p>\mathbf{I} is minimized subject to equilibrium: $\mathbf{w} \times (\mathbf{Wf}) = 0$</p> <p>friction for magnitudes:</p> $f_{ix}^2 + f_{iy}^2 \leq (\mu f_{ci})^2$ <p>where f_{ix} and f_{iy} are the frictional force x and y components at each point contact and f_{ci} is the magnitude of each contact clamping force</p>
Goal	Find: [1] Location of COR [2] Magnitude of f_e which makes the workpiece slip	Find : [1] Location of COR [2] Clamping force for each clamp $f_{necessary} = f_{ci} \frac{\mathbf{I}_c}{\mathbf{I}_{max}}$, where \mathbf{I}_c is the magnitude of the cutting forces vector and \mathbf{I}_{max} is the maximum magnitude obtained from the maximization of the objective function.
Pro	Applicable for any known pressure distribution	Applicable for any number of point contacts
Con	Works only when the COR locus is a line that divides a workpiece symmetrically.	Not applicable for line or continuous pressure distributions.

Table 5.1: A summary of the objective functions, approach and characteristics of the minimum-force and maximum-force methods for solving for the sliding of an object.

Returning to the sliding of rigid objects in a plane, we see that the maximum-force method of Sakurai and the minimum-force method of Phan, Cheung and Yeo are essentially lower-bound and upper-bound methods, respectively. Phan, Cheung and Yeo [1990] begin with an assumed direction of sliding motion and solve for the applied force, obtaining a value that is always greater than or equal to the true value. Sakurai [1990] begins with information about the forces and enforces equilibrium conditions. Therefore, his applied force is always less than or equal to the actual value. However, in the case of strap clamps, since the friction forces are all known, the correct value of the applied force is obtained at the maximum. A summary and comparison of the two methods are given in Table 5.1.

5.4.4 Polynomial solution method

The final method that will be considered is a polynomial solution method that can be applied if the tangential forces and the pressure distribution are both known. Bicchi and Dario [1987] consider the case of a block squeezed between two flat fingers of a parallel-jaw gripper. The resultant friction forces in the x and y directions are assumed to be known (perhaps measured by strain gages in the gripper jaws) along with the pressure distribution over the contact area (perhaps measured by a tactile array sensor). The authors obtain the location of the COR by solving two simultaneous non-linear equations of equilibrium in the x and y directions;

$$f_x = \sum_{i=1}^n \frac{-\mu f_i(y_i - y)}{\sqrt{(x_i - x)^2 + (y_i - y)^2}} \quad (5.13)$$

$$f_y = \sum_{i=1}^n \frac{\mu f_i(x_i - x)}{\sqrt{(x_i - x)^2 + (y_i - y)^2}} \quad (5.14)$$

where n is the number of elements in the pressure sensing array and f_i is a measured normal force at each element, (x_i, y_i) . The values of f_x and f_y are measured directly. Therefore, there are just two unknowns, x and y , corresponding to the location of the COR. The solution of the two simultaneous equations in x and y is straightforward; however, this approach clearly requires more input information than the other

methods.

5.5 Experimental results

In previous sections, the limit-surface approach to representing friction limitations for parts subject to forces and moments has been presented and compared with other methods. An ellipsoidal approximation to the limit surface has been presented and compared with the true limit surface for a variety of pressure distributions. The errors are acceptable, especially when it is considered that there may be large uncertainties in both the pressure distribution and the coefficient of friction. Indeed, the entire approach is based upon the "Coulomb Law" of friction, which is not a physical law at all, but an empirical relationship which has been found to hold approximately true for many hard materials [Tabor 1951].

In light of these assumptions, a number of experiments were conducted in order to see how well the limit-surface approach describes friction limitations with real fixtures and machined components. Two sets of experiments were conducted. The first set of experiments involved measurements of the actual pressure distribution for a part clamped in a vise. The second set involved the application of external forces and moments to a clamped part to determine the onset of slipping.

5.5.1 Experimental measurement of clamping pressures

In certain cases, as in the case considered by Bicchi and Dario [1987] of a block held in gripper, it may be possible to obtain the pressure distribution directly from tactile sensors. However, in the case of machined parts, where the clamping forces may be several hundred *Newtons*(*N*), the development of an array sensor for use in the experiments described in this section was felt to be impractical. Therefore, the resultant clamping force was measured with a load cell and the pressure distribution

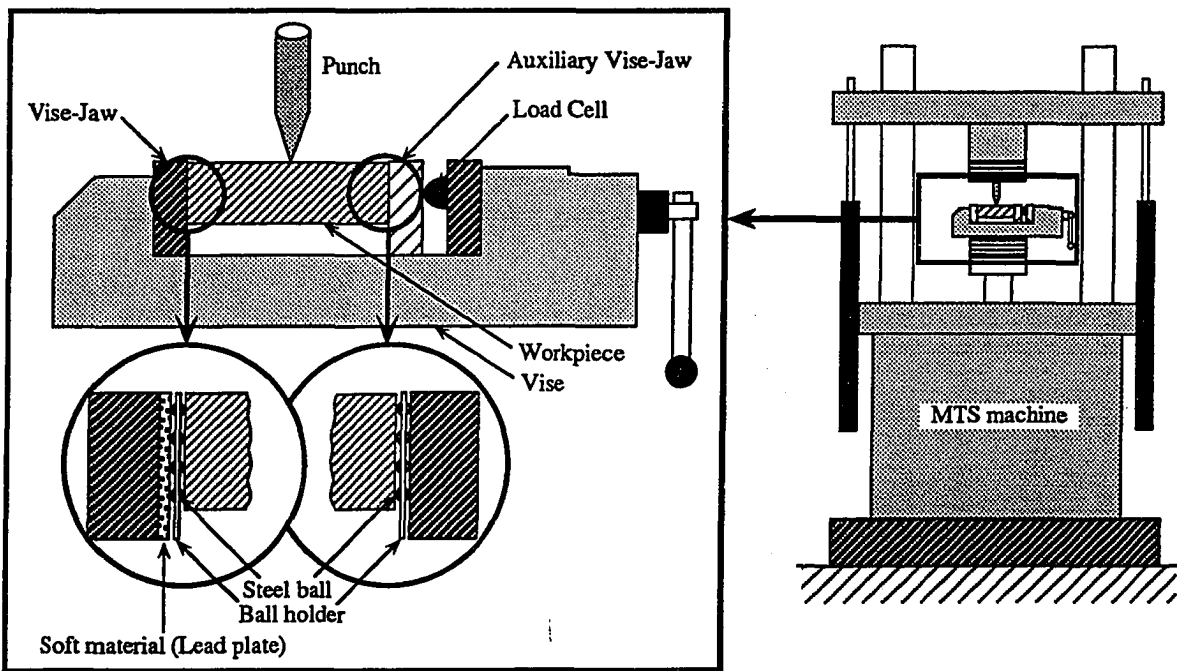


Figure 5.20: The pressure distribution was obtained by using an array of steel balls that indented a soft plate

was obtained using an array of spherical indenters in an approach inspired by the Brinell hardness measurement method. The experimental setup is shown in Figure 5.20 and details are given in Appendix F. The machined part, load cell and vise fixture were mounted on a tensile testing machine to apply controlled external forces to the part.

The steel balls were of diameter, $D = 4.763 \text{ mm}$, and were positioned in a rectangular array. The balls pressed against the workpiece on one side and into a lead plate on the other. The plate was obtained as 1.778 mm thick plate and rolled to 1.651 mm thick to obtain a more uniform thickness and hardness. The tensile flow strength of lead is $U_T = 18 \text{ N/mm}^2$ and the hardness (VPN, Vicker Pyramid Number) is 5.0 [Ross 1972]. The indentation diameter for each ball was measured on an optical micro-measuring machine which is shown in Appendix Figure F.1.

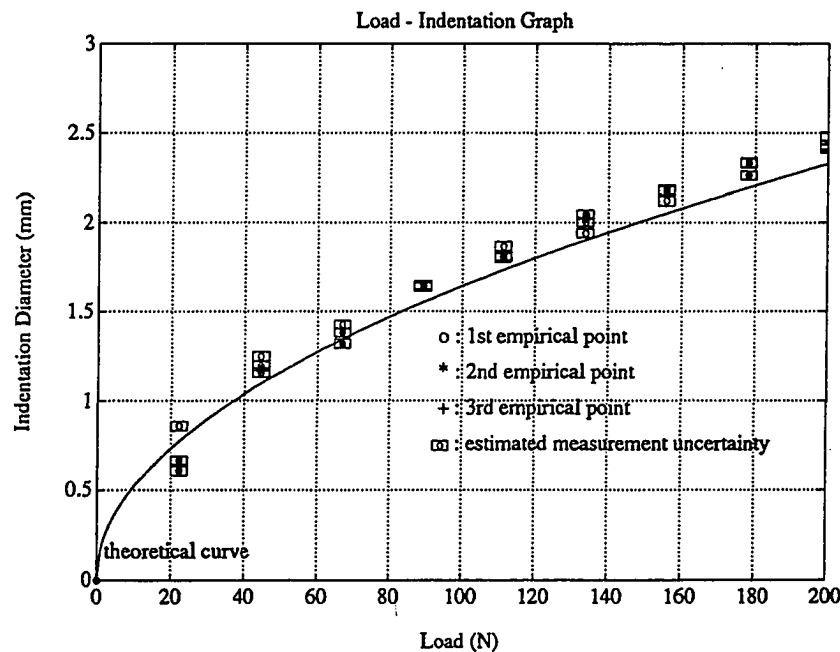


Figure 5.21: Load and indentation diameter relation for 1.778 mm thick lead plate and 4.763 mm diameter spherical indenter: comparison of results from three trials with theoretical result.

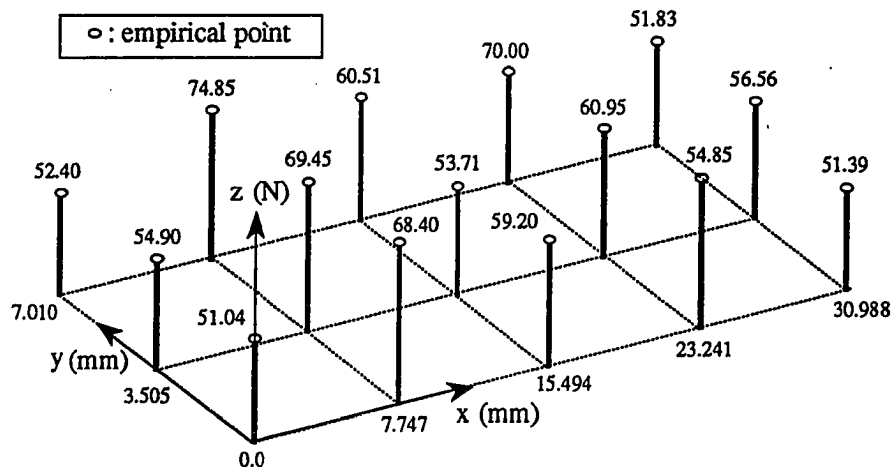


Figure 5.22: 3-D perspective plot of a pressure distribution over a rectangular contact area, obtained by measuring ball indentation diameters. (Total clamping force = $\sum_{i=1}^{15} p_i = 890N$.)

Unfortunately, the empirical Brinell hardness formula only applies for a particular diameter of indenter, which was smaller than the balls used in the experiments. (The ball diameter was chosen to give easily measurable indentations for the applied clamping force and plate hardness.) However, it has been shown [Tabor 1950] that a good approximation to the relationship between applied load, f , and the indentation diameter, d for spherical indenters is Meyer's Law,

$$f = k \cdot d^n \quad (5.15)$$

where k and n are constants for the material under examination. The value of n is generally between 2 and 2.5. This formula correlates well with theoretical studies of indentation with blunt indenters [Shaw 1970; Johnson 1970] in which the relationship between applied load and the indentation diameter can be expressed as

$$f = CAY = \frac{\pi d^2}{4} CU_T \quad (5.16)$$

where U_T is the uniaxial tensile flow stress, and $C \approx 2.66$ for spherical indenters.

Combining equations (5.15) and (5.16) results in

$$f = k \cdot d^2 \quad (5.17)$$

where $k = \frac{2.66\pi U_T}{4}$ for the steel balls used in the current work, and n has been set to 2, corresponding to a material that does not work harden. Substituting in the value of U_T for lead, we obtain

$$d = 0.1627 f^{\frac{1}{2}} \quad (5.18)$$

which is plotted as the theoretical curve in Figure 5.21. As can be seen, this curve has good agreement with the experimental values obtained by measuring forces with a load cell and indentation diameters on the optical micro-measuring machine. Not surprisingly, the agreement is less good for indentation diameters of 1.524 mm and greater, since in this case the indentation diameter is approaching the thickness of the lead plate, whereas the theoretical models assume an infinitely thick plate.

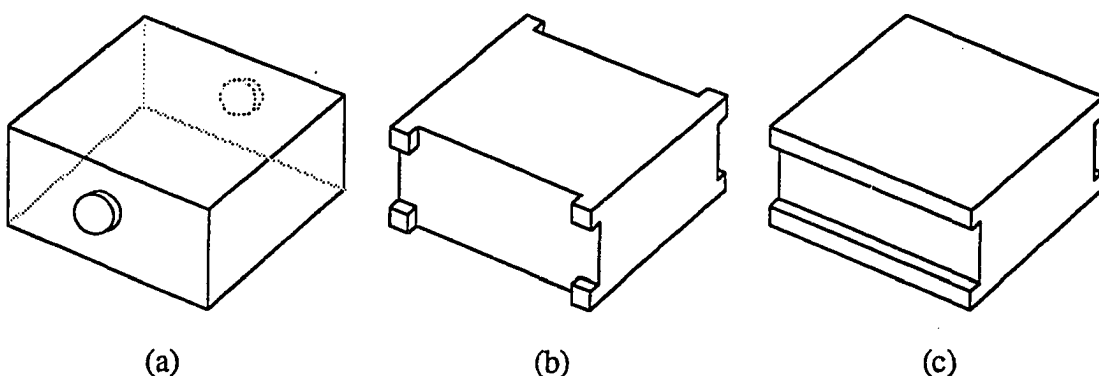


Figure 5.23: Three shapes of workpiece to make an artificial pressure distribution.

When applied to a part clamped in a vise, the apparatus produced typical pressure distributions like that shown in Figure 5.22. It is also straightforward to obtain an approximating limit surface for the array of elements shown in Figure 5.22. However, it was unfortunately discovered that the apparatus could not be used in sliding experiments because as soon as a part slipped, the pressure distribution changed and the indentation diameters became invalid. Therefore a different approach was used to evaluate the accuracy of the limit surfaces as tools for predicting the onset of sliding with real parts, as discussed in the next section.

5.5.2 Comparison of measured and predicted limit surfaces for various contact shapes

The measurement of slipping involved placing workpieces in a vise and subjecting them to controlled external forces and moments using the plunger of a tensile testing machine as shown in Figure 5.20. External moments were produced by applying the forces off-center.

Since it is difficult to obtain a measurement of the pressure distribution for workpieces subject to slipping, an alternative approach was taken in which the contact area itself was controlled. Figure 5.23 shows three different workpieces that were prepared for

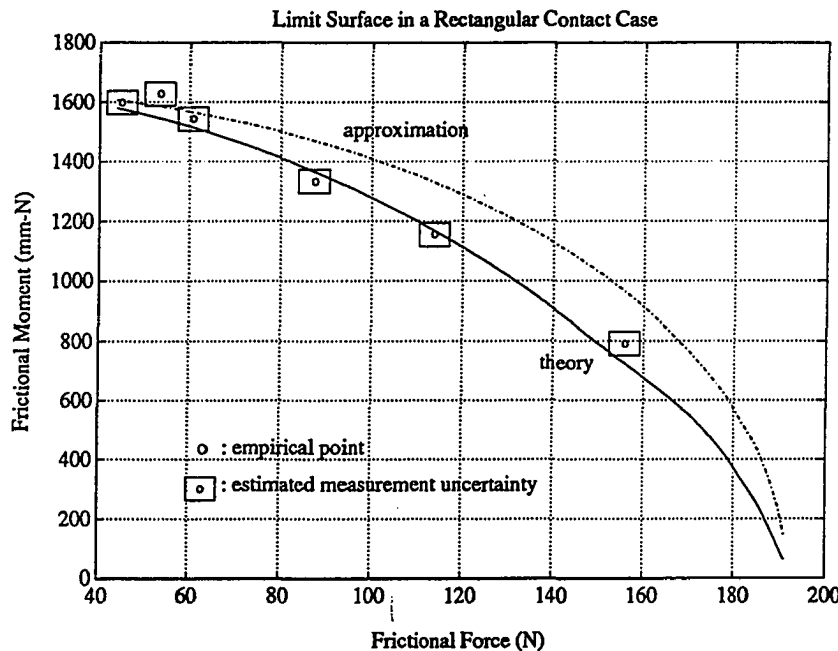


Figure 5.24: Experimental results for uniform rectangular contact case

the experiments. Details of the specimens are given in the Appendix F in Figures F.5, F.6 and F.7. Although the details of the pressure distribution on the contact areas could not be measured, the effects of minor variations in the local pressure distributions are small compared to the effects produced by the very different contact shapes. In addition, the total clamping force was measured for each case and the centroid of the pressure distribution was known to be at the center of the contact face in all cases, due to the use of a ball joint between the load cell and the part. The results are shown in Figures 5.24 - 5.27 and can summarized as follows:

- In the case of Figure 5.24, the plot is for an unprepared rectangular work-piece, assuming uniform pressure over the entire rectangular contact region. The plot is essentially a cross section of the limit surface in the (f_{t_y}, m_z) plane, corresponding to scanning the COR locations along the horizontal axis of the rectangle. In other words, the situation is the same as in Figure 5.18. The

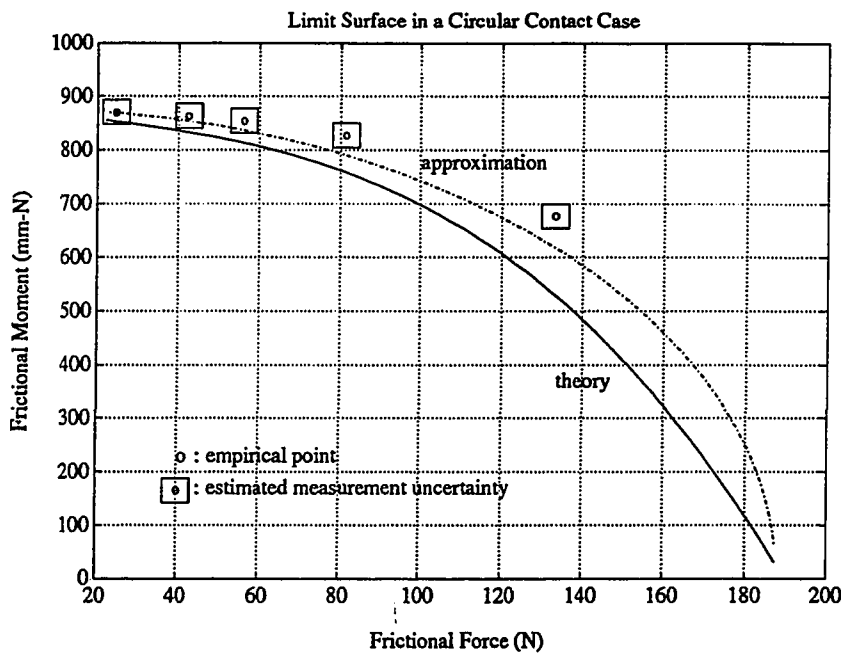


Figure 5.25: Experimental results for circular contact

"approximation" curve is for the ellipsoidal approximation presented in Chapter 5.2.1. The experimental results agree fairly well with the theoretical curves, considering the uncertainty in the pressure distribution and the possibility that the coefficient of friction may not be uniform over the contact area due to minor variations in surface finish and cleanliness. The estimated measurement uncertainty is due to uncertainty in the load cell measurement, measurement errors in the distance between the point of application of the punch and the center of the block, and some uncertainty in judging precisely when the workpiece could be said to have slipped.

- In Figure 5.25 the results are shown for a workpiece prepared as in case (a) in Figure 5.23. In this case, the plot represents any cross-section of the axisymmetric limit surface. The estimated measurement errors are as in the previous case and the "approximation" curve again corresponds to the ellipsoidal approximation. In this case the agreement between the experimental and theoretical

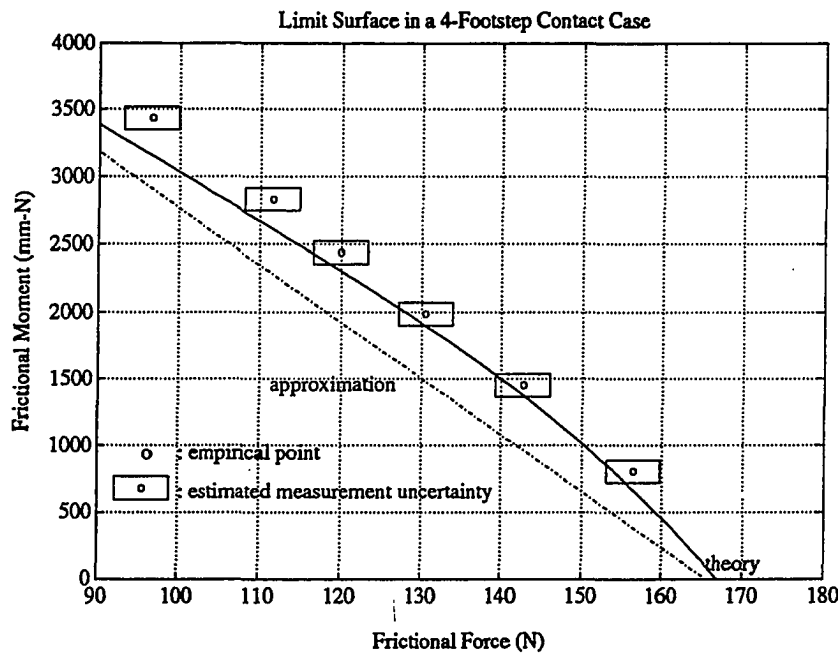


Figure 5.26: Experimental results for four small islands of contact

results is less close. The experimental results appear to be following a broader curve, which suggests that the pressure was not in fact uniform but was higher toward the edge of the circle.

- In Figure 5.26 the results are shown for a workpiece prepared as in case (b) in Figure 5.23. As in the first case, the plot is a cross section of the limit surface in the (f_{t_y}, m_z) plane, corresponding to scanning the COR locations along the horizontal axis of the rectangle. In this case the agreement between the experimental results and the theoretical curve is fairly close again, which is to be expected since there is less margin for error due to variations in the local pressure distribution at each of the four contact areas. The “approximation” curve in this case is a straight line because the four small contact areas were treated as point-contacts, resulting in a limit surface with flat facets, as discussed in Section 5.2.1. As expected, the approximation is therefore somewhat conservative in this case. This plot also gives an idea of how close the point-contact approximation is

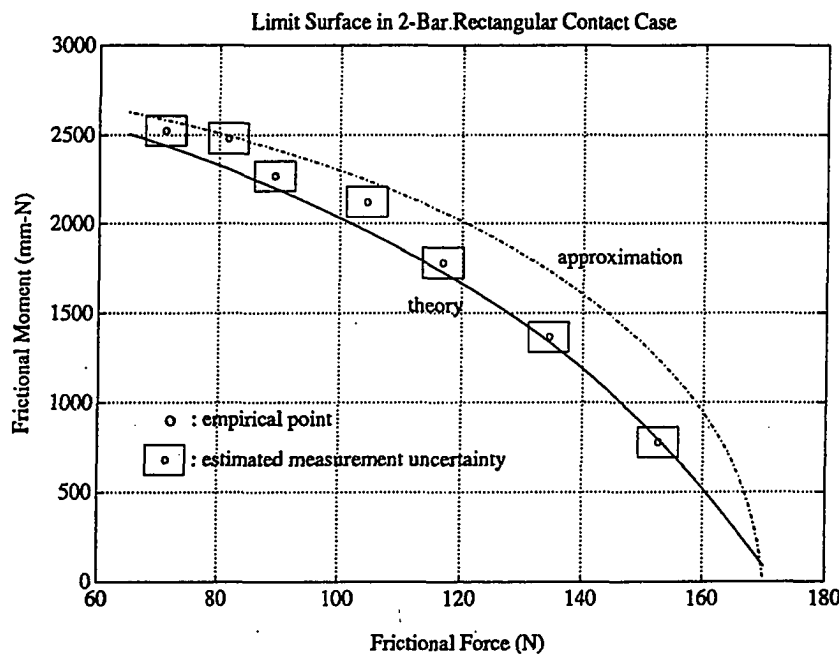


Figure 5.27: Experimental result for two long islands of contact

when the dimensions of the individual contact patches are approximately 1/10 the maximum distance between them.

- In Figure 5.27 the results are shown for a workpiece prepared as in case (c) in Figure 5.23. The cross section again corresponds to the (f_{t_y}, m_z) plane of the limit surface. The “approximation” curve corresponds to the case of two line-contacts. However, in this case the approximation is not conservative because there are no singularities, and therefore no facets, associated with line contacts. There is some scatter in the empirical results which is probably due to variations in the pressure distribution over the two long islands of contact. It should be noted that this case is more sensitive to minor variations in flatness than the previous two cases, due to the length of the contact islands.

5.6 Summary

Limit surfaces form a convenient tool for reasoning formally about friction. However an exact limit surface can only be computed if the pressure distribution for all clamping areas is known. Also, an exact limit surface is hardly necessary when it is considered that cutting forces and the coefficient of friction can only be approximately predicted for typical machining operations. Moreover, the construction of exact limit surfaces is too time-consuming for rapid replanning. A solution proposed in this Chapter was the construction of an approximating ellipsoid. It was found that fitting an ellipsoid, possibly with facets removed for the case of discrete contacts, provided a good approximation to the limit surfaces for commonly encountered contact conditions.

Since the proposed solution is an approximation method, the approximation errors were investigated. The errors were largest when the center of rotation lay on the major principal axis of the contact shape, and were least when the center of rotation lay on the minor axis. While it is difficult to make a general statement about the accuracy of the ellipsoidal approximation that would apply to arbitrary pressure distributions, it should be noted that since the limit surface is convex, the worst-case error can never be greater than the distance between corresponding points on the ellipsoid and a cone with the same base circle and height. For the case of strap clamps, it was found that a provably conservative approximation is to treat the clamp contact areas as point contacts.

The limit surfaces and force analysis also depend directly on the coefficient of friction, which is notoriously hard to predict in the presence of cutting fluids, etc. Therefore experiments were conducted to compare both the limit surfaces and their approximating ellipsoids with measurements. The experiments involved the use of a spherical indentation technique to obtain typical pressure distributions for parts clamped in a vise and the use of prepared specimens with controlled contact areas to investigate the validity of the limit surface predictions. The agreement was generally close, and,

not surprisingly, was best for cases in which the overall results were least sensitive to local variations in the contact pressure.

Chapter 6

Implementation of an incremental and interactive fixture planner

In this chapter the implementation of a fixture planning program is discussed. The analysis procedures of the previous chapters are embedded in a software module called the fixture agent, which interacts with a process planner and geometry module as part of a concurrent design system called Next-Cut. The software was developed in collaboration with other members of the Next-Cut research team.

An important characteristic of the implementation is that instead of bundling geometric computations, fixture planning and process planning into a monolithic program, separate modules were created for each activity. The modules interact through shared representations of designs, plans and ordering constraints as they develop integrated fixture and process plans. One advantage of this approach is modularity. For example, the geometric analysis module surrounds an externally developed constructive solid geometry package called Vantage [Balakumar *et al.* 1988] and isolates the other modules, such as the fixture agent, from its internal details. Similarly, the process planner uses an externally developed planner called PRIAR, [Kambhampati 1990]. Another advantage is the avoidance of redundant code. The fixture agent, process planner and other modules within Next-Cut require many of the same basic geometric

computations and it therefore makes sense to package these in a geometric analysis module that all the other modules can request services from.

The modules interact frequently since the concurrent design system is continually responding to changes in the design imposed by the human user. The need to rapidly assess the fixturing ramifications of design changes has also lead to an incremental style of fixture planning, in which previously computed results are reused whenever possible, to save time.

The main results of the implementation exercise have been a better understanding of how to accomplish interactive, incremental fixture and process planning, and the development of design guidelines for interacting software modules in a concurrent design system.

6.1 Geometric interactions in fixture and process planning

In this section, the basic planning cycle is presented, focusing on geometric issues since these involve the most interactions among the modules. In the following sections, mechanisms for incremental replanning and for working with incomplete information will be discussed.

1. **Tool path pruning:** The first step is to prune the list of tool approach directions to eliminate those that would interfere with the part. The approach to tool path pruning is as described in Chapter 3 and results in lists of “feasible tool approach directions,” $TP(f_j)$ for each feature, f_j .
2. **Generation of the geometric interaction graph:** The next step is to see whether any of the tool paths in $TP(f_j)$ intersects one or more of the other features, f_k . More precisely, we need to know whether the OSR of $TP(f_j)$ intersects f_k or whether the (TSR - OSR) of $TP(f_j)$ intersects f_k . In the former

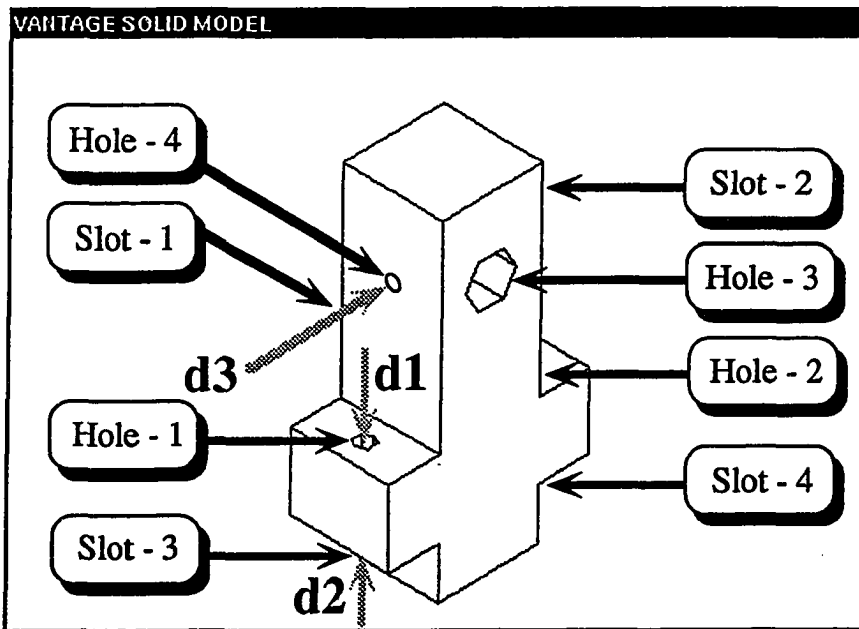


Figure 6.1: A solid model of the component being machined.

case, we have interacting features, which may induce ordering relations in the plan (e.g., if a small hole intersects a large hole then the planner will often drill the small one first). In the latter case, it is necessary that f_k be made prior to f_j , ($f_k \prec f_j$) to avoid a collision. As an example, consider the part shown in Figure 6.1, for which the tool path for machining Hole-4 (shown by the arrow d_3 in the figure) intersects Slot-1. Window I of Figure 6.2 shows the message from the geometry agent, describing this interference. At the end of this step we have ordering constraints to resolve the geometric interactions caused by each tool path. The geometry agent then picks a single toolpath for each feature such that the number of interactions and ordering constraints is minimized. Note that committing to a single tool path based on local optimality criteria such as minimizing the number of geometric interactions can reduce the global optimality of the plan. In Section 6.5 an approach is described to alleviate this problem.

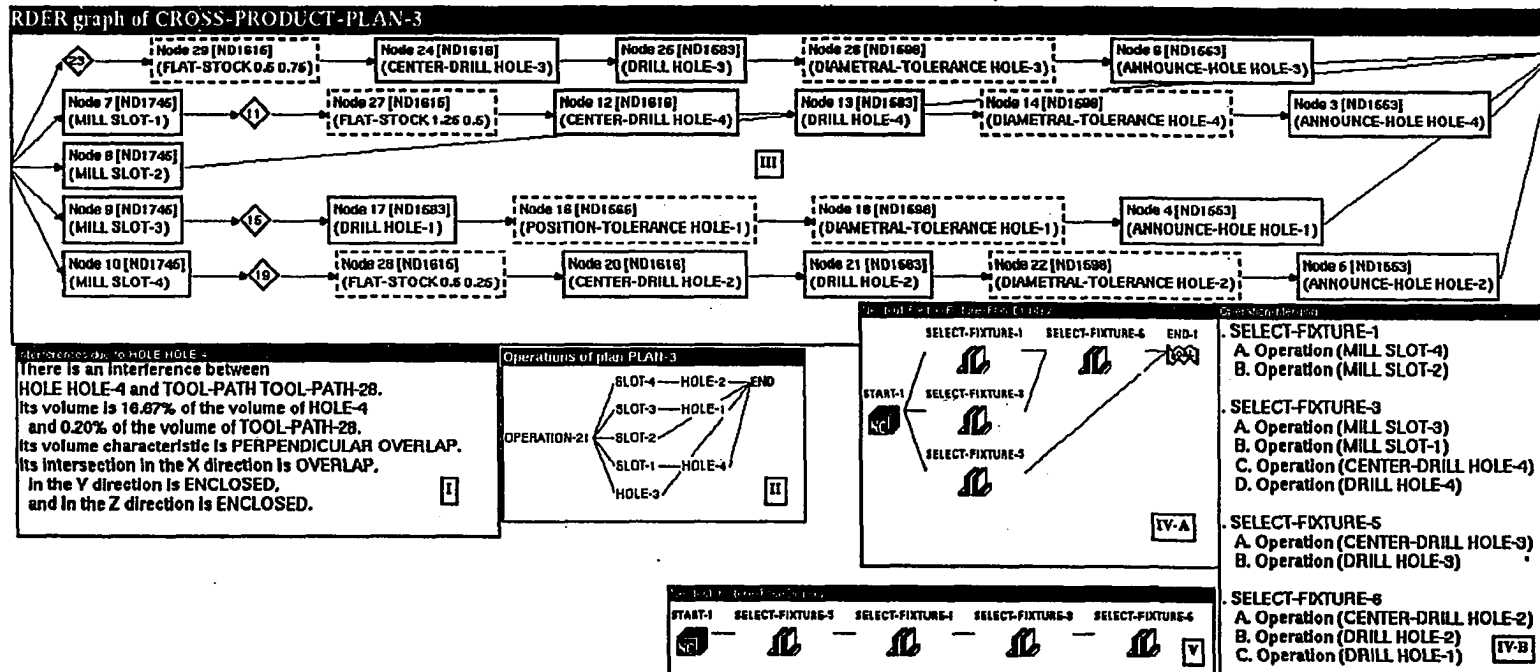


Figure 6.2: Interactive fixture and process planning for the component in Figure 6.1: Window I describes an interference computed by the geometry agent; Window II contains the geometric interaction graph; Window III is a partially-ordered process plan; Window IV-A and IV-B show the setup graph and mergings of operations; Window V shows a particular total ordering of setups selected by the fixture agent.

The final result of this step is a *geometric interaction graph* which represents ordering constraints among the features corresponding to the chosen tool paths. Window II of Figure 6.2 shows the geometric interaction graph for the component of Figure 6.1. The features that precede each other from left to right along a particular path must be made in that order, whereas parallel branches of the graph can be made in any sequence.

3. **Process planning:** The process planner uses the feasible tool approach directions and the geometric interaction graph, along with information about the features themselves, to generate sequences of machining operations. The planner is based on the non-linear planning paradigm, in which high-level tasks (e.g., **MAKE-HOLE**) are successively reduced into simple tasks (e.g., **CENTER-DRILL**; **DRILL**) through the application of task reduction schemata. A more detailed description can be found in [Kambhampati and Cutkosky 1990]. An important attribute of the planner is that ordering constraints are imposed only where necessary to avoid conflicts in the plan. This reduces the need for backtracking when new constraints are imposed by the geometry agent or fixture agent. The output of the planner can be represented as a partially-ordered *process graph*, as shown in Window III in Figure 6.2. The steps preceding each other from left to right must be executed in that order while steps in parallel branches of the plan could be executed in any sequence. Thus, the constraint **SLOT-1** \prec **HOLE-4**, from the geometric interaction graph, is reflected in the partially-ordered process steps in Window III.
4. **Operation mergings and formation of the setups graph:** Using the feasible toolpaths and the process graph, sets of operations with common tool approach directions are merged to form candidate setups for fixture planning. For example, Window IV-B of Figure 6.2 shows mergings of operations (labeled **SELECT-FIXTURE-*i***) for the component of Figure 6.1. The merging step also results in the formation of a *setup graph* that reflects ordering constraints among the candidate setups. An example is shown in Window IV-A of Figure 6.2). Note that the constraint **SLOT-2** \prec **HOLE-4** results in the constraint

SELECT-FIXTURE-1 \leftarrow SELECT-FIXTURE-6.

5. **Fixture planning:** Given the setup graph and mergings of operations, the fixture agent needs to check whether fixture arrangements can actually be generated for each candidate setup. The fixture agent begins by choosing a particular total ordering consistent with the setup graph. This is a departure from the least-commitment approach to planning, and is necessitated by the computational burden of fixture planning. The problem is that fixture planning depends strongly on the part geometry at the start of each setup, which in turn depends on the order in which the setups, and their associated machining operations, have been executed. Therefore, the fixture agent chooses a single total ordering, using heuristics which cause setups that produce minor changes in the external part geometry to be made first (e.g., setups containing mostly holes), as they introduce fewer fixturing complications for subsequent setups. The fixture agent then calls upon the geometry agent to compute the part geometry at the start of each setup and applies rules relating to the dimensions of the part to choose one of the fixture types shown in Figure 5.1. The total ordering that the fixture agent has selected for the component of Figure 1 is shown in Window V of Figure 6.2.

Once the fixture type has been determined, the exact placement of clamping elements can be considered. As mentioned previously, the elements must not prevent access to the features being machined and must not interfere with the swept paths of the cutting tools and tool-holders. These constraints are satisfied by computing safe “clampable regions” for each setup as described in Section 3.1.

The final task of the fixture agent is to arrange clamping elements within the clampable regions. The concerns at this point are to locate the part accurately and to hold it securely so that it will not slip or vibrate when subjected to cutting forces. A number of analyses can be applied at this point using the methods discussed in Chapters 4 and 5 of this thesis. However, the initial placement is based upon heuristics that essentially try to maximize the stability of the

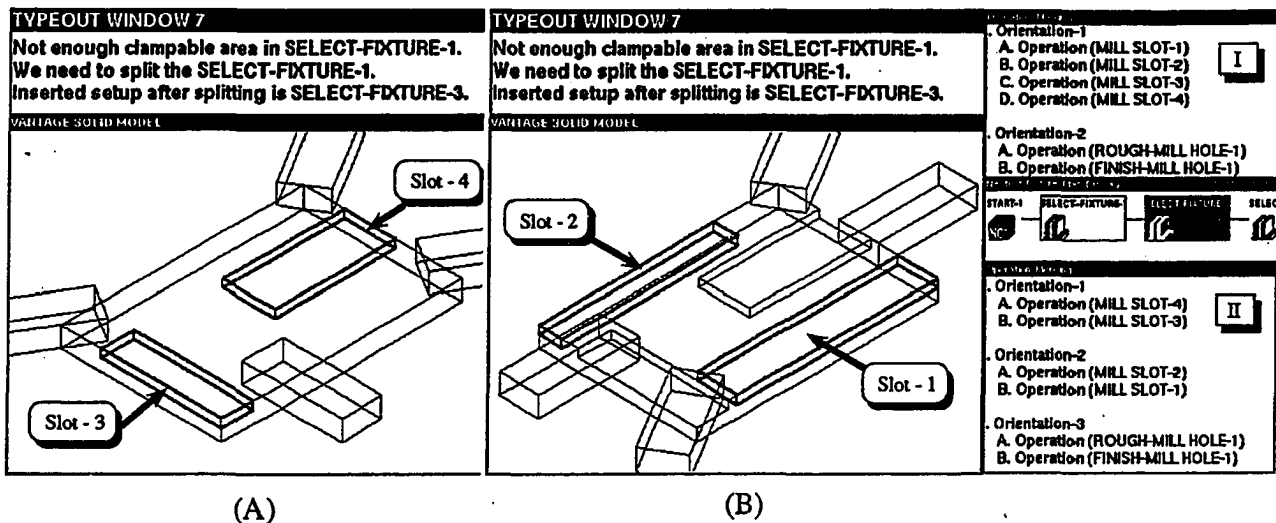


Figure 6.3: The fixture agent was unable to find an adequate clampable region for this part with four slots, so it split the setup into two parts, shifting the clamps between them. Windows I and II show the initial and revised mergings of operations which are communicated back to the process planner.

arrangement.

6.2 Backtracking

The above sequence is the nominal planning cycle followed when generating process and fixture plans for the first time. However, during a design session as the geometry agent, process planner and fixture agent respond to design changes and conflicts that arise in planning, the actual sequence is often different. In this section, we discuss some of the failure modes and the mechanisms for resolving them.

In each case, the approach taken is to first try remedial actions that keep changes in the process or fixturing plan localized. Thus, the process planner avoids making modifications that might render the fixture plan obsolete and vice-versa. This is an important consideration when multiple modules cooperate since the effects of each module's actions on the other modules can bog down the entire system. A second

preference is for remedial actions that involve the fewest computations. In practice, this means that the modules avoid actions requiring the generation of new solid models of the intermediate geometries of the machined part, since the constructive solid geometry computations are the most time-consuming part of the planning process.

The following list summarizes the common geometric problems and remedial actions:

1. Problem description: The swept path of the tool-holder (e.g., collet) for one or more directions in $TP(f_j)$ interferes with the finished part. (This is similar to the preliminary toolpath checks in Steps 1 and 2 of the previous section, except that it is now based upon details of the machining operation and cutting tool.)

Remedial actions:

- (a) Try to eliminate the interference by using a different cutting tool. This requires no changes in the structure of the plan.
- (b) Try a different tool approach direction and prune the list, $TP(f_j)$, accordingly. Then return to Step 3 of Section 6.1.

2. Problem description: The path of the tool-holder for one of the directions in $TP(f_j)$ interferes with one or more features, f_k . Remedial actions:

- (a) Try a different cutting tool.
- (b) Try a different tool approach direction and prune $TP(f_j)$, accordingly. Return to Step 3 of Section 6.1.
- (c) Try to eliminate the interference by machining features f_k first. This case is similar to Step 2 in Section 6.1, and is handled by augmenting the geometric interaction graph to reflect the extra ordering relationships due to tool-holder/feature intersections. The revised geometric interaction graph results in replanning from Step 4. This action affects the fixture agent if the setup graph changes.

3. Problem description: The fixture agent fails to find a sufficient clampable area for a particular setup.

Remedial actions:

- (a) Try to use an alternative set of clamping surfaces on the part. This requires only some additional bounding box tests and clamp placement calculations.
- (b) Try splitting the group of features into two or more setups. This technique is useful for cases such as that shown in Figure 6.3, which can be accommodated by shifting the strap clamps after making the first two slots. This requires additional bounding box tests and clamp placement calculations and results in augmenting the fixture plan to include a new setup and associated clampable region.
- (c) Try a different total ordering, consistent with the setup graph. This will result in a different part geometry at the start of the offending setup and may therefore result in a larger clampable area. This option is attractive if the offending setup was toward the end of the sequence, in which case moving it earlier is likely to result in a significantly different part geometry. Since this approach involves computing new part geometries it is more expensive than the previous two. Note, however, that not all part models may be new. For example, Figure 6.4 shows two total orderings consistent with a partially ordered setup graph. The intermediate part geometries SM-1 and SM-2 are the same for both.
- (d) If the previous actions fail, prune the tool approach directions, $TP(f_j)$, associated with the offending features and backtrack to Step 2 of Section 6.1. This will result in the features being merged differently and made while the part is in a different orientation. New process and setup graphs are generated and the fixture agent replans. A considerably different total ordering is likely, with new intermediate part geometries.

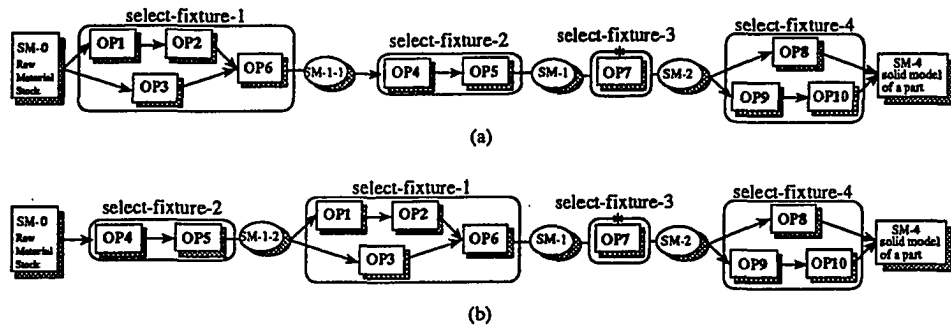


Figure 6.4: Two possible total orders that are consistent with a partially-ordered setups graph and process plan. The two orders result in some different intermediate part geometries.

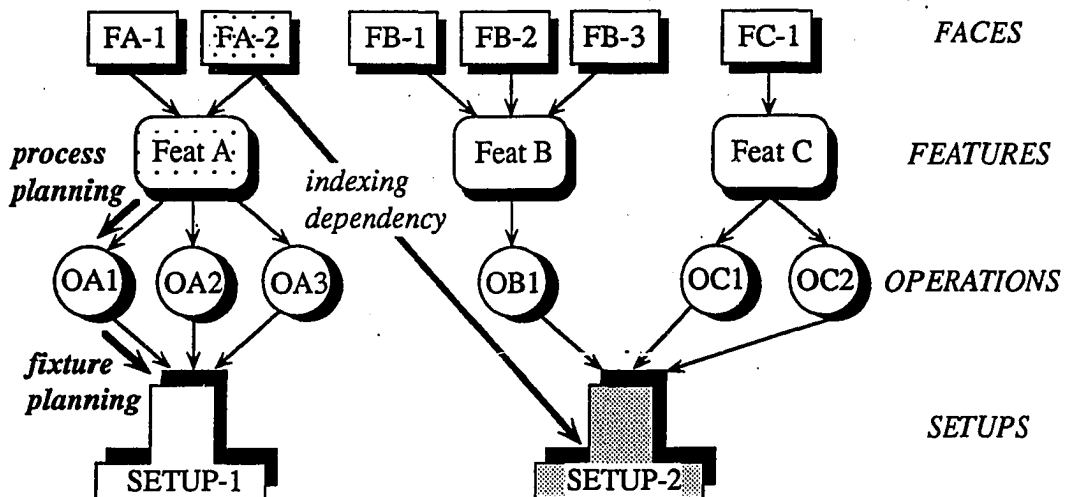


Figure 6.5: Dependencies among features, operations, and fixture setups and primitive geometric elements of features.

6.3 Incremental planning

As seen from the previous sections, there are many occasions when the modules are required to backtrack and modify their results. In addition, the system is continually responding to changes and additions imposed by the designer. For fast response under such circumstances, the process planner and fixture agent both make use of previous results whenever possible. This approach, in which previous plans are continually modified or extended as the design evolves, is called “incremental planning.” It allows the designer to immediately assess the manufacturing implications of changes in the dimensions, locations and tolerances of a component and to experiment with “what if” scenarios. In the case of the process planner, incremental plan reuse is accomplished with the help of a representation of plan causal dependency called *validation structures* [Kambhampati and Cutkosky 1990] which document the preconditions and effects of each step in the plan, as well as the conditions that must hold true for the duration of each step. In the case of the fixture agent, incremental planning is made possible by a graph that captures dependencies among features, feature-elements, operations and setups. An example of how the graph works is shown in Figure 6.5. Features A, B, and C are composed of primitive geometric elements (surfaces and edges) FA-1, FB-3, etc. and are created through machining operations OA1, etc. The fixture agent has merged operations OA1, OA2 and OA3 and created a fixture arrangement, SETUP-1 for them. Similarly, OB1, OC1 and OC2 have an associated fixture arrangement, SETUP-2. Let us suppose that feature A is modified. The process planner reevaluates operations OA1 - OA3 and modifies them as necessary and the fixture agent reevaluates SETUP-1. SETUP-2 might seem to be unaffected, but it must also be reevaluated if there is an indexing dependency between it and the one of the elements of feature A. An example of such a dependency is illustrated in Figure 6.6: the preferred contact faces for clamping the part while Hole-1 is made include one of the component faces of Slot-1. Therefore, the setup associated with Hole-1 is affected by changes in the width of Slot-1.

Once it has been determined which setups must be reevaluated, the fixture agent

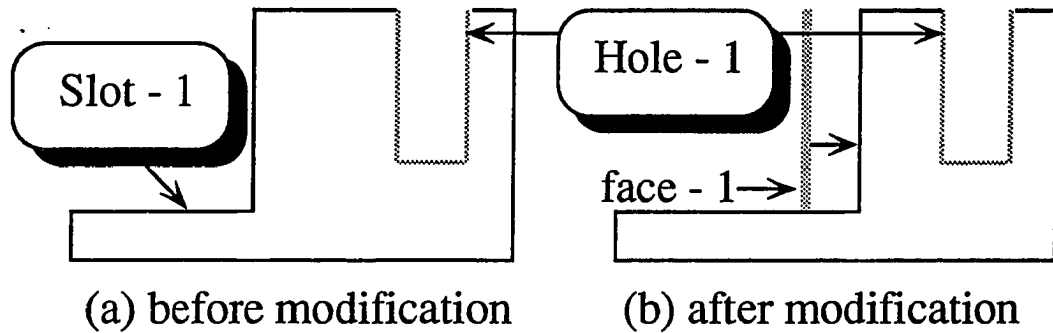


Figure 6.6: Since the setup for Hole-1 depends on face-1, a component face of Slot-1, the fixture agent needs to provide a new fixturing arrangement when Slot-1 is modified.

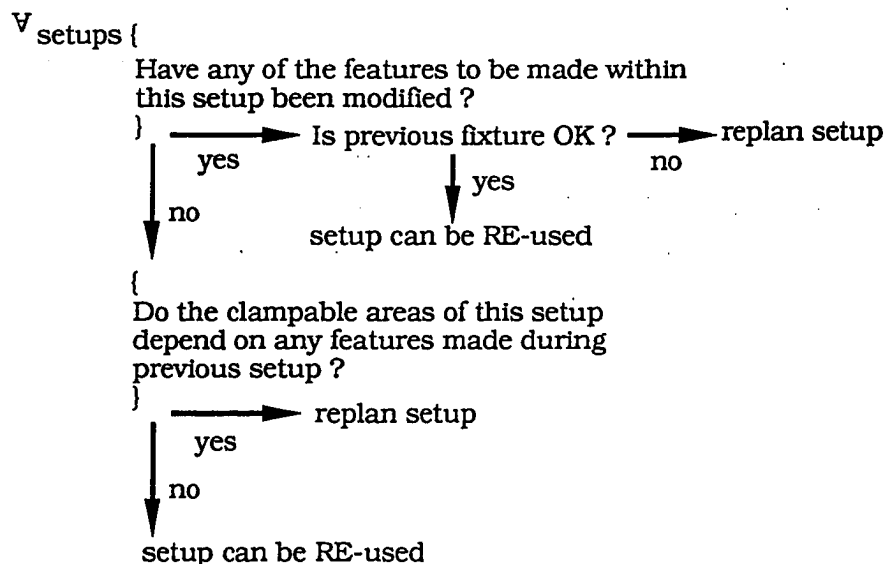


Figure 6.7: A flow chart of the checks involved in incremental fixture planning.

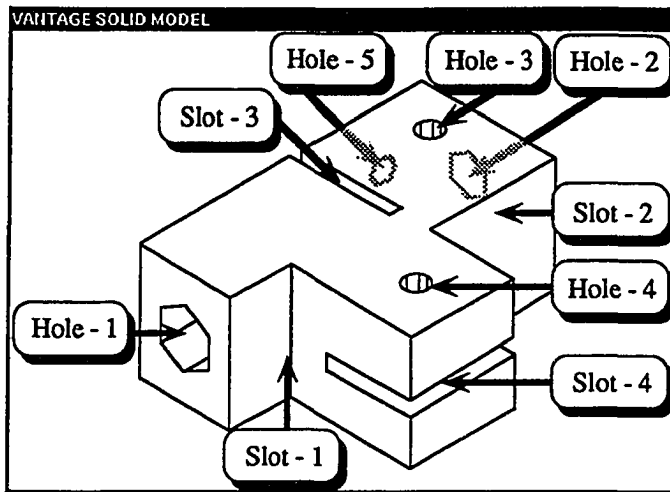


Figure 6.8: Solid model representation of a machined component with several interacting features. Part is shown before modification, in which Slot-3 is deleted and Hole-5 is relocated to the same face as Slot-2.

checks the clampable regions of each and modifies the fixture arrangements as necessary. The basic sequence of checks is shown in Figure 6.7. In many cases, it is not necessary to compute a new intermediate solid model of the part. For example, Figure 6.8 depicts a part that is subsequently modified to eliminate Slot-3 and to relocate Hole-5 from the rear face to the face containing Hole-2. As a consequence, the fixture agent is able to merge setups 2 and 3, as shown in Figure 6.9. Setups 1 and 4, however, are unaffected and are reused from the previous plan.

6.4 Working with incomplete information

Another requirement of modules for a concurrent design system is that they should be able to work at more than one level of detail and with more or less complete input information, so that they can be invoked both during preliminary and final stages in the design of a part. For example, the designer may invoke the fixture agent to check whether a particular combination of features will produce fixturing problems before a process plan has been generated. In this case, the fixture agent performs conservative

geometric tests that do not depend on the order of operations or the magnitudes of cutting forces. The fixture agent works with an unordered list of features and a pointer to a solid model of the part at a point before the features are added. The fixture agent then tries to find an arrangement that works for any feature ordering and for all feasible toolpaths. Failing this, it produces arrangements for subsets of the features. Later, after a process plan has been generated, more detailed analyses of clamping forces and deformations can be performed before releasing the part for production.

A couple of points are worth making about this approach. First, the preliminary geometric checks for clampable regions and kinematic restraint involve the satisfaction of constraints, and not the maximization of an objective function. Also by computing clampable areas that work for all orderings and tool directions (or failing that, for subsets) and by using conservative bounding boxes for all tests, the fixture agent may fail to find acceptable clamping arrangements in some cases, but one knows that the arrangements that it finds will not become invalid when more ordering constraints and more detailed toolpaths are generated at a later time.

Another example of performing conservative checks when faced with incomplete information is the interference checks between the tool paths and the part. In some cases it is impractical to compute new intermediate solid models of the part because the process plan is incomplete or because the designer does not want to wait for new solid models to be generated. In such cases, a previous model can be used, corresponding to the part geometry at any time before the features in question are made. This results in a conservative check because machining is strictly a material removal process. For example, for setup select-fixture-4 in Figure 6.4, if OP7 has been modified, one can use solid model SM-1 as a conservative substitute for the revised version of SM-2 when checking for tool-path/part collisions in OP8-10. Indeed, SM-0, the incoming stock shape, could always be used as a conservative test, although it is likely to be too conservative to be practical.

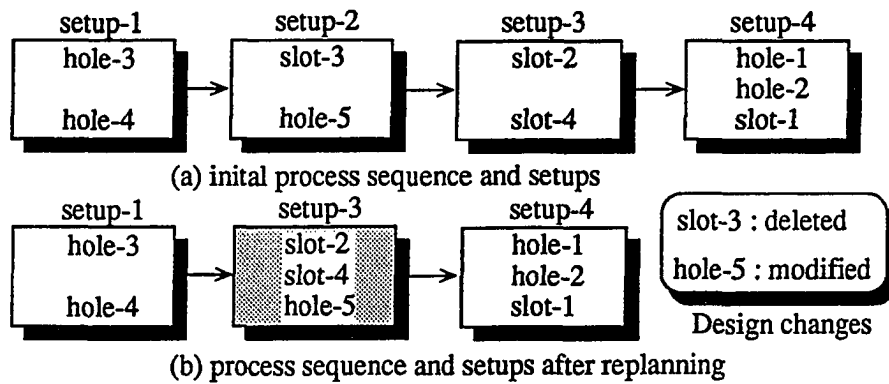


Figure 6.9: Process plan and sequence of setups before and after modifying the part in Figure 10. Setups 2 and 3 have been merged, and setups 1 and 4 have been reused without change.

6.5 Discussion

The previous sections have described the implementation of a fixture planning agent that cooperates with a geometry agent and process planner as part of a concurrent design system. The nominal flow of activities is from geometric interaction tests, to process planning for machining, to fixture planning for holding the part as it is machined. However, this sequence is often disrupted as the system responds to conflicts encountered in planning, changes in the design, and “what if” queries by the designer. To deal with such deviations from the nominal sequence and keep the system as flexible as possible, the software was divided into independent modules that cooperate, but can also work independently if they are unable to obtain up-to-date information from the other modules. The use of specialized modules such as the geometry agent also avoids redundancy; the geometric tests required for process planning are very similar to those required for fixture planning (and for other activities in the NEXT-CUT system, such as the design of assemblies). The geometry agent also offers the advantage of isolating other modules like the fixture agent from the internal details of solids modeling packages that it employs.

To fully realize the potential advantages of a cooperating collection of specialist modules, each module should adhere to some basic design principles. Many of these stem from the need for frequent interaction among the modules. Others stem from the desire to provide rapid feedback about the effects of changes made to the design. The main design principles are summarized below. In concert, they are what distinguishes an "agent" from a collection of analysis and planning routines.

Design principles for cooperating modules in a concurrent design system:

- Communication among the modules takes several forms, including the shared representation of the design and process plan, specialized representations of mutual constraints (e.g., the setups graph) and standardized messages (e.g., the results of intersection tests from the geometry agent). In all cases, there is a tradeoff between expressiveness and abstraction. For example, the intersection results, as in Window I of Figure 6.2, were found after some experimentation to be at the right level of detail for making ordering decisions in process and fixture planning. More generally, it will be impossible to satisfy a variety of modules with messages and representations at a single level of detail. A solution to this problem is to exploit hierarchical representations as discussed below.
- Each module should exploit hierarchical representations where possible, both for reasons of speed and to keep pace with the gradually increasing level of detail in the design. Thus, at an early stage when the designer only knows that some holes will be required, the corresponding process step is "make-hole;" later, when dimensions and tolerances have been assigned, the process steps become "center-drill," "drill" and "ream." Hierarchy also helps to localize changes. If the designer modifies the hole dimensions, we know that we will still be in the "make-hole" branch of the taxonomy of machining operations.
- For fast response, modules should work at a high level where possible and make use of fast, conservative checks to reduce the solution space quickly. Thus, the geometric checks employ conservative bounding-box tests which rapidly prune the tool approach directions and clampable regions.

- Modules should proceed as far as they reasonably can when faced with incomplete input information. This prevents the system from bogging down due to each agent invoking other agents to obtain up-to-date information. For example, a fixture agent should be able to perform preliminary fixture analyses based on part geometry in the absence of a process plan. If reinvoked later, it should be able to refine the fixture plan using the additional information about ordering relationships, tool-paths and expected cutting forces.
- Each agent should reuse previous results whenever practical, both for speed and to make the effects of design changes manifest. Reuse of previous results also helps when scaling the system to more complex designs and to larger numbers of modules. Every time a module computes a new result, it is possible that it may invalidate results previously computed by other modules. However, to the extent that each module reuses previous results, the incidence of new side-effects and interactions with other modules is reduced. Thus, if the process planner makes only minor changes to a previous process plan, it is unlikely that major changes will be needed in the corresponding fixture plan.
- The ability to reuse previous plans (and analysis results) hinges primarily on keeping track of dependencies within the plans and between the plans and the design. In the case of both the fixture agent and process planner, dependency structures permit the modules to rapidly determine which parts of a previous plan *may* be affected by design modifications.
- Once it is determined that parts of a plan or analysis must be recomputed, it is helpful if modules can pick up quickly from where they left off. One way to promote this is to exploit representations that support to incremental revision, even if they are not the most efficient for one-time use. Thus, the clampable-regions are represented as a set of cells, which can easily be added to or subtracted from as features are moved or modified. A second way to promote incremental computation is simply to store extra intermediate “state” information. Thus, the intermediate solid models of the part are stored from one planning iteration to the next, since there is a good chance that some of them

will be reusable. Clearly, this approach involves a tradeoff between response time and memory consumption; for concurrent design systems, the tradeoff is tilted toward responsiveness.

- Modules in a concurrent design benefit from an approach which keeps options open and reduces the need for backtracking in the face of design changes and planning conflicts. We have seen several ways in which the modules in NEXT-CUT employ a least-commitment approach. One is to maintain partially-ordered plans for as long as possible before committing to a single totally-ordered plan. Other examples include the lists of feasible tool approach directions and the representations of clampable areas that correspond to the entire feasible space in which clamps can be placed. Ultimately, it may become impractical to keep all options open; particularly when many computations are needed to test all feasible permutations. Thus, in the example of the fixture agent, a single total-ordering of the setups is ultimately chosen for detailed fixture planning.

More generally, it is important to keep issues of feasibility (constraints) separate from issues of optimality (costs) since the former are far more likely to remain valid from one plan iteration to the next. A short-coming of many previous knowledge-based process planners (e.g., GARI [Descotte and Latombe 1981]; Propel [Tsang 1989]) is that feasibility and optimality issues are melded to arrive at a single plan as quickly as possible, with the result that it is difficult to determine how to modify the plan at a later time.

Future implementation issues

Today, the approach taken with the cooperating fixture agent, process planner and geometry agent in NEXT-CUT is for each module to keep the effects of changes localized, so as to avoid imposing new constraints on the other modules. At the same time, each module treats all externally imposed constraints as non-negotiable. This is a "safe" strategy since modules like the process planner and fixture agent can only reason in detail about those constraints that they impose internally. However, there

are times when it would be desirable to relax this conservative approach. For example, there are some parts for which the fixturing difficulties dominate over process planning. In such cases, it would be desirable for the fixture agent to impose its own ordering constraints *before* invoking the process planner, or even to allow the fixture agent to negotiate with the process planner about relaxing ordering relations in the process plan. After all, many of the rules about which operation "must" be performed first when features interact can be relaxed if there is sufficient reason. This raises a primary requirement for such a negotiation-based approach. The modules must accompany their results with explanations that the other modules can use in making decisions. The explanations can take several forms, including agreed-upon levels of urgency and/or explanations of the circumstances under which a result holds true. We are actively pursuing the latter approach by developing "window of applicability" explanations for the decisions made by the fixture agent and process planner. At the simplest (and least powerful) level, the window of applicability explanations include a list of the quantities upon which a particular result depends. If any of those quantities changes, the result is suspect. A more powerful (and more difficult to construct) explanation provides the sufficient conditions for a result to hold true. For example, can one specify the range of circumstances under which a particular setup will remain valid? This amounts to describing a configuration space of acceptable feature locations, along with the limit-surface of acceptable cutting forces. Evidently, there is a tradeoff between expressiveness and complexity.

Another issue is the tradeoff between saving time by reusing previous results and maximizing the overall efficiency of the plan. At some point, after a number of design modifications have been made and the plan has been "patched" repeatedly, it is better to start the planning process afresh. Knowing when to do this requires information about plan efficiencies which is not presently available to either the process planner or fixture agent. One can side-step this issue by focusing on plan feasibility rather than optimality. The least-commitment approach is also helpful in this regard: the optimal plan is simply one of the many plans consistent with the partial-ordering representations. However, as discussed in Step 5 of Section 6.1, there is a point at

which the fixture agent picks a single total-ordering of setups to avoid requesting a large number geometric computations from the geometry agent. The total order is chosen to reduce the number of setups, and hence the plan cost. As the part is changed, the fixture agent continues to reuse parts of the same sequence, even though a different total-order might be superior. A reasonable alternative would be to periodically launch a background process that would repeat the merging and setup graph generation steps to search for a more efficient sequence without holding up the designer.

Finally, as pointed out in Step 2 of Section 6.1, committing to tool approach directions based on such considerations as geometric interactions may lead to inefficient plans because fixturing issues are not considered. To alleviate this problem, it is worthwhile to modify the approach so that tool paths are selected primarily to minimize the number of setups and secondarily to reduce feature interaction. Thus, Step 4 must be combined with Step 2 and the algorithm must be modified to account for all feasible tool directions, $\text{TP}(f_j)$. Applicable algorithms are presented in the literature (e.g. [Mahanti *et al.* 1991]).

Chapter 7

Conclusions and Future Work

A popular approach to developing automated process and fixture planning programs has been to develop expert systems that encode the knowledge of expert machinists in the form of a rule base. However, a limitation of this approach is that the resulting planners, although they may be able to handle a wide range of standard parts, have no “deep” knowledge of the underlying physics and geometry. As a result of their reliance on expert rules, it becomes difficult to make satisfactory plans when there are competing goals, such as the desire to specify aggressive speeds and feeds, the desire to prevent the part from slipping and the desire to prevent deformation of the workpiece due to clamping and cutting forces. A problem with expert rules is that they do not make it clear how kinematic and geometric constraints bound the space of possible solutions (as opposed to simply asserting that one plan is preferred for reasons of efficiency). A starting point for the work described in this thesis was the belief that fixture planning programs (and related programs for such activities as robot grasp planning and assembly motion planning) will require the ability to reason about relevant aspects of geometry, kinematics and forces. The analyses described in this thesis are an effort to provide this ability for a fixture planning module that forms part of a computational system for concurrent product and process design.

The analysis chapters of this thesis have covered basic geometric, kinematic and

force/friction issues in fixture planning. In all cases, the approach taken was governed by the need to rapidly evaluate the fixturing implications of design changes. In particular, the emphasis has been on fast, approximate methods (as opposed to detailed numerical analyses) and on using representations that can be incrementally updated. Thus, the geometric analysis involved fast, conservative bounding-box interference checks and the construction of "clampable regions" that keep track of the spaces in which clamps can safely be located without interference. Clampable regions are easily added to, or subtracted from, as the features on a part are modified or moved. Similarly, the kinematic analysis involved the construction of contact twist and wrench matrices to which columns can be added or removed as clamping elements are added or removed. However, the most involved of the analyses, and perhaps the most important contribution of this thesis, is the development of a method for rapidly assessing clamping forces and for representing friction constraints.

As mentioned in the introduction, although many common clamping arrangements rely on friction, the analysis of friction in fixturing has received very little attention. The approach to friction analysis developed in this thesis involves the use of limit surfaces in force/moment space and, as far as the author knows, is the first application of limit surface theory to a practical problem. Limit surfaces form a convenient tool for reasoning formally about friction. They are also convenient for planning, since any series of anticipated forces and moments can be tested against a limit surface. If the forces and moments fall inside the surface, the arrangement is "safe."

While the limit surface approach is conceptually attractive, it was found that there are a number of practical issues to be resolved in applying it to realistic fixturing problems. Foremost among these issues is the trade-off between accuracy and computational speed. An exact limit surface can only be computed if the pressure distribution for all clamping areas is known. But an exact limit surface is hardly necessary when we consider that cutting forces and the coefficient of friction can only be approximately predicted for typical machining operations. Moreover, the construction of the limit surfaces is too time-consuming, using either the COR-scanning or Minkowski sum methods, for rapid replanning. A solution proposed in this thesis was the construction

of an approximating ellipsoid. It was found that fitting an ellipsoid, possibly with facets removed for the case of discrete contacts, provided a good approximation to the limit surfaces for commonly encountered contact conditions. The worst-case errors were on the order of 22 % and typical errors were on the order of 7 %. It was also found that errors were largest when the center of rotation lay on the major principal axis of the contact shape, and were least when the center of rotation lay on the minor axis. While it is difficult to make a general statement about the accuracy of the ellipsoidal approximation that would apply to arbitrary pressure distributions, it should be noted that since the limit surface is convex, the worst-case error can never be greater than the distance between corresponding points on the ellipsoid and a cone with the same base circle and height. For the case of strap clamps, it was found that a provably conservative (but not so conservative as to be useless) approximation is to treat the clamp contact areas as point contacts.

Since the limit surfaces and force analysis also depend directly on the coefficient of friction, which is notoriously hard to predict in the presence of cutting fluids, etc., experiments were conducted to compare both the limit surfaces and their approximating ellipsoids with measurements. The experiments involved the use of a spherical indentation technique to obtain typical pressure distributions for parts clamped in a vise and the use of prepared specimens with controlled contact areas to investigate the validity of the limit surface predictions. The agreement was generally close, and, not surprisingly, was best for cases in which the overall results were least sensitive to local variations in the contact pressure.

The final chapter of this thesis discussed the implementation issues associated with making a set of geometric, kinematic and force/friction analyses work together as a fixture agent. What makes a fixture agent different from a package of analysis routines is its ability to interact continually with other software modules and with the designer, sending and responding to messages about the evolving design and process plan. The development of the fixture agent has lead to a set of general guidelines for similar modules that operate in a concurrent design environment. The first of these is that it is preferable to use representations (e.g., of free space) that can be rapidly

updated in response to minor changes in the part geometry or the process plan, and to maintain those representations after each computation is finished so that the next iteration can be performed more quickly. A related point concerns the maintenance of explicit dependencies. In the case of the fixture agent, a dependency graph captures dependencies among operations, setups, features and the primitive geometric elements of features. This is necessary for knowing which parts of a previously constructed fixture plan must be re-evaluated in response to changes in the design and/or process plan.

A more subtle advantage of being able to re-use previous results is that it prevents the concurrent design system as a whole from bogging down. To the extent that each module, such as the fixture agent, re-uses previous results as much as possible, the incidence of new side-effects that other modules must respond to is reduced.

A third desired feature of modules for a concurrent design system is that they should be able to work at more than one level of detail and with more or less complete input information. Thus, in the absence of a machining process plan the fixture agent performs basic geometric checks, chooses fixture types, and makes a first pass at placing fixture elements. If a detailed plan is available, more complete checking of interferences between toolpaths and fixture elements can be performed, the setups can be ordered, and the clamping forces can be tested against expected cutting forces.

A fourth guideline is that modules for a concurrent design system should exploit, where practical, a least-commitment approach to planning. By keeping all options open as long as possible (e.g., by maintaining a representation of the entire "clampable region" as opposed to storing just a single clamping arrangement, and by maintaining a partially-ordered setup graph instead of a single plan) it is possible to reduce the amount of backtracking that must be done when problems arise.

Looking ahead, there are numerous extensions to explore in converting the analysis methods and their prototypical implementation into a versatile fixture planner. The most obvious extensions concern the ability to accommodate wider ranges of geometries (e.g., contoured surfaces) and fixturing types (e.g., modular fixturing). No

fundamental extensions to the analysis methods should be necessary, but considerably more software must be written. Another area of extension concerns the ability to compute deflections of the part as it is cut, due to the action of clamping and cutting forces. This is particularly important for complex parts from which a great deal of material is removed. Such parts are precisely the kinds of parts for which a reliable automatic method of determining fixture placements and clamping forces would be most valuable. Finally, there is additional work to be done on making the fixture agent interact efficiently with other modules of the concurrent design system. In particular, it would be desirable for the fixture agent to accompany its plans with explanations about why they were chosen and what they critically depend on, so that the designer and modules such as the process planner could use this information when contemplating changes to the design or process plan that might affect the fixture agent.

Appendix A

A cylinder in a V-block and a vise-jaw

A.1 Equation of Equilibrium for a cylinder in a V-block and a vise-jaw

As shown in Figure 5.10, we obtain the following equations from the equation of equilibrium.

$$\sum f_x = 0 = f_1 \cdot \cos\phi_1 + f_2 \cdot \cos\phi_2 \quad (\text{A.1})$$

$$\sum f_y = 0 = f_1 \cdot \sin\phi_1 + f_2 \cdot \sin\phi_2 - f_c \quad (\text{A.2})$$

where $\frac{\pi}{2} < \phi_1 < \pi$ and $0 < \phi_2 < \frac{\pi}{2}$.

Solving the equation (A.1) and (A.2) for f_1 and f_2 , we obtain

$$f_1 = \frac{f_c \cos\phi_2}{\sin(\phi_1 - \phi_2)} \quad f_2 = \frac{-f_c \cos\phi_1}{\sin(\phi_1 - \phi_2)} \quad (\text{A.3})$$

Since each line contact has six force/torque components, we have the following equations for each contact. For the contact between a cylinder and a vise jaw, we have

$$f_{x_e} = -\mu f_c \cdot \cos\theta$$

$$\begin{aligned}
 f_{y_c} &= 0 \\
 f_{z_c} &= \mu f_c \cdot \sin\theta \\
 m_{x_c} &= \mu f_c r \cdot \sin\theta \\
 m_{y_c} &= 0 \\
 m_{z_c} &= \mu f_c r \cdot \cos\theta
 \end{aligned} \tag{A.4}$$

For the contacts between the cylinder and a V-block, we have

$$\begin{aligned}
 f_{x_1} &= \mu f_1 \cdot \sin\phi_1 \cdot \cos\theta \\
 f_{y_1} &= \mu f_1 \cdot \cos\phi_1 \cdot \cos\theta \\
 f_{z_1} &= \mu f_1 \cdot \sin\theta \\
 m_{x_1} &= -\mu f_1 r \cdot \sin\phi_1 \cdot \sin\theta \\
 m_{y_1} &= \mu f_1 r \cdot \cos\phi_1 \cdot \sin\theta \\
 m_{z_1} &= \mu f_1 r \cdot \cos\theta
 \end{aligned} \tag{A.5}$$

$$\begin{aligned}
 f_{x_2} &= \mu f_2 \cdot \sin\phi_2 \cdot \cos\theta \\
 f_{y_2} &= \mu f_2 \cdot \cos\phi_2 \cdot \cos\theta \\
 f_{z_2} &= \mu f_2 \cdot \sin\theta \\
 m_{x_2} &= -\mu f_2 r \cdot \sin\phi_2 \cdot \sin\theta \\
 m_{y_2} &= \mu f_2 r \cdot \cos\phi_2 \cdot \sin\theta \\
 m_{z_2} &= \mu f_2 r \cdot \cos\theta
 \end{aligned} \tag{A.6}$$

Since we are interested in the combined three line contacts, we need to add the six force/moment components for the final force/moment. Not surprisingly, all other sliding forces and moments cancel except f_z and m_z . From equations (A.3), (A.4), (A.5) and (A.6), we obtain

$$\begin{aligned}
 \sum f_x &= f_{x_c} + f_{x_1} + f_{x_2} \\
 &= -\mu f_c \cdot \cos\theta + \mu f_1 \cdot \sin\phi_1 \cdot \cos\theta + \mu f_2 \cdot \sin\phi_2 \cdot \cos\theta \\
 &= -\mu f_c \cdot \cos\theta + \mu f_c \cdot \cos\theta \cdot \frac{\cos\phi_2 \cdot \sin\phi_1 - \cos\phi_1 \cdot \sin\phi_2}{\sin(\phi_1 - \phi_2)}
 \end{aligned} \tag{A.7}$$

$$\begin{aligned}
 &= -\mu f_c \cdot \cos\theta + \mu f_c \cdot \cos\theta \cdot \frac{\sin(\phi_1 - \phi_2)}{\sin(\phi_1 - \phi_2)} \\
 &= -\mu f_c \cdot \cos\theta + \mu f_c \cdot \cos\theta \\
 &= 0
 \end{aligned}$$

$$\begin{aligned}
 \sum f_y &= f_{y_c} + f_{y_1} + f_{y_2} \\
 &= 0 + \mu f_1 \cdot \cos\phi_1 \cdot \cos\theta + \mu f_2 \cdot \cos\phi_2 \cdot \cos\theta \\
 &= \mu f_c \cdot \cos\theta \cdot \frac{\cos\phi_2 \cdot \cos\phi_1 - \cos\phi_1 \cdot \cos\phi_2}{\sin(\phi_1 - \phi_2)} \\
 &= \mu f_c \cdot \cos\theta \cdot \frac{0}{\sin(\phi_1 - \phi_2)} \\
 &= 0
 \end{aligned} \tag{A.8}$$

$$\begin{aligned}
 \sum f_z &= f_{z_c} + f_{z_1} + f_{z_2} \\
 &= \mu f_c \cdot \sin\theta + \mu f_1 \cdot \sin\theta + \mu f_2 \cdot \sin\theta \\
 &= \mu f_c \cdot \sin\theta + \mu f_c \cdot \sin\theta \cdot \frac{\cos\phi_2 - \cos\phi_1}{\sin(\phi_1 - \phi_2)} \\
 &= \mu f_c \cdot \sin\theta \cdot \left[1 + \frac{\cos\phi_2 - \cos\phi_1}{\sin(\phi_1 - \phi_2)} \right] \\
 &\neq 0
 \end{aligned} \tag{A.9}$$

$$\begin{aligned}
 \sum m_x &= m_{x_c} + m_{x_1} + m_{x_2} \\
 &= \mu f_c r \cdot \cos\theta - \mu f_1 r \cdot \sin\phi_1 \cdot \cos\theta - \mu f_2 r \cdot \sin\phi_2 \cdot \cos\theta \\
 &= \mu f_c r \cdot \cos\theta - \mu f_c r \cdot \cos\theta \cdot \frac{\cos\phi_2 \cdot \sin\phi_1 - \cos\phi_1 \cdot \sin\phi_2}{\sin(\phi_1 - \phi_2)} \\
 &= \mu f_c r \cdot \cos\theta - \mu f_c r \cdot \cos\theta \cdot \frac{\sin(\phi_1 - \phi_2)}{\sin(\phi_1 - \phi_2)} \\
 &= \mu f_c r \cdot \cos\theta - \mu f_c r \cdot \cos\theta \\
 &= 0
 \end{aligned} \tag{A.10}$$

$$\begin{aligned}
 \sum m_y &= m_{y_c} + m_{y_1} + m_{y_2} \\
 &= 0 + \mu f_1 r \cdot \cos\phi_1 \cdot \cos\theta + \mu f_2 r \cdot \cos\phi_2 \cdot \cos\theta
 \end{aligned}$$

$$\begin{aligned}
 &= \mu f_c r \cdot \cos\theta \cdot \frac{\cos\phi_2 \cdot \cos\phi_1 - \cos\phi_1 \cdot \cos\phi_2}{\sin(\phi_1 - \phi_2)} \\
 &= \mu f_c r \cdot \cos\theta \cdot \frac{0}{\sin(\phi_1 - \phi_2)} \\
 &= 0
 \end{aligned} \tag{A.11}$$

$$\begin{aligned}
 \sum m_z &= m_{z_c} + m_{z_1} + m_{z_2} \\
 &= \mu f_c r \cdot \cos\theta + \mu f_1 r \cdot \cos\theta + \mu f_2 r \cdot \cos\theta \\
 &= \mu f_c r \cdot \cos\theta + \mu f_c r \cdot \cos\theta \cdot \frac{\cos\phi_2 - \cos\phi_1}{\sin(\phi_1 - \phi_2)} \\
 &= \mu f_c r \cdot \cos\theta \cdot \left[1 + \frac{\cos\phi_2 - \cos\phi_1}{\sin(\phi_1 - \phi_2)} \right] \\
 &\neq 0
 \end{aligned} \tag{A.12}$$

As shown in equations (A.7) - (A.12), only two components of force and moment, which are equations (A.9) and (A.12) have non-zero terms

A.2 Example: Equation of limit surface of a cylinder in a V-block and a vise-jaw

When $\phi_1 = 135^\circ$ and $\phi_2 = 45^\circ$, we obtain the following results from equations (A.9) and (A.12).

$$f_z = \mu f_c \cdot \sin\theta \cdot (1 + \sqrt{2}) \tag{A.13}$$

$$m_z = \mu f_c r \cdot \cos\theta \cdot (1 + \sqrt{2}) \tag{A.14}$$

Rearranging (A.13) and (A.14) with respect to θ , we obtain

$$\sin\theta = \frac{f_z}{\mu f_c (1 + \sqrt{2})} \tag{A.15}$$

$$\cos\theta = \frac{m_z}{\mu f_c r (1 + \sqrt{2})} \tag{A.16}$$

By eliminating θ , we have

$$\left(\frac{m_z}{r}\right)^2 + f_z^2 = [\mu(1 + \sqrt{2})f_c]^2 \quad (\text{A.17})$$

Rearranging equation (A.17), we have

$$\left[\frac{m_z}{\mu f_c r(1 + \sqrt{2})}\right]^2 + \left[\frac{f_z}{\mu f_c (1 + \sqrt{2})}\right]^2 = 1 \quad (\text{A.18})$$

Therefore, we obtain that the length of the major axis of the ellipse in Figure 5.12 is $b = \mu f_c r(1 + \sqrt{2})$ and the minor axis is $a = \mu f_c (1 + \sqrt{2})$ where r is the radius of the cylinder and f_c is the clamping force.

Appendix B

Initial fixture placement

B.1 Vise fixture type

For vise fixtures, the agent selects a preferred set of candidate faces by trying to maximize the area of candidate contact faces:

$$\text{Maximize} \quad \sum_{i=1}^2 \text{Area}(F_{\text{contact}_i}) \quad (\text{B.1})$$

where F_{contact_i} represents a contact face.

If this results in a tie, then it picks the pair that minimize distance between the candidate contact faces:

$$\text{Minimize} \quad D_i = \text{distance}(F_{\text{contact}_i}, F_{\text{contact}_j}) \quad (\text{B.2})$$

where F_{contact_i} and F_{contact_j} represents a pair of candidate contact faces.¹

¹Note that in the case of a rectangular block, the above two objectives always give the same result.

The fixture agent searches for pairs of contact faces that maximize the above objectives subject to the following constraints:

1. The dot product of the normal vectors of the candidate faces should be less than zero.
2. Any faces that are component faces of features to be machined in the current setup should not be taken as candidate faces.

Some additional constraints apply in certain situations. These are “soft” constraints in that they can be relaxed if their enforcement makes it impossible to find a pair of candidate clamping faces.

1. Avoid faces with finished surfaces as candidate contact faces (to avoid marring the finish).
2. Avoid reference faces of existing features as candidate contact faces (to avoid a situation in which the cutting tool approaches from the side).

B.2 Strap clamp fixture type

In the case of strap clamp fixture elements, the problem is to determine how many strap clamps to apply and where to locate them within the “clampable region,” which is described in Section 6.1. The number of clamps depends on the size of the part. The placement is determined by a desire to increase the ability of the fixturing arrangement to resist slipping, while also avoiding long segments of the part that have no clamps and might therefore vibrate. A rigorous analysis of resistance to slipping requires the use of limit surfaces, as described in Chapter 5. However, after some experimentation, good results for initial clamp placement were obtained by maximizing the minimum included angle between the clamp placement points:

$$\text{Maximize } \theta_n = \angle (P_{c_n}, P_{c_{n+1}}) \quad (\text{B.3})$$

where P_{clamp_n} and $P_{clamp_{n+1}}$ are the positions of “footprints” of two neighboring strap clamps and θ_n represents the angle between lines radiating from the centroid of the contact face to the two footprints. Thus, the clamps in Figure 3.2 have been placed to maximize the minimum included angle between them.

Appendix C

Friction force versus slipping velocity for a rectangular contact

Let us assume a rectangular block has width, $2a$, and height, $2b$. Let x_c and y_c represent the location of the COR. Then we obtain a total frictional force in the x and y direction for a uniform pressure distribution by applying equation (5.2):

$$\begin{aligned} f_{tx} &= \int_{-a}^a \int_{-b}^b \mu P \frac{-(y - y_c)}{\sqrt{(x - x_c)^2 + (y - y_c)^2}} dy dx \quad (C.1) \\ &= -\frac{1}{2}[(a - x_c)\sqrt{(a - x_c)^2 + (b - y_c)^2} - (a - x_c)\sqrt{(a - x_c)^2 + (b + y_c)^2} \\ &\quad + (a + x_c)\sqrt{(a + x_c)^2 + (b - y_c)^2} - (a + x_c)\sqrt{(a + x_c)^2 + (b + y_c)^2} \\ &\quad + (b - y_c)^2 \ln\{(a - x_c) + \sqrt{(a - x_c)^2 + (b - y_c)^2}\} \\ &\quad - (b + y_c)^2 \ln\{(a - x_c) + \sqrt{(a - x_c)^2 + (b + y_c)^2}\} \\ &\quad - (b - y_c)^2 \ln\{(-a - x_c) + \sqrt{(a + x_c)^2 + (b - y_c)^2}\} \\ &\quad + (b + y_c)^2 \ln\{(-a - x_c) + \sqrt{(a + x_c)^2 + (b + y_c)^2}\}] \mu P \end{aligned}$$

$$\begin{aligned}
f_{t_y} &= \int_{-a}^a \int_{-b}^b \mu P \frac{(x - x_c)}{\sqrt{(x - x_c)^2 + (y - y_c)^2}} dy dx \\
&= -\frac{1}{2} [(b - y_c) \sqrt{(a - x_c)^2 + (b - y_c)^2} + (b + y_c) \sqrt{(a - x_c)^2 + (b + y_c)^2} \\
&\quad - (b - y_c) \sqrt{(a + x_c)^2 + (b - y_c)^2} - (b + y_c) \sqrt{(a + x_c)^2 + (b + y_c)^2} \\
&\quad + (a - x_c)^2 \ln \{(b - y_c) + \sqrt{(a - x_c)^2 + (b - y_c)^2}\} \\
&\quad - (a - x_c)^2 \ln \{(-b - y_c) + \sqrt{(a - x_c)^2 + (b + y_c)^2}\} \\
&\quad - (a + x_c)^2 \ln \{(b - y_c) + \sqrt{(a + x_c)^2 + (b - y_c)^2}\} \\
&\quad + (a + x_c)^2 \ln \{(-b - y_c) + \sqrt{(a + x_c)^2 + (b + y_c)^2}\}] \mu P
\end{aligned} \tag{C.2}$$

For \mathbf{f}_t to be antiparallel to \mathbf{v} , we require that

$$\frac{y_c}{x_c} \cdot \frac{f_{t_y}}{f_{t_x}} = -1 \tag{C.3}$$

Let

$$A = \sqrt{(a - x_c)^2 + (b - y_c)^2} \tag{C.4}$$

$$B = \sqrt{(a - x_c)^2 + (b + y_c)^2} \tag{C.5}$$

$$C = \sqrt{(a + x_c)^2 + (b - y_c)^2} \tag{C.6}$$

$$D = \sqrt{(a + x_c)^2 + (b + y_c)^2} \tag{C.7}$$

By substituting equations (C.1), (C.4), (C.5), (C.6) and (C.7) into the LHS of equation (5.5), we obtain

$$\begin{aligned}
-x_c \cdot f_{t_x} &= \frac{1}{2} \mu P x_c [(a - x_c)(A - B) + (a + x_c)(C - D) \\
&\quad + \ln \frac{(a - x_c) + A}{(-a - x_c) + C} - \ln \frac{(a - x_c) + B}{(-a - x_c) + D}].
\end{aligned} \tag{C.8}$$

Similarly, by substituting equations (C.2), (C.4), (C.5), (C.6) and (C.7) into RHS of equation (5.5), we obtain

$$\begin{aligned}
y_c \cdot f_{t_y} &= \frac{1}{2} \mu P y_c [(b - y_c)(A - C) + (b + y_c)(B - D) \\
&\quad + \ln \frac{(b - y_c) + A}{(-b - y_c) + B} - \ln \frac{(b - y_c) + C}{(-b - y_c) + D}].
\end{aligned} \tag{C.9}$$

In general, equation (C.8) is not equal to equation (C.9). Therefore f_t is not antiparallel to v .

Appendix D

Proof that a limit surface for point contacts is conservative

It has been observed that a limit surface (LS) obtained for several points of support is smaller than or equal to the LS obtained for several small areas of support. For example, let us consider a tripod whose limit surface is LS_{points} and has three supporting points with normal forces f_1 , f_2 and f_3 . Now, consider a pressure distribution that is similar to a tripod, but has three small areas of support such that the resultant of the pressure on each of the three areas is equal to f_1 , f_2 and f_3 , respectively. Also, the location of the centroid of each area is the same as the location of the supporting points in the tripod case. Let the limit surface of the second case be LS_{areas} . It can be shown that no point on the surface of LS_{areas} lies on the interior of LS_{points} . Therefore LS_{points} is a conservative approximation to LS_{areas} .

Proof has two parts:

1. *The LS for a point is contained with the LS for a small area with the same resultant force.*

Proof: Let P_1 be the *LS* for a point contact and P_2 be the *LS* for a corresponding small area of contact with the same resultant force, $f_n = \int_{A_2} p(x, y) dA$, where $p(x, y)$ is the pressure distribution over A_2 , parameterized with respect to an (x, y) coordinate system embedded in the plane of the contact. Let the centroid of the pressure distribution $p(x, y)$ coincide with the origin of the (x, y) coordinate system. The limit surface in the first case is just a circle in the (f_x, f_y) plane of constant radius μf_n [Goyal *et al.* 1991]. The limit surface P_2 will also form a circular intersection with the (f_x, f_y) plane of radius μf_n , but will have a height given by $m_{o,max}$ from equation (5.3). Since P_1 and P_2 have the same base, but P_1 has a height of zero while as P_2 has a nonzero height, it is clear that $P_1 \subseteq P_2$.

2. *The LS for several points of support is smaller than or equal to the LS for several small areas of support.*

Proof: The proof uses a basic lemma of convex set theory. Let P_1, P_2, Q_1, Q_2 and R_1, R_2 , be convex sets such that

$$P_1 \subseteq P_2, \quad Q_1 \subseteq Q_2, \quad R_1 = P_1 \oplus Q_1, \text{ and } R_2 = P_2 \oplus Q_2 \quad (\text{D.1})$$

where \oplus is the Minkowski sum operator. Then it can be shown [Serra 1982] that $R_1 \subseteq R_2$.

Applying the same reasoning of one point contact to the other contacts, Q_1, R_1 , etc., it is seen that $Q_1 \subseteq Q_2, R_1 \subseteq R_2$, etc.

It has been shown by [Goyal *et al.* 1991] that the limit surface for a collection of points or areas moving as a rigid body is given by the Minkowski sum of the limit surfaces for each of the points or areas. Therefore let

$$S_1 = P_1 \oplus Q_1 \oplus R_1 \quad S_2 = P_2 \oplus Q_2 \oplus R_2 \quad (\text{D.2})$$

be the limit surface for the collection of areas. Then, applying the lemma of convex sets repeatedly, we obtain:

$$S_1 = P_1 \oplus Q_1 \oplus R_1 \subseteq P_2 \oplus Q_1 \oplus R_1 \subseteq P_2 \oplus Q_2 \oplus R_1 \subseteq P_2 \oplus Q_2 \oplus R_2 = S_2, \quad (\text{D.3})$$

or $S_1 \subseteq S_2$.

Therefore, the limit surface for a collection of points is enclosed by the limit surface for a collection of areas, each of which has the same centroid and resultant force as the points.

Appendix E

Implementation of Interference Checking

1. Toolpaths, fixture elements, features and the machined part are all members of the class of “spatial objects” in the geometry knowledge base. Each spatial object has its own bounding box (BB) according to the character of the object.
 - workpiece : BB has the exact dimensions of the workpiece.
 - fixture element : BB has the exact dimensions of the fixture elements.
 - feature : There are two kinds of feature BB's. One is an extended BB according to the character of each feature when an explicit tool-path is not defined. The resulting extended BB represents a lower-bound on the volume swept by a cutting tool for making the feature. The other one is the exact dimension of each feature when an explicit tool-path is defined. For the latter case, the construction of the BB is obvious. For the former case, an extended BB is defined as follows.
 - hole - the BB is extended along hole-axis (i.e. in the direction of the normal vector of the feature reference face.)
 - pocket - the BB is extended in the direction of the normal vector of

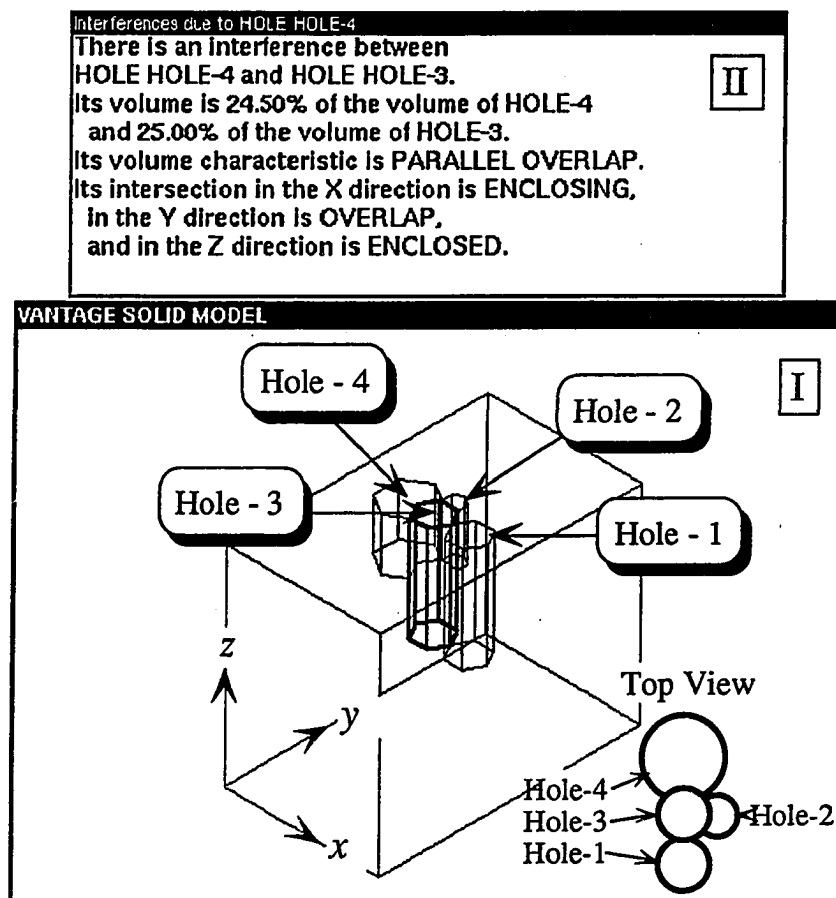


Figure E.1: Four hole features are interacting.

the feature reference face.

- slot – the BB is extended in the direction of the normal vector of each face the slot opens into.

- tool : BB is extended along tool-axis and tool-path. The tool-path is a replacement for the extended features. The extended feature BBs are used when the tool path is not known. However, since they enclose a lower-bound on the actual tool-path, they are anti-conservative (in the sense that [Kim 1990] uses the word) for collision checking.

2. To check for interference it suffices to check for overlap in the X, Y, Z bounds of the boxes for the spatial objects. It is also useful to categorize the interference as viewed from the X, Y and Z directions. The interaction types are enclosed, enclosing and overlapping. For example, in the X direction the conditions are:

if x-interaction = enclosed: $(x1max < x2max) \text{ AND } (x1min > x2min)$
if x-interaction = enclosing: $(x1max > x2max) \text{ AND } (x1min < x2min)$
if x-interaction = nil: $(x1max < x2min) \text{ OR } (x1min > x2max)$
if x-interaction = overlapping: none of the above are true.

The orientation of the spatial objects also used in classifying the interaction type as PERPENDICULAR or PARALLEL. The description of the interference is output as a structure, a typical example of which is displayed in Window II of Figure E.1.

Appendix F

Experiment setups and mechanical drawings

F.1 Experiment procedure

F.1.1 Measurement of μ for indentation case

1. Locate a workpiece between two sets of steel balls as shown in Figure 5.20.
2. Put a lead plate between a fixed vise jaw and a set of steel balls as shown in Figure 5.20.
3. Apply a clamping force until it reaches a chosen value. There may be approximately $\pm 4.45 \text{ N}$ (1.0 lbf) measurement uncertainty.
4. Put a punch tip at the center of the top of workpiece so that any rotational slipping is avoided.
5. Release the punch after 2.5 mm downward movement. Since the initial gap between the workpiece's top face and the punch tip is less than 2.5 mm , slipping is sure to occur.

6. Measure the maximum pushing force when the workpiece slips. From the equation of equilibrium, μ is obtained.

$$\mu = \frac{f_e}{2f_c} \quad (\text{F.1})$$

where f_e is the externally applied force and f_c is the clamping force.

7. After disassembling the workpiece, the indentation diameter is measured using an optical micro-measuring machine, shown in Appendix Figure F.1.

F.1.2 Measurement of external force and moment

Procedures for measuring the external force and moment are the same as described in the previous section except that rotational slippage of the workpiece is permitted, due to external moments. External moments are produced by applying the forces off-center.

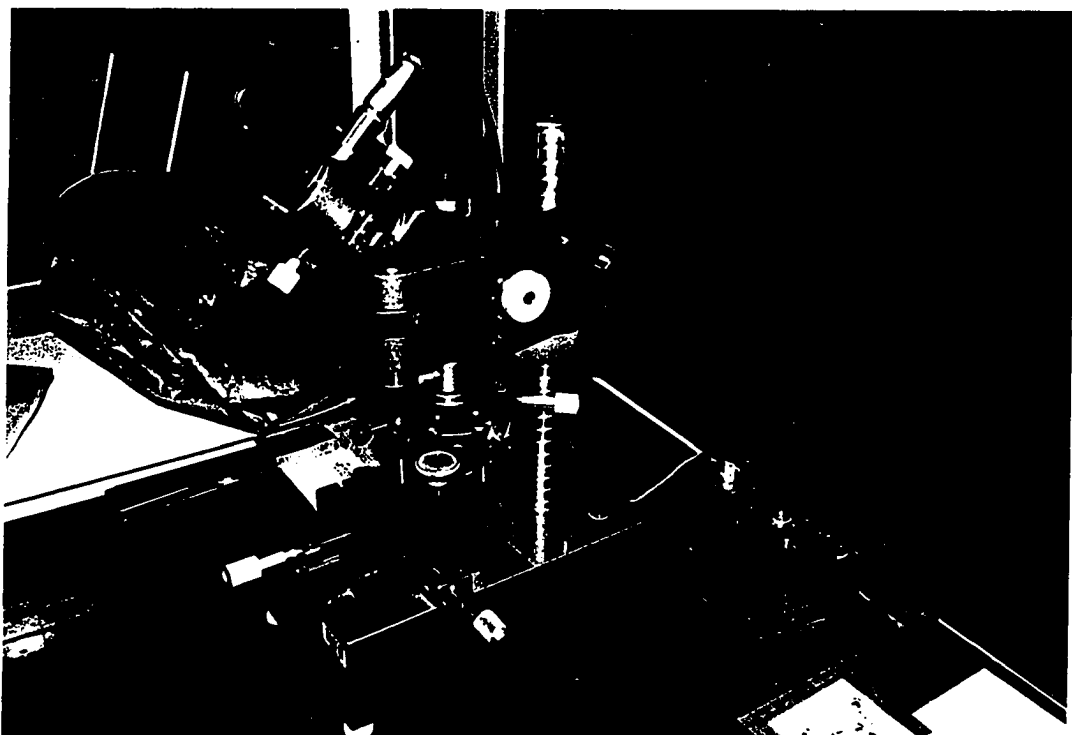


Figure F.1: A measuring device of indented diameter.

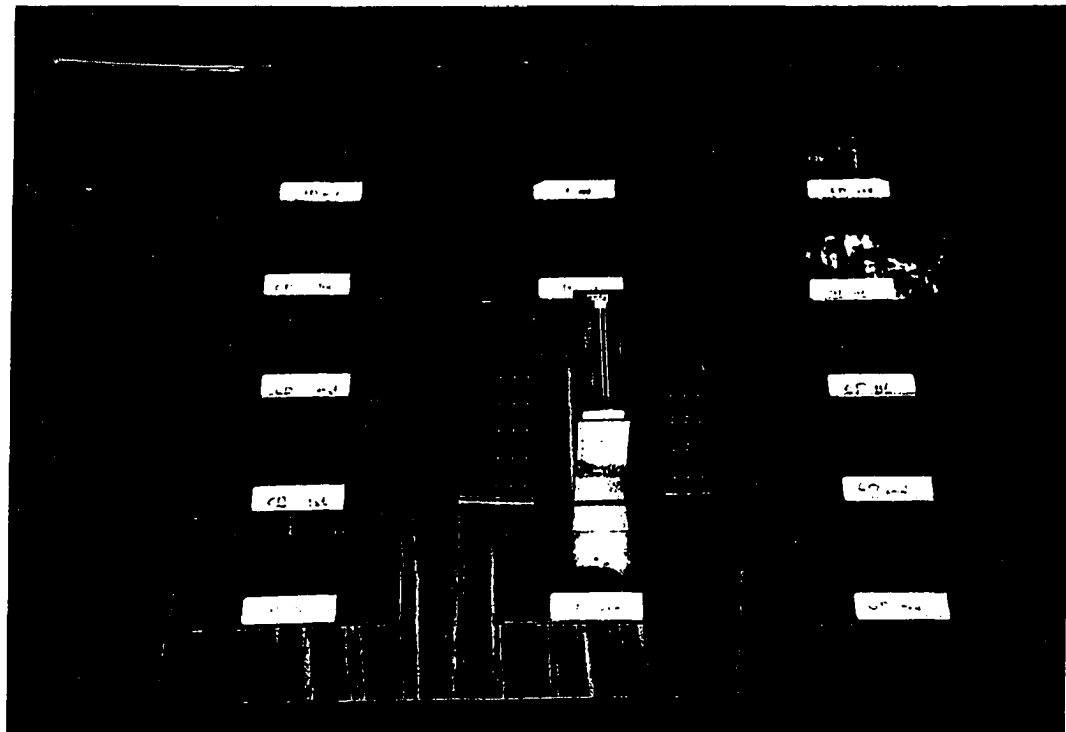


Figure F.2: Indented lead plates.

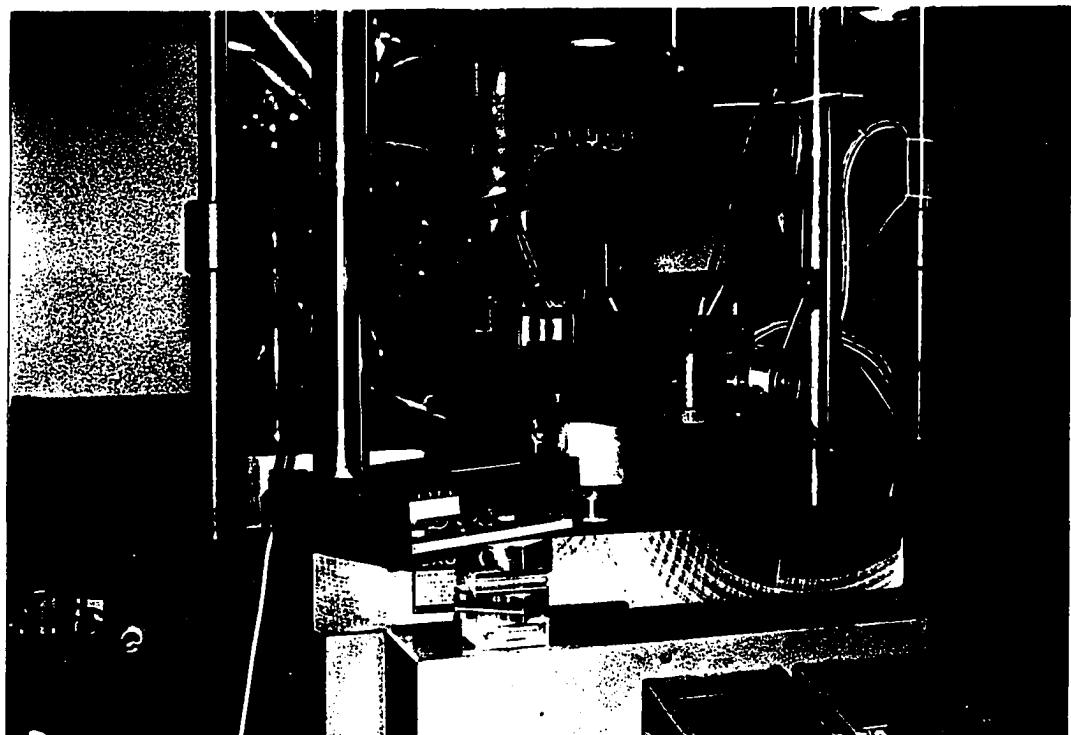


Figure F.3: Experimental setup on MTS machine.

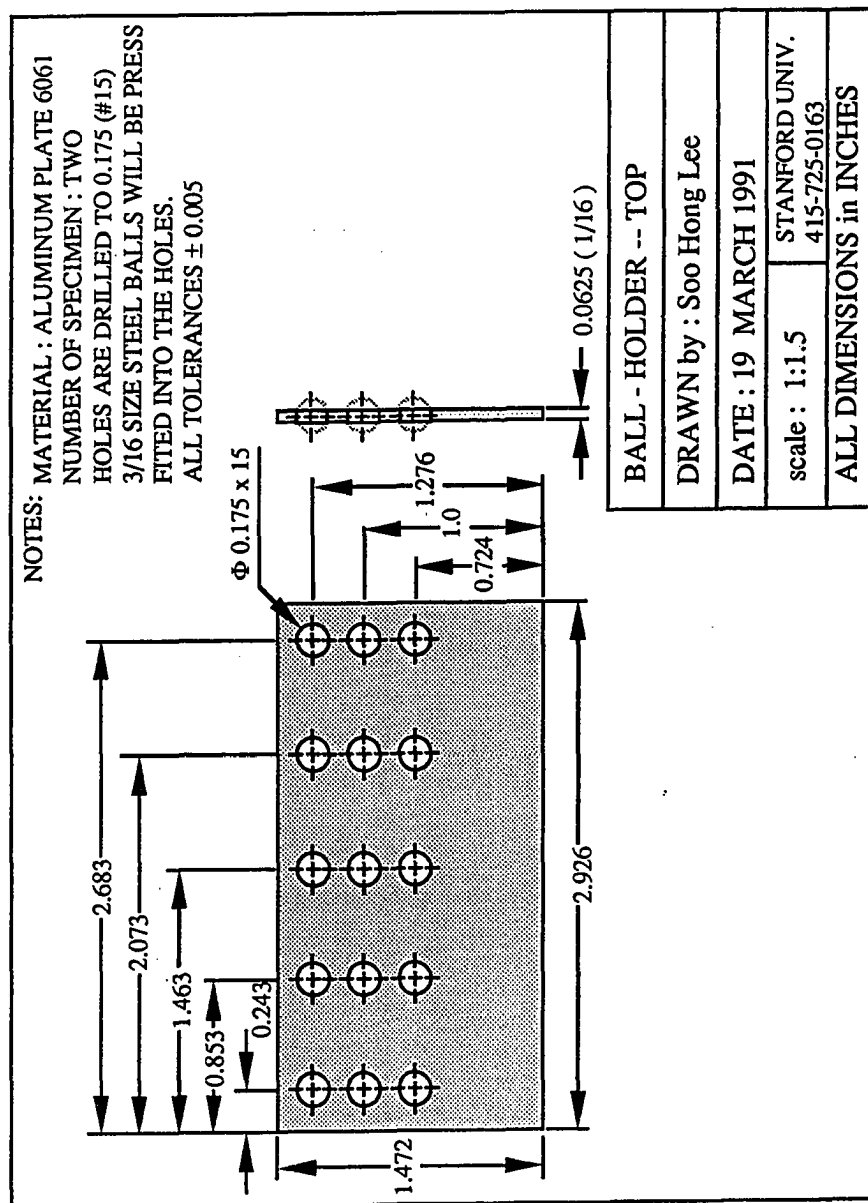


Figure F.4: Mechanical drawing of pressure distribution measuring device.

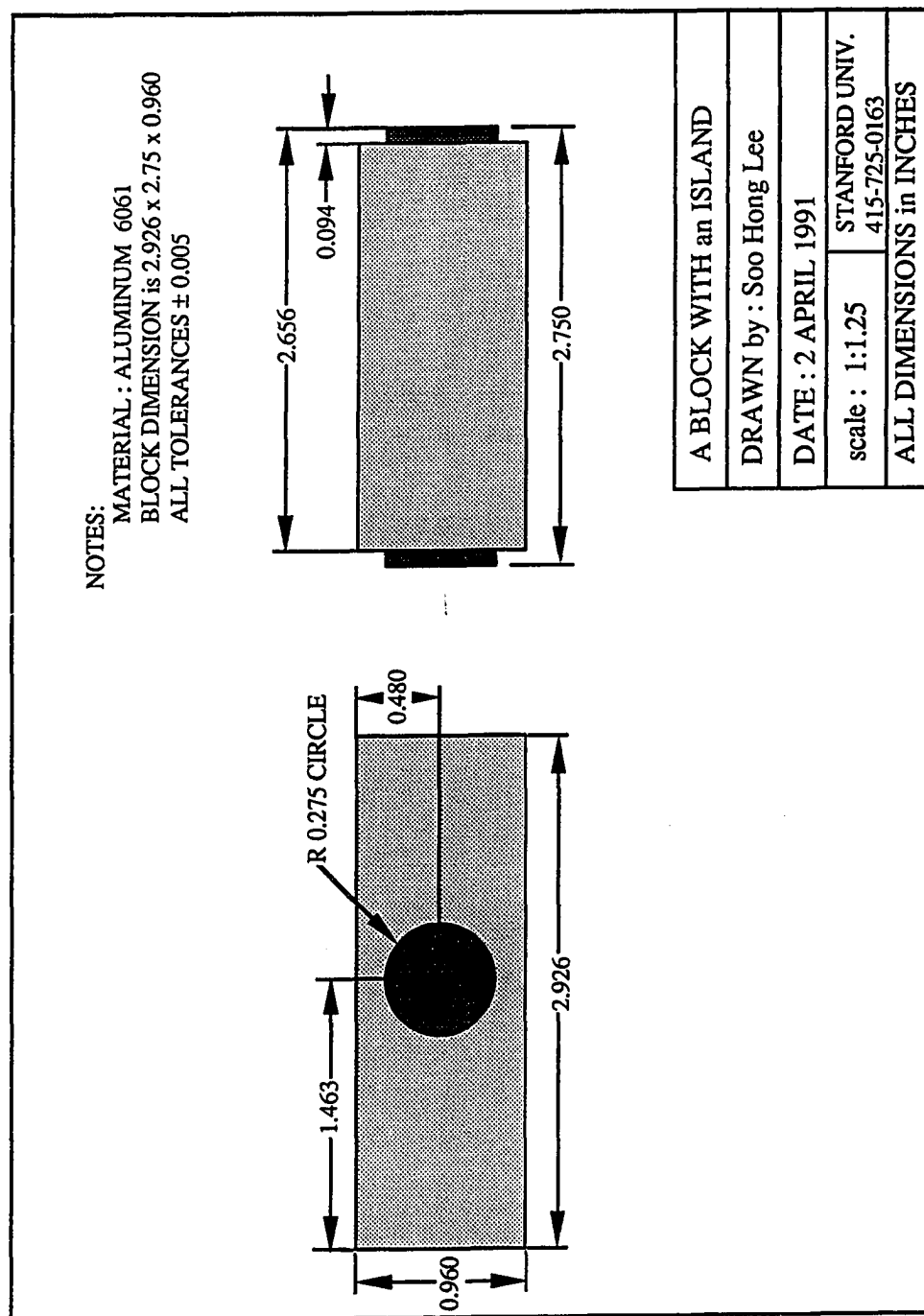


Figure F.5: Mechanical drawing of a workpiece with an island.

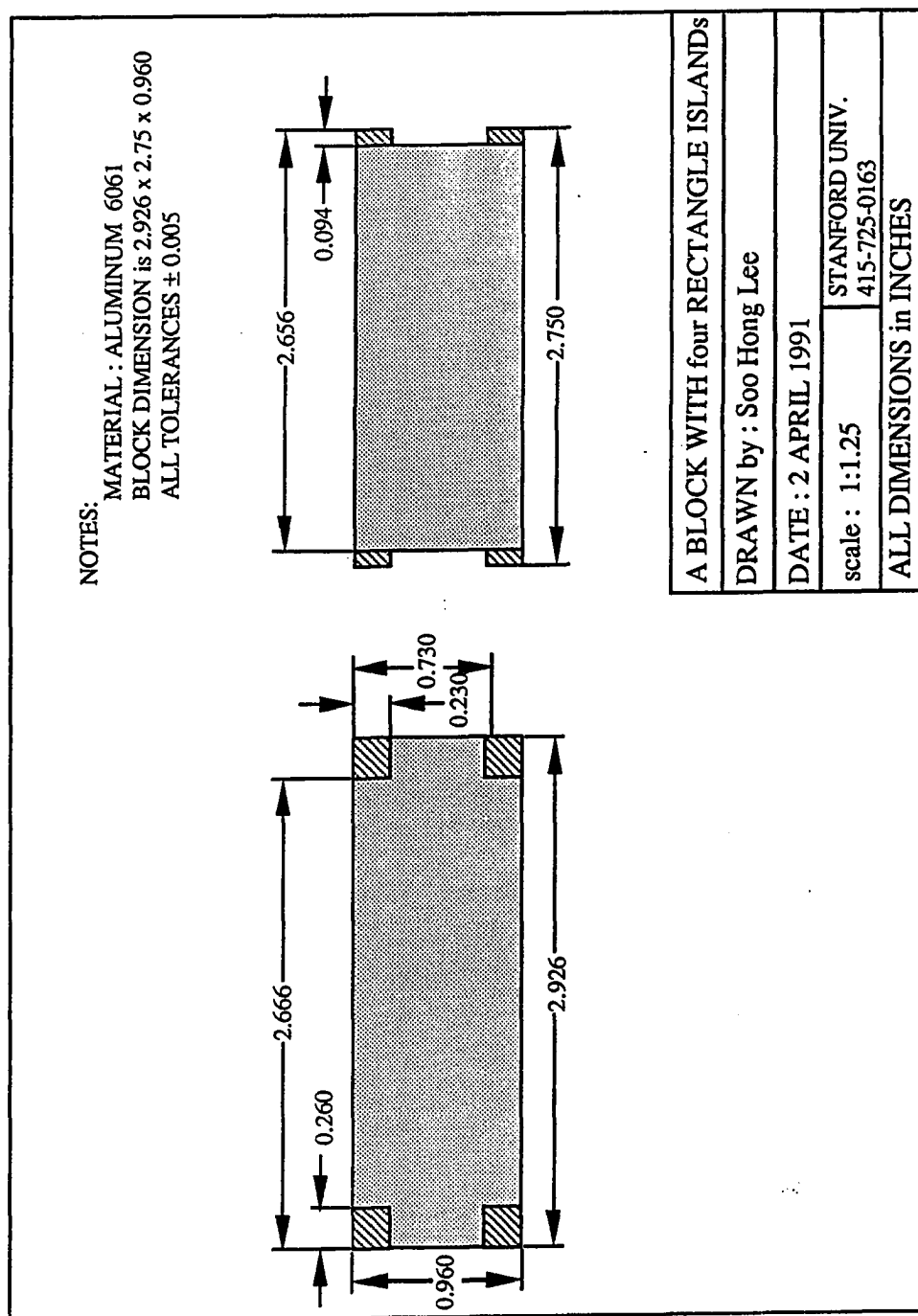


Figure F.6: Mechanical drawing of a workpiece with four rectangular islands.

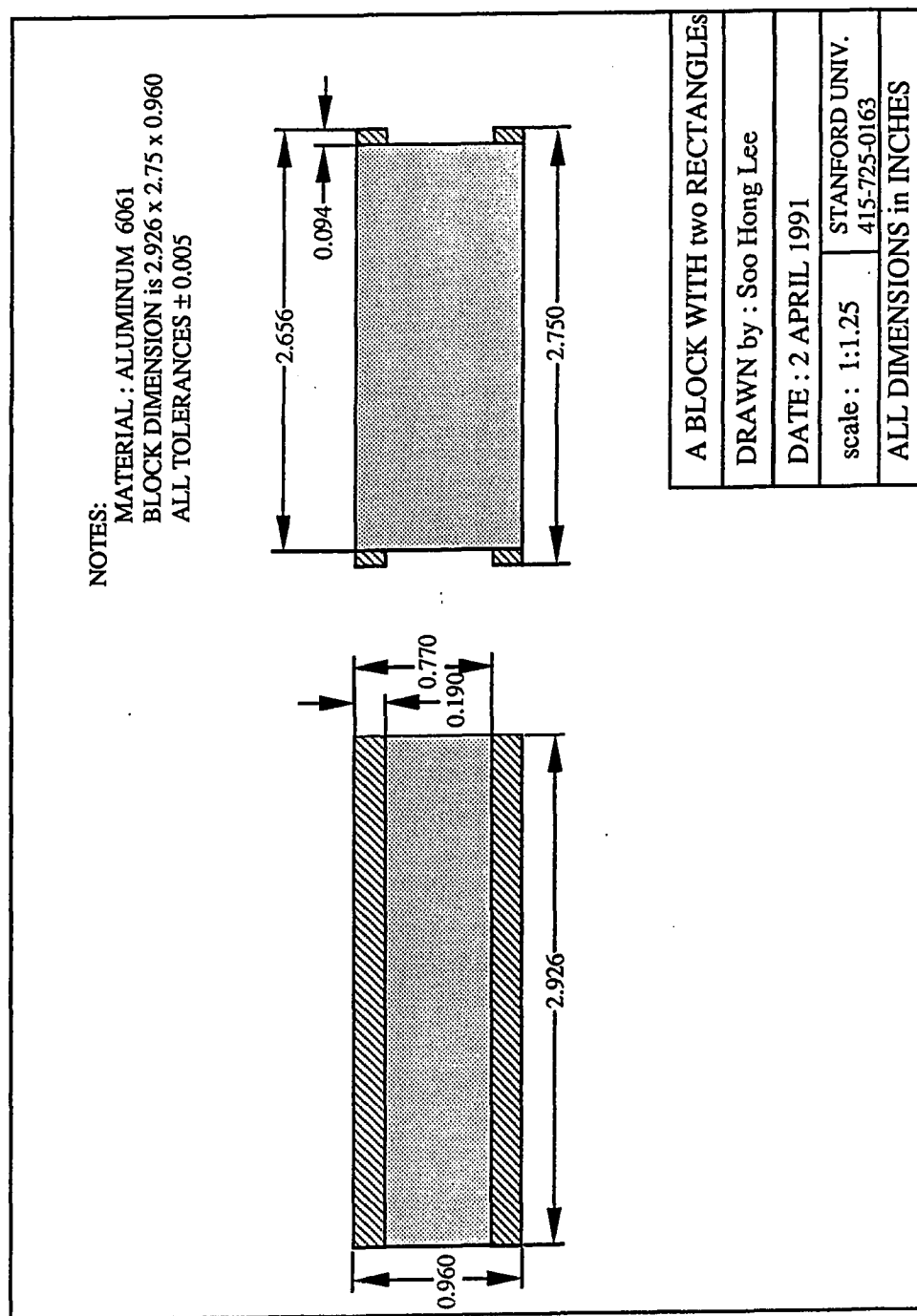


Figure F.7: Mechanical drawing of a workpiece with two long rectangular islands.

Bibliography

- [1] Asada, H. and By, A. B. 1984. Implementing automatic setup change via robots to achieve adaptable assembly. In *Proceedings of the 1984 American Control Conference*, volume 3. 1876–1882. San Diego, California.
- [2] Asada, H. and By, A. B. 1985. Kinematic analysis of workpart fixturing for flexible assembly with automatically reconfigurable fixtures. *IEEE Journal of Robotics and Automation* 86–94.
- [3] Asada, H. and Fields, A. 1985. Design of flexible fixtures reconfigured by robot manipulators. In *3rd International Symposium of Robotics Research*. 251–257.
- [4] Asada, H. and Slotine, J. E. 1986. *Robot Analysis and Control*. John Wiley and Sons. M.I.T.
- [5] Bagchi, A. and Lewis, R. L. 1986. On fixturing issues for the factory of the future. In *Proceedings, 1986 International Computers in Engineering Conference*. ASME.
- [6] Bagchi, A. and Lewis, R. L. 1987. On fixturing issues for the factory of the future. ASME Winter Annual Meeting '87.
- [7] Balakumar, P.; Robert, Jean-Christophe; Hoffman, Regis; Ikeuchi, Katsushi; and Kanade, Takeo 1988. *VANTAGE:A Frame-Based Geometric Modeling System*. The Robotics Institute, VASC-Vision and Autonomous Systems Center, Carnegie-Mellon University.
- [8] Ball, R. S. 1900. *A Treatise on the Theory of Screws*. Cambridge University Press, Cambridge, second edition.
- [9] Bausch, J. J. and Youcef-Toumi, K. 1990. Kinematic methods for automated fixture reconfiguration planning. In *the Proceedings of 1990 IEEE International Conference on Robotics and Automation*. 1396–1401.
- [10] Berenji, Hamil R. and Khoshnevis, Behrokh 1986. Use of artificial intelligence in automated process planning. *Computers in Mechanical Engineering* 47–55.

- [11] Bicchi, A. and Dario, P. 1987. Intrinsic tactile sensing for artificial hands. In *the Proceedings of the 4th Int. Symp. on Robotics Research*, Santa-Barbara, CA. R. Bolles and B. Roth Editors, published by the MIT Press, Cambridge, MA.
- [12] Bidanda, B. and Cohen, P. 1987. An integrated CAD/CAM approach for the selection of workholding devices for concentric rotational components. *Manufacturing Processes, Systems and Machines Book* 265-272.
- [13] Bidanda, B. and Cohen, P. H. 1990. Development of a computer aided fixture selection system for concentric, rotational parts. In *ASME Winter Annual Meeting on Advances In Integrated Product Design And Manufacturing*, Dallas, Texas. 219-226.
- [14] Bowden, F. P. and Tabor, D. 1956. *Friction and Lubrication*. John Wiley and Sons Inc.
- [15] Boyer, Howard E., editor 1987. *Hardness Testing*. ASM International, Metals Park, OH 44073.
- [16] Bralla, J. G. 1986. *Handbook of Product Design for Manufacturing*. McGraw Hill.
- [17] Brost, R. C. 1988. Automatic grasp planning in the presence of uncertainty. *The International Journal of Robotics Research* volume 7:pages 3-17.
- [18] Chan, S. C. and Voelcker, H. B. 1986. An introduction to MPL - a new machining process/ programming language. In *Proceedings of 1986 IEEE Conference on Robotics and Automation*. 333-344.
- [19] Chang, Tien-Chien and Wysk, Richard A. 1985. *An Introduction to Automated Process Planning Systems*. International Series in Industrial and Systems Engineering. Prentice-Hall.
- [20] Chou, Y. C.; Chandru, V.; and Barash, M. M. 1989. A mathematical approach to automatic configuration of machining fixtures: Analysis and synthesis. *Jounral of Engineering for Industry* volume 111:pages 299-306.

- [21] Chou, Y. C. 1990. A methodology for automatic layout of fixture elements based on machining forces considerations. In *ASME Winter Annual Meeting on Advances In Integrated Product Design And Manufacturing*, Dallas, Texas. 181-189.
- [22] Cohen, Paul H. 1991. Automated fixture design. In *1991 NSF Grantees Conference on Production Research and Technology*. 405-413.
- [23] Colbert, J. L.; Menassa, R.; and DeVries, W. R. 1986. A modular fixture for prismatic parts in fms. In *Proceedings, 1986 North American manufacturing Research Conference*. 597-602.
- [24] Craig, J. J. 1989. *Introduction to Robotics*. Addison-Wesley, 2nd edition.
- [25] Crandall, S. H.; Dahl, N. C.; and Lardner, T. J. 1978. *An Introduction to the Mechanics of Solids*. McGraw-Hill Book Company.
- [26] Cutkosky, Mark and Lee, Soo Hong 1989. Fixture planning with friction for concurrent product/process design. In *NSF Engineering Design Research Conference*, Amherst, MA. NSF Design Theory and Methodology Program, College of Engineering, Univ. of Massachusetts. 613-628.
- [27] Cutkosky, Mark R. and Tenenbaum, Jay M. 1990. A methodology and computational framework for concurrent product and process design. *Mechanism and Machine Theory* volume 25:pages 365-381.
- [28] Cutkosky, M. R. and Wright, P. 1986. Friction, stability and the design of robotic fingers. *International Journal of Robotics Research* volume 5:pages 20-37.
- [29] Cutkosky, M. R. 1985. *Robotic Grasping and Fine Manipulation*. Kluwer Academic Publishers, Boston, Mass.
- [30] Cutkosky, Mark R. 1989. Modeling and sensing finger/object contacts for manipulation and control. In *Robotics Research - 1989. Proceedings of the ASME Winter Annual Meeting*, San Francisco, CA. ASME. 181-188.

- [31] Descotte, Yannick and Latombe, Jean-Claude 1981. GARI: A problem solver that plans how to machine mechanical parts. In *Proceedings; International Joint Conference of Artificial Intelligence*, Vancouver. 766–772.
- [32] Drucker, D. C. 1951. A more fundamental approach to stress-strain relations. In *Proceedings of the First U.S. National Congress of Applied Mechanics*, New York. ASME. 487–491.
- [33] Drucker, D. C. 1954. Coulomb friction, plasticity and limit loads. *Journal of Applied Mechanics* volume 26:pages 71–74.
- [34] Drucker, D. C. 1959. A definition of stable inelastic material. *Journal of Applied Mechanics* volume 26:pages 101–106.
- [35] Englert, Paul J. 1987. Principles for part setup and workholding in automated manufacturing environment. Technical report, Department of Mechanical Engineering CMU, Robotics Institute Pittsburgh, Pennsylvania 15213.
- [36] Essenburg, F. 1960. On a class of nonlinear axisymmetric plate problems. *Transactions of the ASME, Journal of Applied Mechanics* 677–680.
- [37] Fenchel, Werner 1953. *Convex Cones Sets and Functions*. Princeton University, Princeton University. chapter 8.16.
- [38] Ferreira, P. M.; Koch, B.; Liu, C. R.; and Chandru, V. 1986. AIFIX: An expert system approach to fixture design. *Symposium on Computer Aided Process Planning* 73–82.
- [39] Ferstenberg, R.; Wang, K. K.; and Muchstadt, J. 1986. Automatic generation of optimized 3-axis NC programs using boundary files. In *Proceedings of 1986 IEEE Conference on Robotics and Automation*. 325–332.
- [40] Fields, Antony; Youcef-Toumi, Kamel; and Asada, Haruhiko 1989. Flexible fixturing and automatic drilling of sheet metal parts using a robot manipulator. *Robotics and Computer Integrated Manufacturing, an International Journal* 5(4):371–380.

- [41] Goyal, Suresh; Ruina, Andy; and Papadopoulos, Jim 1991. Planar sliding with dry friction: Part 1. limit surface and moment function. *Wear* 307–330.
- [42] Hayes, Caroline C. and Wright, Paul K. 1989. Automating process planning: Using feature interactions to guide search. *Journal of Manufacturing Systems* volume 8:pages 1–15.
- [43] Hayes, Caroline C. 1987. Using goal interactions to guide planning. In *Sixth National Conference on Artificial Intelligence*, Seattle, Washington. AAAI. 224–228.
- [44] Hayes, Caroline C. 1989a. A model of planning for plan efficiency: Taking advantage of operator overlap. In *Proceedings of the 11th IJCAI*, Detroit, Michigan. AAAI. 949–953.
- [45] Hayes, Caroline C. 1989b. Setup planning in machining: An expert system approach. In *15th Conference on Production Research and Technology In Advances in Manufacturing Systems Integration and Process*, University of California at Berkeley. SME. 441–443.
- [46] Hayes, Caroline C. 1990. *Machining Planning: A Model of an Expert Level Planning Process*. Ph.D. Dissertation, Carnegie Mellon University.
- [47] Hayes, Caroline Clarke 1991. Incorporating special purpose tool design in planning to make more efficient plans. Technical report, The University of Illinois at Urbana-Champaign, 1304 W. Springfield Ave. Urbana, IL 61801.
- [48] Hill, R. 1950. *The Mathematical Theory of Plasticity*. Oxford University Press, Oxford, first edition. chapter III. Extremum and Variational Principles, 53–67.
- [49] Hoffman, Edward G., editor 1984. *Fundamentals of Tool Design*. Society of Manufacturing Engineers.
- [50] Holzmann, W. and McCarthy, J. Michael 1985. Computing the friction forces associated with a three-fingered grasp. *IEEE Journal of Robotics and Automation* volume RA-1:pages 206–210.

- [51] Ishlinskii, A. Yu.; Sokolov, B. N.; and Chernous'ko, F. L. 1981. Motion of plane bodies with dry friction. *Izv. AN SSSR, Mekhanika Tverdogo Tela* 16(4):17–28.
- [52] Jameson, J. and Leifer, L. 1986. Quasi-static analysis: A method for predicting grasp stability. In *Proceedings of 1986 IEEE International Conference on Robotics and Automation*. 876–883.
- [53] Jameson, J. W. 1985. *Analytic Techniques for Automated Grasp*. Ph.D. Dissertation, Department of Mechanical Engineering, Stanford University.
- [54] Johnson, W. and Mellor, P. B. 1975. *Engineering Plasticity*. Van Nostrand Reinhold Company, London.
- [55] Johnson, K. L. 1970. The correlation of indentation experiments. *Journal of the Mechanics and Physics of Solids* 18:115–126.
- [56] Johnson, K. L. 1985. *Contact Mechanics*. Cambridge University Press, Cambridge.
- [57] Kalker, J. J. 1972. On elastic line contact. *Transactions of the ASME, Journal of Applied Mechanics* 1125–1132.
- [58] Kambhampati, Subbarao and Cutkosky, Mark R. 1990. An approach toward incremental and interactive planning for concurrent product and process design. In *Proceedings of the ASME Winter Annual Meeting, Issues in Design/Manufacture Integration, DE-Vol. 29*. 1–8.
- [59] Kambhampati, Subbarao 1990. A theory of plan modification. In *Proceedings of the Eight AAAI*, Boston, MA. AAAI. 176–182.
- [60] Kanumury, M.; Shah, J.; and Chang, T. C. 1988. An automatic process planning system for a quick turnaround cell- an integrated CAD and CAM system. In *Proceedings of The USA-Japan Symposium on Flexible Automation*, volume 1. Proceedings of The USA-Japan Symposium on Flexible Automation, ASME. 861–868.

- [61] Karinthy, Raghu and Nau, Dana S. 1989. Using a feature algebra for reasoning about geometric feature interactions. In *Proceedings of 11th International Joint Conference on Artificial Intelligence*. Detroit, U.S.A. Morgan Kaufman. 1219–1224.
- [62] Keer, L. M. and Silva, M. A. G. 1972. Two mixed problems for a semi-infinite layer. *Transactions of the ASME, Journal of Applied Mechanics* 1121–1124.
- [63] Keer, L. M.; Dundurs, J.; and Tsai, K. C. 1972. Problems involving a receding contact between a layer and a half space. *Transactions of the ASME, Journal of Applied Mechanics* 1115–1120.
- [64] Kerr, J. and Roth, B. 1986. Analysis of multifingered hands. *The International Journal of Robotics Research* volume 4:pages 3–17.
- [65] Kim, Yong-Se 1990. *Convex Decomposition And Solid Geometric Modeling*. Ph.D. Dissertation, Stanford University.
- [66] Kutz, Myer, editor 1986. *Mechanical Engineer's Handbook*. John Wiley & Sons, New York.
- [67] Lakshminarayana, K. 1978. Mechanics of form closure. ASME paper no. 78-DET-35, Indian Institute of Technology, Madras, India.
- [68] Lee, Soo-Hong and Cutkosky, Mark 1991a. Fixture planning with friction. *ASME Journal of Engineering for Industry* 113(3):320–327.
- [69] Lee, Soo-Hong and Cutkosky, Mark 1991b. Incremental & interactive geometric reasoning for part fixturing in Concurrent Product/Process Design. Technical paper number 19910201, Center for Design Research, Design Division, Mechanical Engineering, Stanford University, Stanford, CA 94305.
- [70] Lee, J. D. and Haynes, L. S. 1987. Finite-element analysis of flexible fixturing system. *Transactions of the ASME* volume 109:pages 134–139.

- [71] Lee, Soo-Hong; Cutkosky, Mark; and Kambhampati, Subbarao 1991. Incremental & interactive geometric reasoning for fixture and process planning. In *Proceedings in 1991 ASME Winter Annual Meeting on Design/Manufacture Intergration session*, Atlanta, Georgia.
- [72] Leu, M. C.; Park, S. H.; and Wang, K. K. 1986. Geometric representation of translational swept volumes and its applications. *Journal of Engineering for Industry* volume 108:pages 113–119.
- [73] Lim, B. S. and Knight, J. A. G. 1987. A foundation for a knowledge-based computer integrated manufacturing system. *International Journal for Artificial Intelligence in Engineering* volume 2:pages 11–22.
- [74] Lozano-Perez, T. 1983. Spatial planning: A configuration space approach. *IEEE Transactions on Computers*.
- [75] Luby, S. C.; Dixon, J. R.; and Simmons, M. K. 1986a. Designing with features: Creating and using a features data base for evaluation of manufacturability. In *Proceedings, International Computers In Engineering Conference, ASME*, volume 1. 285–292.
- [76] Luby, Steven C.; Dixon, John R.; and Simmons, Melvin K. 1986b. Creating and using a features data base. *Computer in Mechanical Engineering* 25–33.
- [77] Luenberger, David G. 1984. *Introduction to Linear and Nonlinear Programming*. Addison-Wesley, second edition.
- [78] Mahanti, Ambuj; Karinthi, Raghu; Ghosh, Subrata; and Pal, Asim 1991. AI search for minimum-cost set cover and multiple-goal plan optimization problems: Applications to manufacturing, planning, and scheduling. In *The Fourth International Conference on Industrial and Engineering Applications of AI and Expert Systems (IEA-AIE-91)*, Kauai, Hawaii.
- [79] Mani, M. and Wilson, W. 1988. Automated design of workholding fixtures using kinematic constraint synthesis. In *Proceedings of the 16th North American Manufacturing Research Conference of SME*, Urbana-Champaign.

- [80] Mason, M. T. and Salisbury, J. K. 1985. *Robot Hands and the Mechanics of Manipulation*. The MIT Press.
- [81] Mason, Matthew T. 1986. Mechanics and planning of manipulator pushing operations. *The International Journal of Robotics Research* volume 5:pages 53–71.
- [82] Menassa, Roland J. and DeVries, Warren R. 1990. A design synthesis and optimization method for fixtures with compliant elements. In *ASME Winter Annual Meeting on Advances In Integrated Product Design And Manufacturing*, Dallas, Texas. 203–218.
- [83] Minagawa, M.; OKINO, N.; and Kakazu, Y. 1984. Automatic dimensioning on 3-D solid geometry. In *Proceedings of the 5th international conference on production engineering Tokyo*. 721–726.
- [84] Moore, D. F. 1972. *The Friction and Lubrication of Elastomers*. Pergamon Press, New York, N. Y.
- [85] Nguyen, V. 1986a. Constructing force-closure grasps. In *Proceedings of 1986 IEEE Conference on Robotics and Automation*, San Francisco. 1368–1373.
- [86] Nguyen, V. 1986b. The synthesis of stable force-closure grasps. Technical Report AI-TR905, MIT, Artificial Intelligence Laboratory.
- [87] Nguyen, V. 1986c. The synthesis of stable grasps in the plane. In *Proceedings of 1986 IEEE Conference on Robotics and Automation*, San Francisco. 884–889.
- [88] Nguyen, V. 1987a. Constructing force-closure grasps in 3d. In *Proceedings of 1987 IEEE Conference on Robotics and Automation*. 240–245.
- [89] Nguyen, V. 1987b. Constructing stable grasps in 3d. In *Proceedings of 1987 IEEE Conference on Robotics and Automation*. 234–239.
- [90] Nguyen, V. 1988. Constructing force-closure grasps. *The International Journal of Robotics Research* volume 7:pages 3–16.

- [91] Nguyen, V. 1989. Constructing stable grasps. *The International Journal of Robotics Research* volume 8:pages 26–37.
- [92] Ohwovoriole, M. S. and Roth, B. 1981. An extension of screw theory. *Journal of Mechanical Design* volume 103:pages 19–39.
- [93] Ohwovoriole, M. 1980. *An extension to screw theory and its applications to the automation of industrial assemblies*. Ph.D. Dissertation, Department of Mechanical Engineering, Stanford University.
- [94] Ohwovoriole, E. N. 1987. Kinematics and friction in grasping by robotic hands. *Journal of Mechanics, Transmissions, and Automation in Design* 109(3):398–404.
- [95] Peshkin, M. A. and Sanderson, A. C. 1988. Minimization of energy in quasi-static manipulation. In *Proceedings of 1988 IEEE Conference on Robotics and Automation*, Philadelphia, Pennsylvania. 421–426.
- [96] Peshkin, M. A. 1986. *Planning Robotic Manipulation Strategies for Sliding Objects*. Ph.D. Dissertation, Department of Mechanical Engineering, Carnegie Mellon University.
- [97] Pham, D. T.; Cheung, K. C.; and Yeo, S. H. 1990. Initial motion of a rectangular object being pushed or pulled. In *Proc. of 1990 IEEE Conf. on Robotics and Automation*, volume 3. 1046–1050.
- [98] Reuleaux, F. 1876. *The Kinematics of Machinery*, volume II. Macmillan, New Jersey, second edition. (Republished by Dover, 1963).
- [99] Ross, Robert B., editor 1972. *Metallic Materials Specification Handbook*. E. & F.N. SPON LTD, London.
- [100] Sakurai, Hiroshi 1990. *Automatic Setup Planning and Fixture Design for Machining*. Ph.D. Dissertation, Massachusetts Institute of Technology.
- [101] Savvin, A. P. 1965. Plane system of friction forces. *Izv. AN SSSR, Mekhanika Tverdogo Tela* 1(3):160–164.

- [102] Serra, J. 1982. *Image Analysis and Mathematical Morphology*. Academic Press, London. chapter II. The Hit or Miss Transformation, Erosion and Opening.
- [103] Shvedenko, V. N. 1986. Equilibrium of a plane system of friction forces. *Izv. AN SSSR, Mekhanika Tverdogo Tela* 21(1):37–42.
- [104] Smithells, C. J., editor 1955. *Metals Reference Book*. Interscience Publishers, Inc., New York, fifth edition.
- [105] Somov, P. 1900. Über gebiete von schraubengeschwindigkeiten eines starren korporis bei verschiedener zahl von stutzflachen. *Zietschrift fur Mathematik and Physik* 45:245–306.
- [106] Stanat, Donald F. and McAllister, David F. 1977. *Discrete Mathematics in Computer Science*. Prentice-HALL, University of North Carolina at Chapel Hill.
- [107] Sungurtekin, Ugur A. and Voelcker, Herbert B. 1986. Graphic simulation and automatic verification of nc machining programs. In *Proc. of 1986 IEEE Conf. on Robotics and Automation*. 156–165.
- [108] Tabor, David 1951. *The Hardness of Metals*. Oxford, Clarendon Press.
- [109] Timoshenko, S. P. and Goodier, J. N. 1970. *Theory of Elasticity*. McGraw-Hill Book Company, New York.
- [110] Trappery, J. C. Amy and Liu, C. Richard 1990. Automatic generation of configuration for fixturing an arbitrary workpiece using projective spatial occupancy enumeration approach. In *ASME Winter Annual Meeting on Advances In Integrated Product Design And Manufacturing*, Dallas, Texas. 191–202.
- [111] Tsang, J. P. 1989. PROPEL: An expert system for generating process plans. In *SIGMAN Workshop on Manufacturing Planning*.
- [112] Tuffentsammer, K. 1981. Automatic loading of machining systems and automatic clamping of workpieces. *Manufacturing Technology* volume 30:pages 553–558.

- [113] Updike, D. P. and Kalnins, A. 1970. Axisymmetric behavior of an elastic spherical shell compressed between rigid plates. *Transactions of the ASME, Journal of Applied Mechanics* 635–640.
- [114] Updike, D. P. and Kalnins, A. 1972. Contact pressure between an elastic spherical shell and a rigid plate. *Transactions of the ASME, Journal of Applied Mechanics* 1110–1114.
- [115] Woodbury, Robert F. and Oppenheim, Irving J. 1986. Geometric reasoning. Technical report, Carnegie-Mellon University, Department of Civil Engineering CMU, Pittsburgh, PA 15213.
- [116] Wright, P. K. and Bourne, D. A. 1988. *Manufacturing Intelligence*. Addison-Wesley.
- [117] Wright, P. K. and Cutkosky, M. R. 1985. *Handbook of Industrial Robotics*. Wiley Press, New York. chapter 7, Design of Grippers.
- [118] Zhukovskii, N. E. 1948. Equilibrium condition for a rigid body resting on a fixed plane with some area of contact, and capable of moving along the plane with friction. In *Collected Works, Vol.1: General Mechanics [In Russian]*. Gostekhizdat, Moscow-Leningrad. 339–354.